EPIGENETIC REGULATION OF PRO-APOPTOTIC GENES IN DROSOPHILA

By

NIANWEI LIN

A DISSERTATION PRESENTED TO THE GRADUATE SCHOOL
OF THE UNIVERSITY OF FLORIDA IN PARTIAL FULFILLMENT
OF THE REQUIREMENTS FOR THE DEGREE OF
DOCTOR OF PHILOSOPHY

UNIVERSITY OF FLORIDA

2010

To Jie, my dear wife and to our families

ACKNOWLEDGMENTS

I would like to thank all of those people who helped make this dissertation possible. First, I wish to thank my advisor, Dr. Lei Zhou for all his guidance, encouragement, support, and patience through out my Ph.D. training. His sincere interest in science has been a great inspiration to me. Since I joined the lab, I have been encouraged to become an independent researcher, but not a technician in the laboratory. As a rigorous scientist, he always told us not to be too excited to make any conclusion that beyong the available evidence. Whe I felt frustrated about the repeated negative data, he taught me how to learn from my failure, and knowing when to make an end of a project is actually a nessesary capability for a successful scientist. From the beginning of my Ph.D. study, I have been trained that a good scientist needs to have good taste about what is worthwhile and what is not. Without this sense of taste and his continuous guidance, I would have not really enjoyed the charm of science as I do today.

I would like to acknowledge the inspirational instruction and guidance of my committee members, Dr. Thomas Yang, Dr. Jorg Bungert, Dr. Suming Huang, as well as the former committee members Dr. Lei Xiao and Dr. Keith Robertson. Their helpful insights, comments and suggestions really shaped my research work. I would also like to acknowledge and thank IDP program for offering me such wonderful opportunity and supportive environment for the graduate training.

My thanks must also go to the current and former members of the Zhou lab, Hailong Meng, Yanping Zhang, Can Zhang, Bo Liu, Guangyao Li, John Pang, Micheal Novo, and etc.. I don’t remember how many ideas were inspired from our discussions

and debating during the lab meetings. More important, we had a delightful and friendly environment which makes any successful work possible.

Finally, I would like to thank my family and my wife for their encouragement and consistent support. A special thanks to my beloved wife Jie Xu, whom I met and married in this small magical town. She fulfills my life and makes everything meaningful to me.

TABLE OF CONTENTS

page

LIST OF TABLES

LIST OF FIGURES

LIST OF ABBREVIATIONS

AEL	After egg laying
AO	Acridine orange
BEAF	Boundary element associated factor
CBP	CREB-binding protein
CDP	CCAAT displacement protein
ChIP	Chromatin Immuno-precipitation
cHS4	Chicken hypersensitive site-4
CNS	Central nervous system
CPE	Chromosomal position effect
CtBP	C-terminal binding protein
CTCF	CCCTC-binding factor
dIAP	*Drosophila* inhibitor of apoptosis protein
Dsp1	dorsal switch protein1
EGFR	Epidermal growth factor receptor
en	*engrailed*
EST	Expressed sequence tag
ESC	Extra sex combs
ESCL	Extra sex combs like
E(z)	Enhancer of zeste
FACS	Fluorescence-activated cell sorting
GAF	GAGA factor
GFP	Green fluorescent protein
Grh	Grainyhead
GSC	Germ line stem cell

H3K9me3	Trimethylated histone 3 lysine 9
H3K27me3	Trimethylated histone 3 lysine 27
HCNE	Highly conserved non-coding element
Hdac1	Histone deacetylase 1
HMTase	histone methyltransferase
HP1	Heterochromatin protein 1
IAP	Inhibitor of apoptosis protein
IBM	IAP-binding motif
ICC	immunocytochemistry
ILB	IRER left barrier
ILF	IRER left fragment
IRER	Irradiation responsive enhancer region
ISH	*in situ* hybridization
JNK	Jun amino-terminal kinase
MG	Midline glial
mx	*michelob_x*
MY	Million years
P53RE	P53 response element
PAT	Photoacoustic tomography
Pc	Polycomb
PcG	Polycomb group
PCR	Polymerase chain reaction
Pcl	Polycomb like
Ph	Polyhomeotic
PHD	Polyhomeotic distal

Pho	Pleiohomeotic
Phol	Pleiohomeotic like
PHP	Polyhomeotic proximal
PIC	Protease inhibitor cocktails
PRC	Polycomb repressive complex
PRE	Polycomb response elements
Psc	Posterior sex combs
Psq	Pipsqueak
puma	p53 upregulated modulator of apoptosis
QPCR	Quantitative polymerase chain reaction
rpr	*reaper*
RT	Room temperature
SAM	Significance analysis of microarrays
Sce	Sex combs extra
scs	Specialized chromatin structure
sickle	*skl*
Su(Hw)	Suppressor of hairy wing
Su(var)3-9	Suppressor of variegation 3-9
Su(z)12	Suppressor of zeste 12
SU(Z)2	Suppressor of zeste 2
TAFII	TATA-box-binding protein (TBP)-associated factor
TBP	TATA-box-binding protein
TRE	Trithorax response element
trxG	Trithorax group
Trl	Trithorax-like

TSS	Transcription starting site
TUNEL	Terminal deoxynucleotidyl transferase dUTP nick end labeling
UAS	Upstream activation sequence
Ubx	Ultrabithorax
USF1	Upstream stimulatory factor 1
VEZF1	Vascular endothelial zinc finger 1
Zw5	Zeste-white 5

Abstract of Dissertation Presented to the Graduate School
of the University of Florida in Partial Fulfillment of the
Requirements for the Degree of Doctor of Philosophy

EPIGENETIC REGULATION OF PRO-APOPTOTIC GENES IN DROSOPHILA

By

Nianwei Lin

December 2010

Chair: Lei Zhou
Major: Medical Sciences — Genetics

It is known that *Drosophila* embryos are highly sensitive to ionizing radiation (IR)-induced apoptosis at early but not later stages, but the underlying molecular mechanism is unknown. The Irradiation Responsive Enhancer Region (IRER), responsible for the induction of pro-apoptotic genes *rpr* and *hid* in response to irradiation, was mapped to a ~33 kb evolutionarily conserved intergenic region upstream of the pro-apoptotic gene *reaper* (*rpr*). The IRER region undergoes a chromatin structure change from a permissive state to a blocked state at developmental stage 12, and stays for the rest of embryonic stages. When blocked, the IRER region is highly enriched with repressive chromatin marks, such as H3K27me3 and H3K9me3, and also bound by PcG proteins. This switch of chromatin structure is responsible for the radiation sensitivity transition during the embryogenesis. The functions of histone-modifyer proteins, including Hdac1(rpd3), Su(var)3-9, Su(z)12 and Pc are required for this process. Thus, direct epigenetic regulation of IRER controls cellular sensitivity to cytotoxic stimuli.

The fact that there is little radiation stress in the natural environment suggests that IRER may have important biological functions during development. Indeed, several IRER deletion mutants showed downregulation of *rpr* in the stripped epidermis at stage

10-11 embryos. To monitor the chromatin accessibility of the IRER region in live animals, a DsRed reporter gene controlled by an *ubiquitin* promoter was inserted into the endogenous IRER locus. The association of DsRed expression level and the chromatin accessibility of IRER were validated by analyzing the FACS sorted cells. The DsRed expressing cells showed some specific pattern in various tissues. Interestingly, rapid induction of DsRed upon irradiation was found in the larval imaginal discs. Also, nutrition-deprivation resulted in increased DsRed in IRER{ubi-DsRed} larvae. Its dynamic epigenetic status suggests that IRER is responsive to environmental stresses and adjusts the cellular sensitivity to stress-induced apoptosis by changing its chromatin configuration.

The chromatin barrier element functions against the propagation of condensed heterochromatin into the euchromaitn regions. The epigenetic blocking is restrained in the IRER without affecting the *rpr* promoter and basic enhancer region, suggesting the existence of a barrier element at the chromatin transition region. The essential chromatin barrier element was narrowed down to a 167bp region at the IRER left barrier (ILB) with a reporter assay. The ILB barrier is sufficient to prevent the propagation of heterochromatin associated with PRE-mediated silencing, and this barrier activity requires the binding of Cut protein, which may recruit the histone acetyltransferase CBP. Unlike all of the known insulators identified from *Drosophila*, the ILB does not contain enhancer-blocking activity. The study of the enhancer specific epigenetic suppression delimited by the ILB barrier greatly contributes to our knowledge of the advanced gene regulation beyond the DNA sequence in eukaryotic genomes.

CHAPTER 1
BACKGROUND AND INTRODUCTION

Apoptosis and Cell Death Regulation

Apoptosis is an essencial biological process in multicellular organisms to eliminate the damaged, aged, infected or excessive cells (Bergmann et al. 1998c; Horvitz 1999; Vaux and Korsmeyer 1999). The apoptotic program is triggered by the activation of caspases. Caspases are ubiquitously expressed as the inactive pro-caspase in most cells. Upon activation, effector caspases will cleave structural proteins, enzyme inhibitors, etc. which in turn will lead to destruction, fragmentation and engulfing of the dying/dead cells (Steller 1995). Although caspase activation and apoptosis can proceed without *de novo* protein synthesis under certain special circumstances, an abundance of evidence suggests that transcriptional mechanisms play a pivotal role in apoptosis initiation. Transcriptional activation of pro-apoptotic genes is especially important for initiating apoptosis in response to cytotoxic stimuli. The genetic requirement of transcription factors such as P53 in irradiation-induced cell death underscores the importance of the transcriptional response (Lowe et al. 1993; Chao et al. 2000).

A general observation of the cell death regulatory pathways reveals that downstream players such as caspases tend to be ubiquitously expressed and with their activity mostly regulated by post-translational mechanisms. In contrast, most, if not all, upstream regulators are regulated at the transcriptional level and are selectively expressed during development or in response to cytotoxic stimuli (Figure 1-1). In the Bcl-2 (ced-9) pathway, the pro-apoptotic upstream initiators, such as the BH3-only protein coded by *egl-1*[*] gene in *C. elegans* (Conradt and Horvitz 1999; Thellmann et al.

[*] All *gene* names are italicized. Protein names are non-italicized and capitalized.

2003), are regulated at the transcriptional level. Human BH3-only pro-apoptotic genes such as *puma* (*p53 upregulated modulator of apoptosis*) and *noxa* are the direct transcriptional targets of P53 (Nakano and Vousden 2001; Yu et al. 2001; Villunger et al. 2003). Correspondingly, p53-dependent irradiation-induced cell death is inhibited or totally blocked in *noxa* and/or *puma* knockout mice, depending on the tissue examined (Jeffers et al. 2003; Shibue et al. 2003).

In *Drosophila*, the Inhibitor of Apoptosis Protein (DIAP) 1 protein plays an essential role in inhibiting programmed cell death during development. Diap1 is ubiquitously expressed and inhibits the activation of caspases. In embryos mutated for *diap1*, essentially all cells die when the maternally deposited Diap1 is exhausted (Wang et al. 1999; Goyal et al. 2000). During development, specific elimination of cells is accomplished by selected expression of the IAP-antagonists, including *reaper* (White et al. 1994), *hid* (Grether et al. 1995), *grim* (Chen et al. 1996), and *sickle* (Christich et al. 2002; Srinivasula et al. 2002; Wing et al. 2002), which remove the IAP inhibition and cause caspase activation (reviewed in (Cashio et al. 2005; Ditzel and Meier 2005; Vaux and Silke 2005)). Interestingly, all of the 4 genes are located in a genomic region of about 350kb and are transcribed in the same direction. During development, *reaper*, *grim*, and *sickle* are specifically expressed in cells that are destined to die (White et al. 1994; Chen et al. 1996; Christich et al. 2002; Srinivasula et al. 2002; Wing et al. 2002), suggesting the importance of a transcriptional mechanism in achieving the appropriate level of cell death in each tissue. The expression of *hid* is largely limited to dying cells although it is expressed in cells that do not die, possibly due to the fact that unlike the other three, the pro-apoptotic activity of Hid is subject to post-translational modification

(Bergmann et al. 1998b). In addition to mediating developmental cell death, transcriptional activation of these genes is responsible for the tissue degeneration induced by ecdysone during metamorphosis. Not surprisingly, *reaper*, *hid*, and *sickle* are transcriptionally activated following ionizing irradiation to mediate cell death (White et al. 1994; Christich et al. 2002; Brodsky et al. 2004; Zhang et al. 2008a; Zhang et al. 2008b). In mutant embryos lacking *reaper* and *hid*, irradiation induces little apoptosis (White et al. 1994).

Patterns of Cell Death during Embryogenesis

Cell death has long been noticed for embryos mutated for genes which govern differentiation and development (Magrassi and Lawrence 1988; Smouse et al. 1988). Systematic analysis of cell death during *Drosophila* embryogenesis in wild type embryos was first carried out by Abrams et al (Abrams et al. 1993). They showed that most cell death during *Drosophila* embryogenesis share the canonical characteristics of apoptosis. The vital dye Acridine Orange (AO) was found especially sensitive to the apoptotic cells in *Drosophila* embryos, although it seems to preferentially label cells in later stage of apoptosis. Often, it also labels the apoptotic bodies phagocytosed by migrating macrophages (Abrams et al. 1993). AO-positive cells first appear at embryonic stage 11 (about 7 hour after egg laying (AEL)) in the precephalic region. However, the AO-labeling pattern quickly spreads out to the other segments and reaches a peak level at stages 12 and 13 (8-10hr AEL), when nearly all segments have AO-positive cells. The level of cell death wanes after stage 14, and becomes mainly restricted to the ventral nerve cord at the end stage of embryogenesis (Stage 16-17, after 15hr AEL).

The overall pattern of cell death is quite dynamic throughout the course of *Drosophila* embryogenesis after 7 hr after egg laying, as revealed by AO staining or terminal deoxynucleotidyl transferase dUTP nick end labeling (TUNEL) (Abrams et al. 1993; Pazdera et al. 1998). Although the general pattern associated with a particular developmental stage is highly reproducible, the exact number and positions of dying cells at a given point may vary significantly. For instance, the pattern of AO or TUNEL – positive cells in the ventral epidermis between stages 12-14 shows a rough segmentally-repeated pattern associated with segment boundaries (Pazdera et al. 1998). However, the positions and numbers of dying/dead cells are only partially symmetrical on the two sides of the midline.

A genetic screen identified that the genomic region deleted in the H99 deficiency mutant is required for almost all developmental cell death in *Drosophila* embryogenesis (White et al. 1994). Three genes in this region, *reaper* (White et al. 1994), *hid* (Grether et al. 1995), and *grim* (Chen et al. 1996), encode pro-apoptotic proteins that function as IAP (Inhibitor of Apoptosis) -antagonists. These proteins share an IAP-binding motif (IBM), which can bind to IAP and relieve its inhibition on caspases. A 4th IAP-antagonist, *sickle*, reside just upstream of *reaper*, but was not deleted in the H99 deficiency (Christich et al. 2002; Srinivasula et al. 2002; Wing et al. 2002). The four IAP-antagonists reside in a ~350kb region that is highly conserved as a synteny in the sequenced *Drosophila* genomes. With the exception of *hid*, expression of the IAP-antagonist genes appears to be limited to cells destined to die during embryogenesis. The pro-apoptotic function of Hid can be suppressed by the MAP kinase pathway and *hid* is the only one of the four whose mRNA can be detected in cells that do not die.

The central nervous system (CNS) of the H99 mutant embryo is about 3-4 times larger than the wild type at the end of embryogenesis, indicating that approximately 70% of the cells in the embryonic CNS die during embryogenesis (White et al. 1994). A similar ratio was observed in monitoring the developmental cell death of the glia cells at the CNS midline (Sonnenfeld and Jacobs 1995a; Zhou et al. 1995). Cell lineage–specific makers allowed monitoring of these cells during wild type embryogenesis as well as in H99 mutant. While there are about 8 *slit1.0-lacZ* expressing midline glial (MG) cells per segment at early stage 12, only 3 cells remain there at the end of embryogenesis. The rest undergo cell death, which depends on the function of the three IAP-antagonist genes deleted in H99 mutant (Zhou et al. 1995). However, not every cell lineage undergoes cell death during embryogenesis. For instance, the number of ventral unpaired neurons in the CNS midline remains unchanged during both wild type and H99 embryogenesis (Zhou et al. 1995).

Interestingly, many dying cells are quickly phagocytosed by migrating hemocytes / macrophages during embryogenesis (Abrams et al. 1993; Tepass et al. 1994; Sonnenfeld and Jacobs 1995b; Zhou et al. 1995). It seems that dying cells are “pushed” from their original location towards the space through which hemocytes will migrate. The display of phagocytotic signal on the dying cells depends on the function of IAP-antagonists and caspase activation. On the macrophage side, *Croquemort,* is required for recognizing the apoptotic cells (Franc et al. 1996; Franc et al. 1999). However, the genesis of hemocytes in the cephalic mesoderm and their stereotypic migration in the embryo are independent of cell death, as both were largely normal in the H99 mutant

background (Tepass et al. 1994; Zhou et al. 1995). Reciprocally, cell death can proceed normally in embryos that lack macrophages (Tepass et al. 1994).

The majority of cell death during embryogenesis occurs between stage 11 to stage 13. In post stage 15 embryos, only discrete cells in the ventral nerve cord can be detected as AO or TUNEL –positive (Abrams et al. 1993; Zhang et al. 2008a). Most of these late-dying cells appear to be neuroblasts (Karcavich and Doe 2005; Rogulja-Ortmann et al. 2007). Unlike cell death at earlier stages, dying neuroblasts do not appear to be phagocytosed by macrophages.

Why should cells be generated in the embryo only to be eliminated in just a few hours? The reason may differ depending on the circumstance. For example, the midline glial cells guide the crossing over of the axons from each hemisphere, eventually forming the commissural axon tract. Interestingly, midline glial cell death concurs with the end of commissural axon formation and separation, suggesting that the MG cell death may be a mechanism to eliminated obsolete cells (Sonnenfeld and Jacobs 1995a). On the other hand, cell death of the abdominal neuroblasts cells is timed to terminate their potential to proliferate (Bello et al. 2003; Maurange et al. 2008). In H99 deficiency mutant that lacks *reaper*, *hid*, and *grim*, the rescued neuroblasts continue to proliferate and generate supernumerary cells. This indicates that cell death also serves to prevent over-proliferation.

Toyama et al. also demonstrated that cell death in the aminoserosa cells actually contribute to the movement of cell sheet during morphogenesis (Toyama et al. 2008). The delamination and extrusion of the apoptotic cell produces a force that is required for bringing the cell sheet together during dorsal closure. This was a rather surprising

finding. Clearly, the functional significance of cell death may well surpass what we have already known or thought about so far.

Polycomb Silencing and Genomic Programmes

DNA is compacted into the nucleus as the chromatin in eukaryotic genomes. The nucleosome is the subunit of chromatin, and is composed of 147 bp of DNA wrapped around an octamer of histones. Each nucleosome core consists of two copies of each of the histones- H2A, H2B, H3 and H4. The nucleosomes form an approximately 11 nm "beads-on-a-string" fibre. The N-terminal tails of histones are subject to different post-transcriptional modifications, such as methylation, acetylation, phosphorylation and ubiquitination. Different combinations of histone modifications, also known as histone code, will confer the chromatin different structure, and thereby control the expression of the associated genes.

Epigenetics refers to the study of a heritable gene expression pattern that is due to the information contained in chromatin, other than the associated DNA sequence. There may be several mechanisms involved in epigenetic regulation: (1) ATP-dependent chromatin remodeling (Flaus and Owen-Hughes 2004), (2) post-translational covalent modifications of the histones, (3) histone variant replacement (Kamakaka and Kadonaga 1994), and (4) DNA methylation at CpG sites (Scarano et al. 2005). These mechanisms may work in an inexclusive way in higher eukaryotes.

The cell fate is determined by the specific gene expression pattern and maintained by epigenetic mechanism. This process is also known as cellular memory, and Polycomb group (PcG) proteins play important roles in maintaining the silenced state of their target genes, while trithorax group (trxG) proteins are required for "memorizing" the active expression.

PcG Complexes

Polycomb group (PcG) proteins are required to prevent inappropriate expression of Hox genes (Lewis 1978). The expression pattern of homeotic genes is initially established by proteins coded by segmentation genes which act as activators and repressors. After early embryogenesis, the PcG silencing mechanisms take over to maintain the repressed state through the rest of development (Zhang and Bienz 1992; Qian et al. 1993; Pirrotta 1998). PcG silencing involves at least three kinds of polycomb repressive complexes (PRC), including PRC1, PRC2 and PhoRC complexes (Table 1-1) (Schwartz and Pirrotta 2007).

PRC1 complex

The core of *Drosophila* PRC1 contains Polycomb (Pc), Polyhomeotic (Ph), Posterior Sex Combs (Psc), and dRING (also known as Sex Combs Extra [Sce]). The PRC1 complex contains multiple chromatin modifying activitie, and is believed to be the maintenance unit directly responsible for actual repression of gene expression through the combination of two mechanisms- chromatin compaction or direct interaction with general transcription machinery (Shao et al. 1999; King et al. 2002; Francis et al. 2004; Lavigne et al. 2004; Levine et al. 2004; Wang et al. 2004a). For instance, the PRC1 and hPRC-H complexes interact with chromatin and block the chromatin remodeling process by the SWI/SNF complex (Shao et al. 1999; Francis et al. 2001), as well as the transcription by RNA polymerase II (King et al. 2002; Dellino et al. 2004). TATA-box-binding protein (TBP)-associated factors (TAFIIs) were also found as one of the components of PRC1 (Breiling et al. 2001; Saurin et al. 2001).

Pc protein contains an N-terminal chromodomain and a Pc box at the C-terminal domain. The chromodomain is responsible for the binding of Pc to H3K27me3 (Fischle

et al. 2003; Min et al. 2003), whereas the small Pc box is necessary for the transcriptional repression function of Pc protein, and is required for its interaction with dRING. Mammalian PRC1 component RING1B contains the E3 ubiquitin ligase activity, and this enzymatic activity is stimulated by two other components BMI1 and RING1A (Cao et al. 2005). Similarly, dRING in *Drosophila* PRC1 complex also has the ubiquitin ligase activity (Wang et al. 2004a). Psc, another component of *Drosophila* PRC1, is responsible for the inhibition of nucleosome remodeling *in vitro* (King et al. 2005). Psc is also a co-factor for dRING, and is essential for its H2A ubiquitination function. Finally, it is proposed that Ph protein might be necessary for the spreading of PcG complexes (Kim et al. 2002).

PRC2 complex

In PRC2 complex, the SET domain-containing subunit E(z) is the only catalytically active component, which is responsible for trimethylation of H3K27 (Cao et al. 2002; Czermin et al. 2002; Muller et al. 2002; Cao and Zhang 2004a), and may also trimethylate H3K9 *in vitro* (Czermin et al. 2002). H3K27 trimethylation recruits PRC1 through the chromodomain of PC protein, and consequentially repress gene expression by condensing the chromatin structure and inhibiting transcriptional processes. The histone methyltransferase (HMTase) activity requires a minimum of three components- E(z), Esc and Su(z)12 (Cao and Zhang 2004b; Nekrasov et al. 2005). In vitro studies showed that the Su(z)12 and Nurf-55 form the minimal nucleosome-binding module of PRC2, but this is not sufficient for HMTase activity (Nekrasov et al. 2005). It is shown that Esc is crucial for the HMTase activity of E(z), and also required for the nucleosome-binding of PRC2 (Ketel et al. 2005; Nekrasov et al. 2005). Studies of mammalian PRC2

showed that SUZ12 is also essential for HMTase activity and the silencing function of the mammalian PRC2 complex (Cao and Zhang 2004b; Pasini et al. 2004).

Recently the Polycomb-like (Pcl) protein has been discovered in a variant of the PRC2 complex in flies, which was only found on polytene chromosomes (Tie et al. 2003; Papp and Muller 2006). This Pcl-PRC2 has a very similar HMTase activity as the PRC2 complex containing the core subunit –E(z), Esc and Su(z)12, but it seems that their functions are not completely redundant (Tie et al. 2003; Nekrasov et al. 2007). Pcl mutants did not show significant changes in the genome-wide H3K27 mono- and dimethylation, but the high level of H3K27me3 at PcG target genes demonstrated a great reduction in the mutants (Nekrasov et al. 2007).

PhoRC complex

A novel PcG protein complex called PhoRC was discovered and characterized with recent biochemical purification of the Pho protein complex. Pho and Pho-like (Phol) are sequence-specific DNA binding proteins (Brown et al. 1998; Fritsch et al. 1999; Busturia et al. 2001; Mishra et al. 2001; Brown et al. 2003; Klymenko et al. 2006). dSfmbt is another component of PhoRC, which contains the MBT (malignant brain tumour) repeats responsible for the interaction with mono- or dimethylated H3K9 or H4K20 (Klymenko et al. 2006). Specifically, in the *in vitro* GST pull-down assays conducted by Wang *et al.* (Wang et al. 2004b) showed that Pho directly interacts with E(z) and Esc, while Phol directly interacts with Esc but not E(z). PhoRC-dependent E(z) recruitment and H3K27me3 deposit are required for Pc binding to the *Ubx* PRE. Also the study using DNA mobility shift assays showed that Pho and a PRC1 core complex bind synergistically to the *bxd* PRE (Mohd-Sarip et al. 2005). Moreover, it has been suggested that the spacer region of Pho is implicated in interactions with Pc and Ph in

both *in vitro* binding assays (Mohd-Sarip et al. 2002) and tethering assays (Klymenko et al. 2006). It is worth noting that in *phol;pho* double mutant imaginal discs, derepression of *Ubx* was observed accompanying with disrupted distribution of PRC1 and/or PRC2 components. However, mutation of Pho and Phol did not show significant affect on the binding of PRC1 and PRC2 on polytene chromosomes (Brown et al. 2003), suggesting that the Pho/Phol-dependent PcG recruitment is absent in nonmitotic tissues.

Targeting of PcG Repression

It is always an enigma in the study of PcG mechanisms how the PcG complexes are recruited to their target genes. In *Drosophila*, it has been known for a long time that Polycomb Response Elements (PREs), the specific regulatory region of several hundred base pairs, serve as docking platforms for PcG proteins and confer PcG-dependent repression on their associated reporter genes. Cytological studies during the 90s suggested that there may be more than a hundred PREs in the *Drosophila* genome, and some of them had been verified experimentally (Ringrose and Paro 2007; Schwartz and Pirrotta 2008). However, their DNA sequences did not show clear homology, so it is very difficult reveal a PRE consensus sequence only by sequence homology.

Some sequence-specific DNA binding proteins were found at the PREs, including Pleiohomeotic (Pho), Pleiohomeotic-like (Phol), GAGA factor (GAF; also known as Trithorax-like [Trl]), Pipsqueak (Psq), Zeste, Grainyhead (Grh; also known as neuronal transcription factor 1 [NTF-1]), dorsal switch protein1 (Dsp1) and Sp1/KLF family members (Muller and Kassis 2006). These proteins have been proposed to recruit PcG complexes to PREs, and Ringrose *et al.* (Ringrose et al. 2003) developed an algorithm based on the clustered pairs of these transcription factors binding sites and predicted 167 PREs in the *Drosophila* genome. However, three *Drosophila* genome-wide ChIP-

on-chip analyses (Negre et al. 2006; Schwartz et al. 2006; Tolhuis et al. 2006) found only limited overlap between the identified PcG protein binding sites and the predicted PREs described in the Ringrose *et al.* study. Actually mutations of many of these DNA binding proteins do not show any of the classic PcG phenotypes, and the number and distribution of their binding sites is quite variable. In addition, none of them can be found at all identified PcG sites. It is possible that the recruitment of PcG complexes to the PREs is independent of some individual “recruiters”, or the most essential “recruiters” have yet to be discovered. Alternatively, PcG complexes can be recruited to their target genes by different sets of combination of the DNA binding proteins in a tissue-specific or developmental stage-specific manner.

Recruitment of PcG Complexes

Wang *et al.* (Wang et al. 2004b) described a hierarchical recruitment pathway of PcG complexes at the *Ubx* PRE in the *bxd* region in both *Drosophila* SL2 cells and larval wing imaginal discs. In this model, the only DNA-binding PcG protein, Pho, in the PhoRC complex binds to sites within PREs, and recruits the PRC2 complex through direct interaction with E(z) and/or Esc. The PRC2 subunit E(z) trimethylates H3K27 at the PREs, which contributes to the recruitment and/or stabilization of the PRC1 complex to these particular sites. After sequentially recruited to the PREs, the PcG complexes interact with the preinitiation complex at the remote promoter by looping out the chromatin region in between, and repress expression of the associated genes. However, this model was challenged by the findings of recent chromatin mapping experiments by ChIP and microarray techniques. These studies detected PcG proteins of both PRC1 and PRC2 complexes peaking sharply at known or putative PREs in *D. melanogaster*, whereas the Pc protein covers a broader domain than other PcG

proteins. On the other hand, the distribution of H3K27me3 at a silenced gene usually covers more than ten kilobases including the entire transcribed region and the upstream regulatory region (Kahn et al. 2006; Papp and Muller 2006; Schwartz et al. 2006). Inconsistent with Wang's model (Wang et al. 2004b), the distribution of Pc protein does not correlate with that of H3K27me3, and dropped down gradually from the PRE peak. Moreover, the PREs seem to have very low occupancy of methylated H3, which may be due to the depletion of nucleosomes at these regions (Kahn et al. 2006; Mohd-Sarip et al. 2006; Papp and Muller 2006; Schwartz et al. 2006). Based on this evidence, Schwartz and Pirrotta (Schwartz and Pirrotta 2007) proposed an alternative looping model in which DNA-binding proteins such as Pho and GAF bind to the nucleosome-free PRE and recruit PRC1 and PRC2 complexes. The PRE-bound complexes methylate flanking nucleosomes, and the methylation domain is extended by looping of the PRE-bound complexes to contact nuceosomes over a broad domain. The looping is facilitated by the interaction between the Pc chromodomain and methylated nucleosomes, and possibly other methyl-binding domains, such as PHD fingers, MBT repeats, Tudor and SET domains in other PcG proteins.

PcG Silencing and Biological Functions

Besides the best studied *Drosophila* Hox genes, there are many other PcG target genes. Recent genome-wide studies suggested that, PcG mechanisms are involved in processes of development and cell-fate decisions, cell cycle progression, and possibly programmed cell death in both mammals and *Drosophila* (Sanchez-Elsner et al. 2006; Struhl 1983; Riley et al. 1987; Kuziora and McGinnis 1988; Jones and Gelbart 1990; Moazed and O'Farrell 1992; Simon et al. 1992).

PcG proteins and development

PcG proteins were first discovered in *Drosophila melanogaster* as negative *trans*-regulators that are required to prevent inappropriate expression of homeotic (Hox) genes (Lewis 1978). In *Drosophila*, segmentation requires expression of the *engrailed* (*en*) gene in the posterior group of cells in each segment, while segmental identity is specified by the selective expression of the Bithorax and Antennapedia complexes, two clusters of genes known as Hox genes. In early embryogenesis, the homeotic genes are first turned on in the 3-hour-old embryo, and their characteristic domains of expression are shaped by maternal and transiently expressed zygotic proteins coded by pair-rule genes, gap genes, and segmentation genes (McGinnis and Krumlauf 1992). The majority of the early transcription factors disappear at mid-embryogenesis when gastrulation begins (Orlando et al. 1998), and the expression pattern of homeotic genes is spatially maintained by PcG and trithorax (trxG) proteins throughout development. The derepression of *engrailed* and Hox genes in the PcG mutants is only observed after the completion of the early tiers of regulation that establish and refine the pattern of these genes (Struhl 1983; Riley et al. 1987; Kuziora and McGinnis 1988; Jones and Gelbart 1990; Moazed and O'Farrell 1992; Simon et al. 1992), suggesting that the maintenance of patterned expression involves a molecular mechanism distinct from those that guide pattern establishment. As a consequence of this cellular memory, if a homeotic gene was not previously active in the early embryos at a specific tissue or cell lineage, it remains repressed by PcG silencing over cell cycles. In contrast, a gene is activated at later stages only in the progeny of cells in which it was active in the early embryos. Genetic analysis has suggested that PcG proteins maintain the repressed gene state possibly through setting a repressive mark, such as H3K27me3. At the same

time, trxG proteins maintain the active state of those previously transcribed genes by depositing the active mark, such as H3K4me3 ans acetylated histones.

In addition to Hox genes, there is a growing list of PcG target genes that are important for cell-fate decision and development. The products of many of these genes are transcription factors, as well as secreted morphogens (*wingless*, *hedgehog*, *decpentaplegic*), and even some PcG protein themselves (*Psc*, *Ph*) (Schwartz and Pirrotta 2007). These genes are regulated in a tissue-specific or developmental stage-specific manner. In any given cell type, only those genes required for specifying the cell identity are active, while others remain silenced by PcG mechanisms.

Recently, several studies have noted that non-coding RNAs play a role in regulating PcG silencing, and might also involved in the switching or resetting epigenetic state. Schmitt et al. showed that (Schmitt et al. 2005) the establishment of PcG-mediated silencing was abolished by intergenic transcription through the *Fab-7* PRE. Although this model is supported by some other reports (Bender and Fitzgerald 2002; Hogga and Karch 2002; Rank et al. 2002), another study did not detect such non-coding transcription after resetting of the state mediated by a minimal *Fab7* PRE (Dejardin and Cavalli 2004). Interestingly, a recent paper reported that non-coding transcripts of a Trithorax Response Element (TRE) play an important role in epigenetic activation of gene expression by recruiting *Drosophila* ASH1 histone methyltransferase to the TRE of the *Ubx* gene (Sanchez-Elsner et al. 2006). Although the mechanisms of how these non-coding RNAs are regulated and recruited to the target genes still remain unknown, more investigation in this field will definitely broaden our understanding in epigenetic maintenance and switching.

PcG proteins and the cell cycle

It has long been noticed that *Drosophila* PcG mutations can cause cell cycle defects. For example, $E(z)^{1}$ alleles display a small-disc phenotype with no discernible mitotic figures (Phillips and Shearn 1990). However, it remains unclear how PcG complexes control cell cycle progression. Martinez et al. (Martinez et al. 2006) found that depletion of PcG protein PC by RNAi alters the cell cycle in proliferating S2 cells, then they identified a PRE as the target region for PC and PH within the promoter, the first exon and the first intron of the *CysA* gene. This PRE sequence can cause PcG-dependent variegation of the min-*white* reporter gene in transgenic files, as this phenotype is reversed in a PcG mutant background. Remarkably, in homozygous $Pc^{-/-}$ embryos, endogenous *CycA* expression is upregulated, while downregulation of *CycA* was observed when *Pc* and *Ph* are overexpressed in dividing embryonic cells. They thus proposed that PcG complexes can act as direct transcriptional repressors of cell cycle genes. It has been known that CycA level is crucial for controlling mitosis as the only essential mitotic cyclin in *Drosophila* (Jacobs et al. 1998). CycA inhibits the Fizzy related protein (Fzr), which is a single inhibitor of mitosis (Dienemann and Sprenger 2004). Another study found that PcG complexes inhibit the accumulation of mitotic CycA and affect the G2/M transition (Martinez et al. 2006).

In addition to directly regulating cell cycle genes, PcG complexes might regulate the cell cycle by modulating general chromatin condensation. For instance, chromatin perturbations could result in genome instability and mitotic defects. Lupo et al. (Lupo et al. 2001) showed that *Drosophila* Topoisomerase II and Barren proteins, which are required for proper mitotic condensation, interact in vivo with PcG target sequences in the bithorax complex. Similarly, another study reported that a *Drosophila* centrosomal

and chromosomal factor Ccf, also required for condensation in mitosis, shares the same binding sites on polytene chromosomes with Psc protein (Kodjabachian et al. 1998). Finally, mutations in *Ph*, *Pc* and *Psc* demonstrated segregation defects with the formation of anaphase bridges during syncytial embryonic mitoses (O'Dor et al. 2006). All of this evidence suggests an important function of PcG proteins in mitosis.

Insulators

The eukaryotic genome is organized in the way that discrete functional domains lie next to one another. Insulator/boundary elements are regulatory DNA sequences that create the boundaries between these domains and prevent promiscuous gene regulation. There are two biochemical activities associated with insulators/boundaries: one is enhancer-blocking activity which prevents enhancer-promoter communication when positioned in between them; the other is chromatin barrier activity, which blocks the silencing effect mediated by heterochromatin (Gaszner and Felsenfeld 2006). Several functional assays were developed to evaluate these two activities. The enhancer-blocking function was demonstrated by the ability of the potential insulator to prevent an enhancer from activating a reporter gene on the other side (Kellum and Schedl 1992). The reporter assays for testing barrier activity were based on the postulate that the candidate barrier sequences should protect a reporter gene against position effects due to the local chromatin environment (Kellum and Schedl 1991), or preventing the silencing effect initiated by some silencing elements such as Polycomb Response Elements (PREs) in *Drosophila* or *HM* silencers in yeast (Sigrist and Pirrotta 1997; Bi and Broach 1999; Donze et al. 1999).

Although the molecular mechanism of insulator/boundary elements is not as clear as other well-studied regulatory elements such as promoters and enhancers, some

models for insulator action have been proposed in the light of recent investigations on yeast, *Drosophila* and chicken. There are three models for how enhancer-blocking insulators disrupt the interaction between enhancers and promoters, namely the promoter decoy model, the physical barrier model, and the loop domain model (Bushey et al. 2008; Raab and Kamakaka 2010). Each of these models has its own supporting evidence and may not be exclusive. Meanwhile, the working models for chromatin barrier function are mainly derived from the studies on yeast and chicken cells. The observations in several yeast boundary elements prompted the proposition of the nucleosome gap model (Bi and Broach 2001). In this model, recruitment of specific transcription factors, such as Rap1 and Reb1, at a barrier precludes nucleosome assembly and creates a gap in a regular nucleosome array (Bi and Broach 1999; Donze et al. 1999; Fourel et al. 1999). This nucleosome-free gap prevents the spread of heterochromatin mediated by Sir2/Sir3/Sir4 complexes which may otherwise propagate along the chromatin fiber to the neighboring regions (Bi and Broach 1999). Another barrier model was inspired by the molecular details of the 5' HS4 insulator at the chicken β-globin locus, one of the best-studied insulators in vertebrates. A series of elaborate analyses in this insulator indicated that its enhancer-blocking and barrier activities are separable and carried out by distinct DNA elements (Bell et al. 1999; Recillas-Targa et al. 2002; West et al. 2004; Gaszner and Felsenfeld 2006). Deletion of the CTCF binding site (footprint II or FII), which is responsible for the enhancer-blocking activity, did not affect the barrier activity mediated by the other four footprints (Recillas-Targa et al. 2002). The DNA sequences required for the barrier activity can be further dissected into two functional units. FIV interacts with upstream stimulatory factor 1

(USF1) which recruits specific chromatin-modifying enzymes that catalyze the histone modifications favoring euchromatin, including histone acetylations, H3K4 and H4R3 methylations (West et al. 2004; Huang et al. 2007). This results in a local chromatin environment that is unfavorable to the propagation of heterochromatin. Whereas another three footprints FI, FIII and FV restrict the spread of DNA methylation through the recruitment of vascular endothelial zinc finger 1 (VEZF1) (Dickson et al. 2010).

Although the enhancer-blocking and barrier activities are separable in chicken cells, it is not clear whether this is common in other organisms. There are at least five types of insulators reported in *Drosophila* defined by their associated proteins, including Suppressor of Hairy Wing [Su(Hw)] in *gypsy* insulator, Zeste-white 5 (Zw5) in *scs* element, Boundary Element Associated Factors (BEAF32) in *scs'* element, *Drosophila* CTCF (dCTCF) in Fab-8 insulator, and GAGA binding Factor (GAF) in multiple insulators (Maeda and Karch 2007; Gurudatta and Corces 2009). The reporter-based assays revealed that most if not all of the known *Drosophila* insulators exhibit both enhancer-blocking and barrier activities (Kellum and Schedl 1991; Roseman et al. 1993; Sigrist and Pirrotta 1997; Barges et al. 2000; Majumder et al. 2009). However, there is a good possibility that separable elements responsible for either activity resides within the *Drosophila* insulators. One evidence comes from the observation that evolutionarily conserved E(y)2/Sus1 protein is required for the barrier activity of the Wari insulator as well as Su(Hw)-dependent insulators in vivo (Kurshakova et al. 2007; Erokhin et al. 2010). It is likely that different domains of Su(Hw) interact with different protein complexes that are responsible for either enhancer-blocking or barrier activities. In addition, a recent study on the *Drosophila* SF1 insulator showed that the chromosomal

position effect (CPE)-blocking activity was independent of GAF-binding sites that are essential for the embryonic insulator activity (Majumder et al. 2009). Therefore the SF1 may contain multiple non-overlapping regions responsible for diverse functions, though the *cis*-elements accounting for the CPE-blocking activity and the related *trans*-factors have yet to be determined.

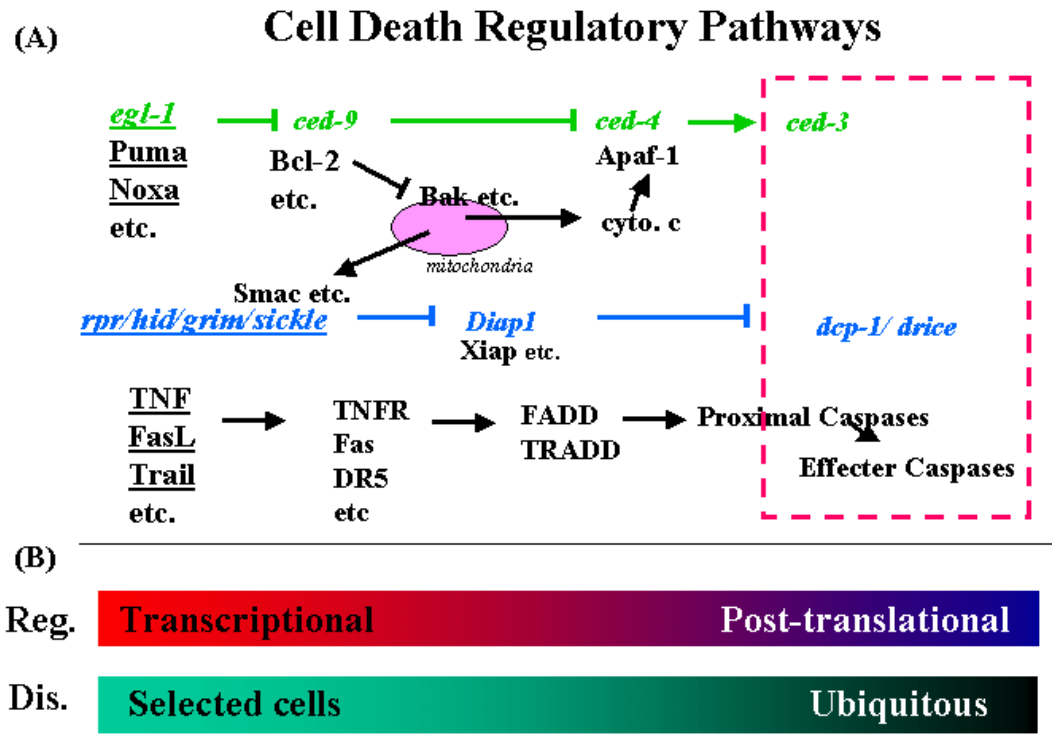

Figure 1-1. Cell death regulatory pathways in different organisms. A) Simplified schematic presentation of the three major apoptosis pathways, which, when activated, all lead to the activation of caspases (in dashed square). Colors distinguish the organism to which the gene/protein belongs (eg. *C elegans*, *Drosophila* and Mammals). Upstream pro-apoptotic genes that are subject to transcriptional regulation were underlined. B) Summarization of the observation of that many downstream players in the apoptotic pathways tends to be ubiquitously distributed (Dis.) and their activities are mostly regulated (Reg.) by post-translational mechanism such as cleavage of pro-caspases. In contrast, most up-stream regulators tend to be transcriptionally regulated and are only expressed in selected cells.

Table 1-1. Components of PcG complexes

PcG protein paralogs			Protein domains	Functions
Drosophila melanogaster	Human	Mouse		
PRC1 maintenance complex				
Pc*	CBX2/HPC1 CBX4/HPC2 CBX8/HPC3	CBX2/M33 CBX4/MPC2 CBX8/PC3	Chromodomain	Preferentially binds to H3K27me3 SUMO E3 ligase
Ph*	EDR1/HPH1 EDR2/HPH2 EDR3/HPH3	EDR1/MPH1/Rae28 EDR2/MPH2 EDR3/MPH3	Zinc-finger SPM domain	Stoichiometric components of PRC1 and required for silencing
Psc*	BMI1/PCGF4 MEL-18/RNF110/ZFP144 MBLR/RNF134/PCGF6	BMI1/PCGF4 MEL-18/RNF110/ZFP144 MBLR/RNF134/PCGF6	RING-finger domain	Co-factor for dRING, essential for its H2A ubiquitination function
dRING*	RING1/RNF1/RING1A RNF2/RING2/RING1B	RING1/RNF1/RING1A RNF2/RING1B	RING-finger domain	E3 Ubiquitin ligase for H2AK119
Scm	SCMH1 SCMH2	SCMH1	Zinc-finger SPM domain	?
PRC2 initiation complex				
E(z)*	EZH1 EZH2	EZH1/ENX2 EZH2/ENX1	SET domain	Methylation of H3K9, H3K27
Su(z)12*	SUZ12	SUZ12	Zinc-finger	Co-factor for E(z)
Esc*	EED	EED	WD40 repeats	Co-factor for E(z)
Escl	EED	EED	WD40 repeats	Co-factor for E(z)
Nurf-55	RbAp46/48		WD repeat	Binds to histone, involved in nucleosome remodeling
Pcl	PHF1	PHF1/PCL1	PHD, Tudor	Interacts with E(z) via PHD domain, required for high levels of H3K27me3 specifically at PcG target genes
PhoRC sequence specific DNA binding complex				
Pho*	YY1	YY1	Zinc-finger	Sequence-specific DNA binding
Phol	YY2	YY2	Zinc-finger	Sequence-specific DNA binding
dSfmbt*	L3MBTL2/SFMBT1	L3MBTL2	Zinc-finger MBT repeat, SAM	Binds to mono- and dimethylated H3K9 and H4K20

Owing to the tremendous diversity of PcG homologues in vertebrates, this table is not exhaustive. *These proteins are the core components of each PcG complex they belong to. Nurf-55: *nu*cleosome-*r*emodeling *f*actor 55. Sfmbt: Scm-related gene containing four mbt domains. MBT: malignant brain tumor. SAM: sterile α motif.

CHAPTER 2
EPIGENETIC BLOCKING OF AN ENHANCER REGION CONTROLS IRRADIATION-INDUCED PRO-APOPTOTIC GENE EXPRESSION IN DROSOPHILA EMBRYOS

Abstract

Drosophila embryos are highly sensitive to γ-ray induced apoptosis at early but not later, more differentiated stages during development. Two pro-apoptotic genes, *reaper* and *hid*, are up-regulated rapidly following irradiation. However, in post-stage 12 embryos, in which most cells have begun differentiation, neither pro-apoptotic gene can be induced by high doses of irradiation. Our study indicates that the sensitive-to-resistant transition is due to epigenetic blocking of the Irradiation Responsive Enhancer Region (IRER), which is located upstream of *reaper* but is also required for the induction of *hid* in response to irradiation. This IRER, but not the transcribed regions of *reaper*/*hid*, becomes enriched for trimethylated H3K27/H3K9 and forms a heterochromatin-like structure during the sensitive-to-resistant transition. The functions of histone modifying enzymes Hdac1(rpd3), Su(var)3-9, and PcG proteins Su(z)12 and Polycomb are required for this process. Thus, direct epigenetic regulation of two pro-apoptotic genes controls cellular sensitivity to cytotoxic stimuli.

Introduction

Although caspase activation and apoptosis can proceed without *de novo* protein synthesis under certain special circumstances, abundant evidences suggest that transcriptional and translational mechanisms play crucial roles in regulating apoptosis induced by cytotoxic stimuli. The genetic requirement of transcription factors such as P53 in irradiation-induced cell death underscores the importance of the transcriptional response. Several pro-apoptotic genes, including *puma* (*p53 upregulated modulator of apoptosis*), are the direct transcriptional targets of P53. In *puma* knockout mice,

irradiation-induced cell death in hematopoietic cells and the developing nervous system is almost completely blocked (Jeffers et al. 2003). Although much has been revealed about the molecular mechanism of P53-mediated pro-apoptotic gene expression and apoptosis, we understand very little as to why different tissue/cell types can have dramatically different sensitivity to irradiation.

In *Drosophila*, the Inhibitor of Apoptosis Protein (IAP) -antagonists play a pivotal role in regulating programmed cell death during development. Upon its initial identification, the IAP-antagonist *reaper* was found to be transcriptionally activated upon irradiation (White et al. 1994). The H99 genomic region, which also includes two other IAP-antagonists *hid* and *grim*, is required for mediating irradiation-induced cell death in *Drosophila*. A reporter construct containing the immediate 11kb sequence upstream of the *reaper* transcribed region gives a much broader expression pattern in transgenic animals than that of the endogenous *reaper* mRNA (Nordstrom et al. 1996), suggesting that key inhibitory *cis*-regulatory function is not present in the reporter construct. This 11kb reporter construct is responsive to ionizing irradiation and contains at least one putative P53 response element (P53RE) that conforms to the patterns of mammalian P53 binding sites (Brodsky et al. 2000). Correspondingly, genetic analysis indicated that the function of *Drosophila* P53 (DmP53) is required for mediating ionizing irradiation induced *reaper* expression and apoptosis (Lee et al. 2003; Sogame et al. 2003; Brodsky et al. 2004). However, several questions remain to be addressed. First, the sensitivity to irradiation-induced cell death is tissue/cell type-specific and restricted to certain developmental stages. The difference in sensitivity has no direct correlation with the availability of DmP53. Rather, the windows of sensitivity seem correlated with

developmental marks such as high proliferation. Second, over-expression of DmP53 failed to induce *reaper* expression or apoptosis in many tissues, indicating that DmP53 alone is not sufficient in inducing *reaper* expression, or (and) the P53RE is not always accessible.

It has been observed that during development, the sensitivity to irradiation-induced cell death can change rapidly even for the same cell linage. For instance, while the proliferating neural precursor cells in the mammalian hippocampus are extremely sensitive to ionizing irradiation, differentiating or differentiated neurons in the same region are resistant (Peissner et al. 1999; Mizumatsu et al. 2003). A similar switch of sensitivity to irradiation was observed during *Drosophila* embryogenesis. While both *reaper* and *hid* are induced to mediate cell death in young embryos with mostly proliferating cells, neither can be induced in embryos developed a few hours further when most cells are differentiating or differentiated. This system offered us a valuable model to explore the molecular mechanisms underlying the sensitive-to-resistant transition accompanying cellular differentiation. In this study, we found that the IRER upstream of the *reaper* locus, including the putative P53RE, is subject to epigenetic regulation during development. Histone modification and chromatin condensation specific to the IRER, but not the promoter region, are capable of switching off the sensitivity to irradiation-induced pro-apoptotic gene expression and cell death. To our knowledge, this is the first evidence that direct epigenetic regulation of pro-apoptotic gene(s) controls cellular sensitivity to cytotoxic stimuli.

Materials and Methods

Fly Strains and Genetic Crosses

Canton S and yw *Drosophila* strains were used as wild type in this study. The Exelixis insertion strains were obtained from Dr. Artavanis-Tsakonas's group at Harvard Medical School. The Hdac mutant alleles 303, 313, 326, 328, def 8, and def24 were kindly provided to us by Drs. Mottus and Grigliatti (Mottus et al. 2000). The Su(z)12 alleles were provided to us by Dr. Jurg Muller (Birve et al. 2001). The E(z) alleles were obtained from Dr. Rick Jones. Other mutant strains were obtained from the Bloomington Stock Center. Genetic crosses for generating defined deletions using the Exelixis insertional strains and tool kit were performed strictly as described (Thibault et al. 2004).

Embryo Staging and Irradiation

Wild type as well as mutant embryos were collected for a defined period on standard juice/agar plates and aged to the desired developmental stages. Collections of embryos were randomly sorted into treatment and control groups. The control group was sham treated while the treatment group was subjected to γ-ray irradiation applied using a Model M Gammator (Radiation Machinery Corporation, NJ). For microarray and *in situ* hybridization RNA analysis, embryos were incubated at room temperature (RT) for 15-30 min after irradiation. For quantitative PCR experiments, embryos were incubated for the indicated time length following irradiation. After incubation, embryos were dechorionated using 50% bleach, rinsed three times with ddH_2O, and snap frozen with the dry ice/ethanol bath. Samples were stored at –80°C prior to RNA extraction.

Gene Expression Analysis

Total RNA and mRNA were extracted with RNeasy Mini Kits (QIAGEN, CA) or Poly(A) Pure (Ambion, TX), respectively.

Real time PCR. Total RNA samples were treated with DNase I to remove genomic DNA. cDNA were prepared by reverse transcription of total RNA with High-Capacity cDNA Archive Kit (Applied Biosystems). Quantitative real-time PCR (QPCR) followed protocols provided by the manufacturer. The real-time PCR step used 100ng total cDNA/PCR well with triplicates per gene per sample. For primer sequences and detailed procedures please refer to the supplementary information.

Microarray Data Analysis

Identifying γ-ray –responsive genes: Gene expression levels in γ-ray treated and control samples were first compared using Affymetrix Analysis Suite 5.0 by setting the untreated sample as “Baseline”. A “Change p-value” was obtained for each probe-set through this analysis. To minimize the non-systematic error caused by random fluctuation, the “Signal log ratio” [Log2(Exp./Control)] outputs of repeated measurements were analyzed by “one-class” Significance Analysis of Microarrays (SAM) (Tusher et al. 2001). Genes (Probe-sets) ranked at the top 50 based on the “relative difference” value by the SAM analysis (Tusher et al. 2001), and whose “Change p-value” was less than 0.001 in at least one array measurement, were selected as potential γ-ray responsive genes.

Comparison and visualization of array data: For further analysis and visualization of array data, outputs from the Affymetrix Analysis Suite were loaded into the GeneSpring (Silicon Genetics) array analysis package. Genomic sequence and coordinates for each gene were extracted from datasets obtained from the Berkeley Drosophila Genome Project (http://www.fruitfly.org/). Gene lists for functional groups,

such as apoptosis genes, were compiled based on functional annotations from Flybase (http://www.flybase.org/) using the "ListG" program.

Functional annotation of gene lists. Initial analysis of DNA array data as outlined above resulted in extensive gene (probe-set) lists. To facilitate functional analysis, we annotated the lists using a Python-based "ListPro" program (See supplementary data ST1).

Statistical Analysis

We performed comparisons on the proportions of detectable genes to be cell death regulatory genes using the Chi-square test for paired samples. A 95% confidence interval was calculated for the proportion difference, e.g.,

$(p_s - p_r) \pm [1.96SE(p_s - p_r) + \frac{1}{2n}]$, where p_s and p_r are detectable proportions at the sensitive and resistant stages respectively and *n* equals 39. In addition, exact p-value was evaluated for the statistical significance of observing two cell death related genes among 11 induced genes at the sensitive stage based on hyper-geometric probability distributions.

DNase I Sensitivity Assay

Using the Apollo Genome Annotation and Curation Tool**,** sequences and annotations were inputted covering the 75C1-2 locus (18,060k-18,460k) from the *Drosophila melanogaster* Genome Annotation 4.0 (http://www.fruitfly.org/). For each selected 1,000 bp interval the sequence was used as input to Primer3 for designing/selecting a set of primers that are 150-400 bp apart. The specificity of the primer set for quantitative PCR was first verified by dissociation curve as well as checking on agarose gel after electrophoresis. Only primer sets that consistently

amplified one fragment of the predicated size were used for downstream experiments. The amplified fragments were also sequenced to further verify the accuracy of the selected primer sets. For the simplification of our discussion, the primer sets are referred to using the middle three digits. For instance, primer set designed for 18,363,000-18,363,999 is referred to as primer set “363” throughout this paper.

DNase I sensitivity assay was performed based on modification of published methods (Carr and Biggin 2000; Kalmykova et al. 2005). About 50-150ul of staged embryos were washed with distilled water, dechorionated with 3% sodium hypochloride, and washed again to remove traces of bleach. The embryos were then transferred to 10 ml cold Buffer A (15 mM Tris pH 7.4, 60 mM KCl, 15 mM NaCl, 1 mM EDTA, 1 mM EGTA) supplemented with 1% protease inhibitor cocktails (PIC, Sigma, P8340) and homogenized on ice with a 15ml Wheaton Dounce Tissue Grinder using the “Loose” pestle. The homogenate was then centrifuged at 400g for 1 min to remove tissue chunks. The supernatant was transferred to a new tube and centrifuged at 1,100g for 10 min to pellet the cells. The cell pellet was then resuspended with Buffer B (10mM Tris, PH 7.5, 5mM $MgCl_2$, 10mM NaCl, 25% Glycerol) supplemented with 1% protease inhibitor cocktail (PIC) (2 times the starting volume of embryos). The resuspended cells were aliquoted, snap frozen with dry ice/ethanol bath and kept at –80^{O}C. For DNase I treatment, about 100 ul samples were thawed briefly on ice and resuspend with 1,000ul cold Buffer A supplemented with PIC. NP-40 were added to final concentration of 0.1% and incubated on ice for 5 min. The permeablized cells were pelleted by centrifuge at 1,500g for 8 min at 4 ^{O}C. The cell pellet was then resuspended in 1x DNase I buffer (New England Biolab), and aliquoted (200ul) to three tubes each treated with 0U

(control), 5U, and 50U per ml DNase I (New England Biolab), respectively. After 5 min the treatment was stopped by adding EDTA to 25 mM. Cells were then lysed with 45ul 6xSDS lysis buffer (6% SDS, 300 mM Tris-HCl, pH 8.0, and 120 mM EDTA) and incubated overnight with 0.5mg/ml protease K. Geomic DNA was then purified with phenol and phenol/chloroform extraction and resuspended in 10 mM Tris (PH 8.0) and diluted to 5ng or 10ng per ul.

Two to three 1ul samples of the treated or control DNA were then analyzed with QPCR. The primer sets for each 1,000bp region of the IRER were designed with the help of Apollo and Primer 3 (Rozen and Skaletsky 2000; Lewis et al. 2002) and verified by dissociation curves, gel electrophoresis, and DNA sequencing. Ct values for each locus were obtained with an ABI 7500Fast Real-Time PCR System using manufacturer-recommended protocol and PCR labeling kits.

Chromatin Immuno-precipitation (ChIP) Assay

ChIP analysis of staged embryos were performed essentially using a protocol provided to us by Ian Birch-Machin and Shan Gao (Birch-Machin et al. 2005). Dechorionated embryos (200-500ul) were fixed for 15 min in 3.7% formaldehyde in the presence of n-haptane. After fixation, embryos were homogenized with a Wheaton Dounce Tissue Grinder (pestle Loose) in cold PBT (0.1% triton in PBS) supplemented with PIC. Tissue chunks were removed by centrifugation for 1 minute at 400g, after which cells were pelleted by centrifugation for 10 min at 1,100g. The cell pellet was then resuspended in 15ml ice-cold Cell Lysis Buffer (5mM PIPES pH 8, 85mM KCL, 0.5% NP40, 1% PIC), and dounced (10X) using a Wheaton 15ml Dounce Tissue Grinder with the “Tight” pestle. The homogenate was centrifuged at 2000g for 4min at 4^{o}C to pellet the nuclei, which was resuspended in Nuclear Lysis Buffer (50mM Tris.HCl pH 8.1,

10mM EDTA.Na_2, 1% SDS, 1% PIC) and incubated for 20 min at 4^{o}C. At the end of the incubation, 0.3g of acid washed glass beads (Sigma, G-1277) were added, and the samples were sonicated on ice using a Branson Sonifer 450 to obtain fragmented DNA with an average size of approximately 500bp. For immunoprecipitation, the sheared fixed chromatin samples (~5mg DNA) were diluted (1:5) with IP buffer (1% Triton X-100, 2 mM EDTA, 20 mM Tris–HCl, pH 8.0, 150 mM NaCl, 1% PIC) and incubated for 1 hr at 4^{o}C with 50 ul of equilibrated Protein A beads (Protein A– Sepharose CL-4B; Amersham Biosciences). After removing the Protein A beads, the samples were aliquoted and each equal volume aliquot was incubated with appropriate antibody or served as input control. After overnight incubation, the complex was precipitated by adding Protein A beads. The pelleted beads were resuspended with 500ul TSE I buffer (1% Triton X-100, 0.1% SDS, 2 mM EDTA, 200 mM Tris–HCl, pH 8.0 and 150 mM NaCl) and transferred to the basket of a Spin-X column. Using the column, the beads were washed again with 500 ul TSE I buffer and twice with 500ul TSE II buffer (1% Triton X-100, 0.1% SDS, 2 mM EDTA, 200 mM Tris–HCl, pH 8.0 and 500mM NaCl). Then the beads were washed twice with Wash Buffer III (0.25M LiCl, 1% NP-40, 1% sodium deoxycholate, 1 mM EDTA and 10 mM Tris–HCl, pH 8.0) and twice with TE. The DNA samples were eluted with freshly prepared elution buffer (1% SDS and 0.1 M $NaHCO_3$) and incubated for 6 h at 65°C to reverse formaldehyde cross-links. DNA was then purified using the Qiagene PCR purification kit. Two to three 1ul samples of each elute (including the parallel processed input control sample) were subjected to QPCR quantification.

Histology

The Procedures for TUNEL, *in situ* hybridization (ISH), and immunocytochemistry (ICC) were performed as described (Zhou and Steller 2003). For distinguishing homozygous mutant embryos, embryos collected from Df(3L18,365-399)/TM3Ubi-GFP were first subjected to ICC with anti-GFP (Santa Cruz, 1:2000) and then subjected to ISH or TUNEL procedures.

Results

Sensitivity to γ-Ray Induced Apoptosis Is Developmental-Stage Dependent

During the 20 hrs of embryogenesis, the sensitivity of fly embryos to irradiation changes dramatically between 7-9 hr after egg laying (AEL). When measured by embryonic lethality, embryos before 7 hr AEL (developmental stage 1-11) (Campos-Ortega and Hartenstein 1985) are extremely sensitive to γ-irradiation (Figure 2-1A), while embryos after 9hr AEL (developmental stage 12) become highly resistant. This dramatic change of sensitivity to irradiation was first noticed decades ago (Wurgler and Ullrich 1976; Ashburner 1989), but the underlying cellular and molecular mechanisms remain unclear.

This shift of sensitivity to irradiation at the organismic level coincides with changes of sensitivity at the cellular level. Irradiation-induced cell death, as measured by TUNEL, appears about 45-60 mins post irradiation and reaches the peak at about 75-90 mins. The most dramatic induction of TUNEL-positive cells following γ-ray was observed in stage 10-11 embryos (Figure 2-1 C vs. B). In sharp contrast, there is little increase of TUNEL-positive cells in germ band retracted embryos post developmental stage 12 (Figure 2-1 E vs. D). For the clarity of the discussion, we will refer to embryos before or

at stage 11 as sensitive (stage) embryos, and those after stage 12 as resistant (stage) embryos.

To gain a comprehensive picture of genomic responses to γ-ray irradiation, we used the Affymetrix DrosGenome1 GeneChips to measure the immediate transcriptional response elicited by γ-ray. For both sensitive and resistance stage embryos, total RNA was extracted 15 mins after irradiation from treated and parallel processed control samples. Among the 11 genes induced significantly in the sensitive stage, two are known cell death regulatory genes, *reaper* and *hid* (Figure 2-1G). The probability of observing two or more known pro-apoptotic genes in 11 randomly selected genes from the genome is calculated as 2×10^{-4}, indicating that cell death genes are selectively activated following γ-ray treatment in sensitive embryos. In contrast, none of the two genes, or any other pro-apoptotic gene, was significantly induced by γ-ray in resistant embryos (Table 2-1).

The specific induction of *reaper* and *hid* by γ-ray in sensitive but not resistant embryos was verified by both Northern hybridization (Figure 1H) and quantitative PCR (QPCR) (Figure 2-1I). The QPCR result indicates that, in sensitive embryos, both *reaper* and *hid* are induced rapidly (within 20 mins), and reach a peak at about 40-60 min after irradiation. In contrast, neither can be significantly induced in resistant stage embryos at any time points (up to 2 hrs). Interestingly, a similar responsive pattern was observed for another IAP-antagonist *sickle*, which is upstream of *reaper* (Figure 2-2A). The other IAP-antagonist, *grim*, showed no radiation induction in either sensitive or resistant stage.

Irradiation-induced cell death is largely blocked in the H99 deficiency mutant that lacks *reaper*, *hid, and grim* (White et al. 1994). The selective and rapid induction of *reaper* and *hid* post irradiation indicates that the two genes are responsible for mediating irradiation-induced cell death in sensitive stage embryos. Their coordinated induction is likely essential for the rapid induction of apoptosis, as has been demonstrated before (Zhou et al. 1997). The IAP-antagonists *sickle* is not deleted in the H99 mutant; however it is also induced upon ionizing irradiation (Christich et al. 2002; Brodsky et al. 2004). In this study, we focus on the immediate induction of *reaper* and *hid* in sensitive embryos and the sensitive-to-resistant transition of the responsiveness of these two genes.

Rapid Sensitive-to-Resistant Transition of Pro-Apoptotic Gene Responsiveness during Developmental Stage 12

To pinpoint the timing of the sensitive-to-resistant transition during development, pooled embryos (0-16 hr AEL) were treated with 20Gy γ-ray and then monitored for expression of pro-apoptotic genes at 20-30 mins following irradiation. The pooled embryos were collected overnight, irradiated on the same plate, fixed together, and processed for in situ hybridization in the same tube. Our data indicated that both *reaper* and *hid* can be induced by γ-ray in embryos developed beyond developmental stage 6, when the gastrulation begins. The responsiveness of the two pro-apoptotic genes peaks at stage 10 and remains responsive at developmental stage 11 (Figures 2-2 D vs. A; E vs. B; F vs. C). However, once the germ band starts to retract at early stage 12, the responsiveness begins to diminish rapidly (Figures 2-2 G-L). By the time most of the germ band has retracted to the ventral side (late stage 12), the responsiveness of both genes is totally lost (Figures 2-2 K vs. H; L vs. I; Figure 2-3). The contrast of *reaper* or

hid in situ hybridization (ISH) signals in sensitive versus resistant embryos following irradiation is most apparent when viewed under low magnification (Figure 2-3). Increasing the γ-ray dosage up to 120 Gy failed to induce any detectable increase of *reaper* and *hid* expression at 30 mins post irradiation (data not shown). The rapid sensitive-to-resistant transition was also verified independently with QPCR (Figure 2-2M). It is clear that compared to embryos at stage 9-11 (4-7 hr AEL), there is little induction of *reaper* or *hid* at stage 12 or 13.

The change of radiation responsiveness of pro-apoptotic genes is unlikely due to reduced amount of DNA damage or a suppressed cellular signaling response in resistant stage embryos. Two DNA repair genes, *ku70* and *ku80*, were also significantly induced by irradiation in sensitive stage embryos through a DmP53 dependent mechanism (Brodsky et al. 2004). However, in sharp contrast to the pro-apoptotic genes, not only did the two genes remain responsive to irradiation at resistant stage, but their induction levels were significantly higher in the resistant stage than in the sensitive stage (Figure 2-4). This suggests that the loss of responsiveness is specific to the pro-apoptotic genes.

Mapping the Genomic Region Responsible for Mediating γ-Ray Responsiveness

To map the genomic region responsible for mediating the γ-ray responsiveness of *reaper* and *hid*, we took advantage of the insertional mutants generated by Exelixis (Thibault et al. 2004). These insertion lines were generated in an isogenic background with transposon vectors containing the Su(Hw) insulator sequences. If the insertion is located between the promoter and the enhancer region mediating γ-ray responsiveness, it could interrupt the responsiveness of the pro-apoptotic genes. In addition, these

transposons have FRT sequences that can be used for making well-defined genomic deletions (Parks et al. 2004).

Both *reaper* and *hid* reside in the 75C1-2 region, together with the other two IAP-antagonists *grim* and *sickle*. The organization of the genomic region harboring the four genes is depicted in Figure 2-5A. Interestingly, all four pro-apoptotic genes are transcribed in the same direction. Remarkably long gene-less regions surround the *reaper* locus: from *grim* to *reaper* is approximately 93 kb and from *reaper* to *sickle* is about 40 kb. In contrast, left of *hid* and right of *sickle* are gene dense regions (more than five genes in 50-60 kb). When compared to homologous regions in *D.Pseudoobscura* (*D.pseu*) and *D.virilis* (*D.viri*), the intergenic genomic region is better conserved than the transcribed and coding region of *reaper* at the nucleotide level (Figure 2-5B). The two species diverged from *D.mela* 40 and 60 MY ago, respectively. The exceptional conservation of non-transcribed sequences around *reaper* suggests that vital regulatory functions may reside in these regions.

From the Exelixis collections, we obtained a total of 45 strains that were recorded as having a single insertion in the 75C1-2 region. Their insertion sites were verified by inverse PCR (Table 2-2). Analysis of these strains indicated that a 20kb region between 3L: 18,366,171 and 18,386,107 is required for the γ-ray responsiveness of *reaper*. Three insertions (R1, R2, and R3) between this region and the *reaper* promoter all blocked the γ-ray responsiveness of *reaper* (Figures 2-5 C-E). In contrast, the insertions (R4, R5, and R6) after this region did not block the γ-ray responsiveness (Figures 2-5 F and G). Significant γ-ray responsiveness of *reaper* transcription was clearly visible in homozygous R4 and R5 embryos, indicating that the essential γ-ray responsible region

for *reaper* transcriptional regulation is located between R3(18,366,171) and R4(18,386,107). However, there may be additional enhancer element(s) in the DNA region between R5(18,387,288) and R6(18,398,861), as the γ-ray responsiveness of *reaper* is conceivably stronger in homozygous R6 embryos than that in R5 and R4. In terms of *reaper* transcriptional response to irradiation, there is no detectable difference between R6 and wild type embryos, indicating all essential elements are on the left side of R6.

We then generated deletions that removed the interval 3L:18,365,736 - 18,398,898 between R2 and R6 (referred to as Df(3L:18,366-398)), the interval 3L:18,365,736-18,386,300 between R2 and R4 (Df(3L:18,366-386)), and the interval 3L: 18,386,300 - 18,398,898 between R4 and R6 (Df(3L:18,386-398)). For each deficiency, 5-10 independent deletion strains were obtained. The span of the deletion was verified by PCR using primers flanking the deletion, and the breaking point was verified by sequencing the PCR product. None of these deficiencies removed the transcribed region of *reaper* or *sickle*. The left breaking points for the deficiencies are more than 2 kb away from the *reaper* transcription starting site.

In embryos homozygous for either Df(3L:18,366-386) or Df(3L:18,366-398) (identified with a GFP balancer), the responsiveness of *reaper* to γ-ray irradiation was totally abolished (Figure 2-6 A-H), indicating that essential enhancer elements are located in the Df(3L:18,366-386) interval. Homozygous Df(3L:18,386-398) showed a significantly decreased level of *reaper* responsiveness (Figure 2-6 C and G), which reconfirms that the region between R4 and R6 has non-essential enhancer(s). These results are in perfect agreement with our insertion mapping data described above. The

insulators in the original insertions were removed during the deletion generation process so there is no Su(Hw) insulator in Df(3L:18,366-386) or Df(3L:18,366-398). There is one remaining insulator left in Df(3L:18,386-398), but that should not affect the conclusion of the results.

Thus both approaches unequivocally indicated that the enhancer region responsible for mediating *reaper* irradiation responsiveness resides in the interval between R2 and R6, i.e. 3L: 18,365,736 - 18,398,861. We named this region Irradiation Responsive Enhancer Region (IRER). The previously identified putative P53RE (18,368,516) is within this region and close to the left boundary. Since over-expression of P53 alone was not sufficient to induce *reaper* expression in the embryo, it is very likely that other enhancer element(s) in this region is(are) also required for mediating irradiation-induced *reaper* expression. In addition, our data indicate that there is(are) non-essential enhancer element(s) in the region between R5 and R6. To facilitate the discussion, we will refer to the region between R2 and R6 as IRER, and the deletion of this region as Df(IRER). Correspondingly, we will refer to the genomic region between R2 and R4 as IRER_left, and the region between R5 and R6 as IRER_right. For the responsiveness of *reaper*, IRER_left is essential, and IRER_right is supplemental.

An unexpected result from the deletion analysis is that the responsiveness of *hid* to γ-ray irradiation was also significantly reduced in the Df(IRER_left) mutant and abolished in the Df(IRER) mutant (Figure 2-6 I-P). This is surprising since the insulator-containing insertions (R1, R2, R3) did not have any effect on γ-ray induced *hid* expression (data not shown). It indicates that there may exist a high-order arrangement which enables the IRER to interact with the *hid* promoter. The essential region

mediating this interaction most likely resides in the interval between R4 and R6 (IRER_right). In homozygous Df(IRER_right), *hid* responsiveness is lost even though *reaper* is still responsive (albeit reduced). To rule out the possibility of unintended damage to the *hid* locus in the process of the FLP/FRT mediated deletion, we performed complementation tests between Df(IRER) and *hid* mutant alleles, including [05014], [A206], and [8d]. All of the *hid* mutant alleles are homozygous lethal and homozygous Df(IRER) has greatly reduced viability. Invariably, the lethality of the *hid* alleles was complemented by the Df(IRER) chromosome, indicting the developmental function of *hid* is intact in the Df(IRER) mutant. In addition, we tested *hid* responsiveness in the X38 deletion mutant, which removes the *reaper* transcription unit and all of the IRER region (Peterson et al. 2002). In both X38/X38 and Df(IRER)/X38, the responsiveness of *hid* is abolished, indicating that indeed *hid* responsiveness to irradiation is mediated by IRER.

Formation of DNaseI-Resistant Structure in the IRER But Not the Promoter and Transcribed Region of *reaper* in Post Stage 12 Embryos

Like its mammalian ortholog, *DmP53* is required for mediating irradiation and DNA-damage -induced cellular responses including apoptosis and/or DNA repair. However, the sensitive-to-resistant transition we observed for the induction of pro-apoptotic genes is unlikely due to the unavailability of DmP53 since it is ubiquitously expressed in the embryo at both sensitive and resistant stages (Jin et al. 2000)(Figure 2-4B). DmP53 mediated induction of DNA-repair genes *ku70* and *ku80* is not diminished, and actually incressed, after the transition observed for the pro-apoptotic genes (Figure 2-4A). We tried over-expressing *DmP53* using UAS-*DmP53* but it failed to convey any detectable radiation sensitivity in resistant stage embryos (data not

shown). Previous studies using reporter constructs containing part of the IRER_left have found that the reporter remained responsive to x-ray till the end of embryogenesis (Qi et al. 2004). All of these evidences suggest that the transition is not due to unavailability or lack of activation of DmP53, rather they point to epigenetic regulation of the IRER that controls its accessibility.

A DNase I sensitivity assay was performed to scan the DNA accessibility around IRER. A primer set was designed and verified for a selected 1,000 bp interval, e.g. 18,363,000-18,363,999 (referred to as “363” in the paper) (Table 2-3). Unless otherwise stated, the ΔCt values mentioned thereafter refer to Ct(50U)-Ct(0U). For constitutively active genes such as the *act5c* transcribed region, the ΔCt value is between 4-5 in resistant stage embryos. In contrast, heterochromatin areas such as the H23 (22,000 to 24,000 of chr2 heterochromatin) locus are refractory to the DNase I treatment, with the ΔCt value close to zero (Figure 2-7A and Figure 2-8). In resistant stage embryos, the *reaper* transcribed region and proximal promoter and enhancer regions (363-365) remain as sensitive to DNase I as the constitutively active *actin5c* locus. In sharp contrast, most of the IRER region is almost as inaccessible as the heterochromatin locus (H23). The only region in IRER that remains relatively open at the resistant stage is 18,386-387, which is probably the shared enhancer/promoter region of two putative non-coding RNAs that are transcribed in opposite directions (represented by EST sequences RE73107 (3L: 18,383-379) and RE07245 (3L: 18,388-392), respectively). It is also where R4 and R5 insertions are located. This is unlikely just a coincidence, rather we believe the relative openness of this region allowed R4 and R5 to be recovered from the mutagenesis.

To monitor the dynamics of the accessibility of IRER, we performed the DNase I sensitivity assay in staged embryos that were 3.5-5 hr, 5.5-7.0 hr, 9-10 hr, 10-13 hr, and 14-17 hr AEL (Figure 2-7B). A significant decrease of DNase I sensitivity was found in IRER between 7 and 9 hr AEL, consistent with the sensitive-to-resistant transition observed for irradiation-induced *reaper*/*hid* expression and cell death. When the ΔCt values of different loci were normalized against the ΔCt value of the *act5c* locus, it was apparent that the *reaper* transcribed region and immediate promoter and enhancer region (primer set 363, 365, respectively) remained as open as the *act5c* locus throughout embryogenesis. However, the IRER region (detected with primer sets 368, 370, 372, 377, 382) underwent a dramatic shift of accessibility between the 7 hr and the 9 hr AEL (Figure 2-7B). Within the IRER, it seems that the center of the IRER_left, represented by probe sets 371-382, becomes inaccessible first. While the left boundary of IRER, represented by probe sets 368-370, becomes inaccessible to DNase I at relatively later stages. The control H23 heterochromatic region also changes dramatically in DNase I sensitivity between sensitive and resistant stages, which is consistent with the timing of heterochromatin formation in *Drosophila* embryogenesis (Lu et al. 1998).

Histone Modifications in the IRER Region

The formation of heterochromatin-like structure is associated with post-translational modification of histones (Jenuwein and Allis 2001). To monitor histone modification in and around IRER, Chromatin Immuno-Precipitation (ChIP) experiments were performed in parallel with sensitive and resistant stage embryos (Figure 2-9 B and C) using antibodies against trimethylated H3K9 and H3K27 (Gift from T. Jenuwein). As shown in Figure 2-9B, we observed a dramatic increase of H3K27 trimethylation in the

IRER at the resistant stage. For the region 18,366-368, the recovery rates of resistant embryos are over 100-fold higher than those of sensitive embryos. As expected, the level of H3K27Me3 in the positive control *Ultrabithorax* (*Ubx*) promoter region also increased at the resistant stage. However, the magnitude of the increase in the *Ub*x promoter is much smaller than that observed for 18,366-368, probably reflecting the fact that the *Ubx* promoter remains open in the posterior segments while the blocking of IRER is for the whole embryo.

There is also a significant increase of H3K9 trimethylation throughout the IRER (Figure 2-9C), especially in the center of IRER_left (18,371-382), which corresponds to the region that has the strongest resistance to DNase I (Figure 2-7). It is interesting to note that, in comparison, the highest level of H3K27 trimethylation is at the left boundary of IRER (18,366-368). To test whether trimethylated H3K9 is indeed associated with the formation of heterochromatic structure in IRER, the antibody against Heterochromatin Protein 1 (HP1) was used for ChIP assay. The distribution profile of HP1 in the tested region is quite similar with that of trimethylated H3K9 (Figure 2-9E), further indicating that the IRER indeed undergoes the transition from a relatively open structure to a heterochromatin-like structure.

Just as trimethylated H3K9 is often bound by HP1, trimethylated H3K27 is associated with the Polycomb Repressive Complex 1 (PRC1), including Polycomb (Pc) and Posterior Sex Combs (Psc). The Bithoraxoid Polycomb Response Element (BXD-PRE) region, known to be bound by PRC1, was used as the positive control. Significant increase of specific Pc and Psc binding to the IRER was detected in the resistant embryos (Figure 2-9 D and F), suggesting that PcG-mediated silencing is involved in

blocking the IRER. However, instead of specifically binding to a localized PRE, we found that the binding of Pc and Psc is widespread in all of the tested loci in IRER.

Several other types of histone modification, including di- and tri-methylation of H3K4, di-methylation of H3K9 and H3K27, acetylation of H3K9, and phosphorylation of H3S10 were investigated in the same region as well (data not shown). Of those, only a moderate decrease (30-50%) of H3 acetylation was observed in resistant stage embryos compared to sensitive stage ones (Figure 2-9G). This may also contribute to the structural transition since acetylated H3 is considered as one of the euchromatic marks (Jenuwein and Allis, 2001). However, the magnitude of change is not comparable to that observed for trimethylated H3K27 and H3K9.

To determine the timing of histone modifications, we performed ChIP analysis in embryos between 7-9 hr AEL (late stage 11 and stage 12) (“Middle”; Figures 2-9 H and I). Compared to sensitive stage, both H3K27 and H3K9 trimethylation profiles changed significantly in the IRER during the transitional “middle” stage. Thus, it is impossible to distinguish which of the two modifications happens first. It is quite possible that the two distinct modifications happens in parallel. Interestingly, the enrichment of trimethylated H3K27 at region 366 during middle stage is already as high as that at the resistant stage, while at other sites in IRER there is an increase of H3K27 trimethylation between the middle stage and the late resistant stage. This suggests that this modification may be initiated from the left boundary of IRER. Another difference between H3K9 and H3K27 trimethylation is that there is a relatively low level, but significant increase, of H3K27 trimethylation in the *reaper* promoter and immediate enhancer region (363 & 365), whereas the H3K9 trimethylation is much more limited to the core of IRER.

Histone Modifiers Are Required for the Sensitive-to-Resistant Transition

Trimethylation of H3K27 is carried out by the Polycomb Repressive Complex 2 (PRC2), which contains three core components, Suppressor of zeste 12 (Su(z)12), Extra sexcombs (ESC), and Enhancer of zeste (E(z)). Trimethylation of H3K9 is catalyzed by the histone methyltransferase Su(var)3-9. The histone deacetylase (Hdac1/rpd3) is involved in and required for both modifications. In searching for the key chromatin modifiers responsible for putting the inhibitory markers in IRER, we examined the γ-ray responsiveness in embryos mutated for genes involved in chromatin modulation. The list of the genes/alleles tested is presented in Table 2-4. In summary, we found that a significant delay of the sensitive-to-resistant transition was observed in embryos mutated for Hdac1, Su(var)3-9, Su(z)12, and Pc. The timing of the transition is monitored via in situ hybridization for *reaper* and *hid*, respectively, in irradiated embryos. There is a remarkable synchronicity between the responsiveness of *reaper* and *hid* in all of the tested mutants (Table 2-4), which strongly indicates that the same mechanism controls the responsiveness of both genes.

In wild type embryos the sensitivity of *reaper* and *hid* to γ-ray is diminished once the germ band begins to retract (early or middle stage 12). In all of the Hdac, Su(var)3-9, Su(z)12, and Pc mutants, the responsiveness remained during the germ band shortening process and in some mutant alleles, after the germ band has fully retracted to the ventral side (stage 13-14) (Figure 2-10 A-F). There is a noticeable increase of base level *reaper* (and *hid*) expression in untreated Hdac mutant embryos (Figure 2-10 C vs. A), which probably reflects the general loss of suppression in these mutants. However, there is no increase of base level *reaper* (*hid*) expression in the Su(z)12

mutants which nonetheless showed similar delay of the sensitive-to-resistant transition. All of these alleles were originally identified as dominant modifiers. For instance, the Hdac alleles were identified as dominant suppressors of position effect variegation observed for In(1)w^{m4} (Mottus et al. 2000). For most of the alleles tested, we noticed that the delay of transition was perceivable even in heterozygous embryos although it was much more profound with homozygous mutants (distinguished with GFP balancer). When pooled embryos laid by heterozygous parents were tested for DNase I sensitivity, there is a detectable difference in the center of IRER_left (18,371-382) between the mutant strains and the wild type strain at 10-13 hr AEL (stage 12-13) (Figure 2-11).

Although the function of Su(z)12 and Pc is required for turning off the sensitivity, we were not able to observe similar delay in mutant alleles of E(z) or Psc. This may due to the rescuing effect of the maternal deposit of E(z), which has been shown to have a longer lasting effect than that of Pc (or Su(z)12). However, there is also little delay of transition in mutant eggs laid by homozygous E(z)S2e or transheterozygous S2e/S4e mutant female at the restrictive temperature (29^{o}C) (Table 2-4). This discrepancy needs to be clarified in future studies and seems to indicate that the blocking of IRER, although involving trimethylation of H3K27 and requiring the function of some PcG proteins, is distinct from the canonic silencing mechanism observed for PRE-mediated silencing. Furthermore, we did not observe any significant precociousness or delay of the sensitive-to-resistant transition in trithorax group mutants (Table 2-4).

In all of the mutants tested, eventually the sensitivity is lost after about 13 hr AEL, indicating that these mutants delayed but did not block the sensitive-to-resistant (open-to-closed chromatin) transition. The timing of transition varied among the mutant alleles,

however, by developmental stage 15 (about 13-14 hr AEL), none of the mutants was responsive to irradiation as measured by *reaper* or *hid* ISH. Since the P53RE reporter construct remained responsive to irradiation till the end of embryogenesis (18-20hr AEL)(Qi et al. 2004), the loss of responsiveness in these mutants is unlikely due to the absence of trans factor(s). Our DNase I sensitivity data also indicate that although there is a delay, eventually IRER in the mutants becomes as inaccessible as in wild type embryos. The blocking of IRER in embryos mutated for the key epigenetic regulators (Hdac1, Su(var)3-9, Su(z)12, and Pc) may be mediated by other proteins that have overlapping function with the four genes. In addition, given the fact that trimethylation of H3K27 and H3K9 were initiated at about the same time, it is possible that they represent redundant mechanisms in blocking IRER.

Discussion

The irradiation responsiveness appears to be a highly conserved feature of *reaper*-like IAP-antagonists. A recently identified functional ortholog of *reaper* in mosquito genomes, *michelob_x*(*mx*), was also responsive to irradiation (Zhou et al. 2005). These evidences highlighted that stress responsiveness is an essential aspect of functional regulation of upstream pro-apoptotic genes such as *reaper*/*hid*. It is also worth mentioning that several mammalian BH3 domain-only proteins, the upstream pro-apoptotic regulators of the Bcl-2/Ced-9 pathway, are also regulated at the transcriptional level.

In this study we showed that the irradiation responsiveness of *reaper* and *hid* is subject to epigenetic regulation during development. The epigenetic regulation of the IRER is fundamentally different from the silencing of homeotic genes in that the change of DNA accessibility is limited to the enhancer region while the promoter of the pro-

apoptotic genes remains open. Thus, it seems more appropriate to refer this as the "blocking" of the enhancer region instead of the "silencing" of the gene. This region, containing the putative P53RE and other essential enhancer elements, is required for mediating irradiation responsiveness. Our ChIP analysis indicates that histones in this enhancer region are quickly trimethylated at both H3K9 and H3K27 at the sensitive-to-resistant transition period, accompanied by a significant decrease in DNA accessibility. DNA accessibility in the putative P53RE locus (18,368k), when measured by the DNase I sensitivity assay, did not show significant decrease until sometime after the transition period. It is possible that other enhancer elements, in the core of IRER_left, are also required for radiation responsiveness. An alternative explanation is that the strong and rapid trimethylation of H3K27 and association of PRC1 at 18,366-368 are sufficient to disrupt DmP53 binding and/or interaction with the Pol II complex even though the region remains relatively sensitive to DNase I. Eventually, the whole IRER is closed with the exception of an open island around 18,387.

The finding that epigenetic regulation of the enhancer region of pro-apoptotic gene controls sensitivity to irradiation-induced cell death may have implications in clinical applications involving ionizing irradiation. It suggests that applying drugs that modulate epigenetic silencing may help increase the efficacy of radiation therapy. It also remains to be seen as to whether the hyper-sensitivity of some tumors to irradiation is due to the de-differentiation and reversal of epigenetic blocking in cancer cells. On the other hand, loss of proper stress response to cellular damage is implicated in tumorigenesis (Baylin and Ohm 2006). The fact that the formation of heterochromatin in the sensitizing enhancer region of pro-apoptotic genes is sufficient to convey resistance to stress-

induced cell death suggests it could contribute to tumorigenesis. In addition, it could also be the underlying mechanism of tumor cells evading irradiation-induced cell death. This is a likely scenario given that it has been well documented that oncogenes such as Rb and PML-RAR fusion protein cause the formation of heterochromatin through recruiting a human ortholog of Su(v)3-9. In this regard, the *reaper* locus, especially the IRER, provides an excellent genetic model system for understanding the *cis* and *trans* acting mechanisms controlling the formation of heterochromatin associated with cellular differentiation and tumorigenesis.

Differentiation Stage-Specific Sensitivity to Irradiation-Induced Cell Death

The developmental consequence of epigenetic regulation of the IRER is the tuning down (off) of the responsiveness of the pro-apoptotic genes, and thus decreasing cellular sensitivity to stresses such as DNA damage (Figure 2-10G). Epigenetic blocking of the IRER corresponds to the end of major mitotic waves when most cells begin to differentiate. Similar transitions were noticed in mammalian systems. For instance, proliferating neural precursor cells are extremely sensitive to irradiation-induced cell death while differentiating/differentiated neurons become resistant to γ-ray irradiation, even though the same level of DNA damage was inflicted by the irradiation (Nowak et al. 2006). Our findings here suggest that such a dramatic transition of radiation sensitivity could be achieved by epigenetic blocking of sensitizing enhancers.

Later in *Drosophila* development, around the time of pupae formation, the organism becomes sensitive to irradiation again, with LD50 values similar to what was observed for the 4-7 hr AEL embryos (Ashburner 1989). Interestingly, it has also been found that during this period, the highly proliferative imaginal discs are sensitive to

irradiation-induced apoptosis, which is mediated by the induction of *reaper* and *hid* through P53 and Chk2 (Brodsky et al. 2004). However, it remains to be studied as whether the reemergence of sensitive tissue is due to the reversal of the epigenetic blocking in IRER or the proliferation of undifferentiated stem cells that have an unblocked IRER.

Silencing by a Non-Canonic Mechanism?

The blocking of IRER differs fundamentally from the silencing of homeotic genes in several aspects. First, the change of DNA accessibility and histone modification is largely limited to the enhancer region. The promoter regions of *reaper* (and *hid*) remain open, allowing the gene to be responsive to other stimuli. Indeed, there are a few cells in the central nervous system that could be detected as expressing *reaper* long after the sensitive-to-resistant transition. Even more cells in the late stage embryo can be found having *hid* expression. Yet, the irradiation responsiveness of the two genes is completely suppressed in most if not all cells, transforming the tissues into radiation-resistant state.

Secondly, the histone modification of IRER has a mixture of features associated with pericentromeric heterochromatin formation and the canonic PcG- mediated silencing. Both H3K9 and H3K27 are trimethylated in IRER. Both HP1, the signature binding protein of the pericentromeric heterochromatin, and the PRC1 are bound to IRER. As demonstrated by genetic analysis, the function of both Su(var)3-9 and Su(z) 12/Pc are required for the silencing. Preliminary attempts to verify specific binding of PRC2 proteins to this region was unsuccessful. The fact that none of the mutants tested could completely block the transition seems to suggest that there is a redundancy of the two pathways in modifying/blocking IRER. It is also possible that the genes we tested

are not the key regulator of IRER blocking but only have participatory role in the process.

Finally, within the IRER, there is a small region around 18,387 (18,386k-388k) that remains relatively open till the end of embryogenesis (Figure 2-7A). Interestingly, this open region is flanked by two putative non-coding RNA transcripts represented by EST sequences. If they are indeed transcribed in the embryo as suggested by the mRNA source of the cDNA library, then the “open island” within the closed IRER will likely be their shared enhancer/promoter region. Sequences of both cDNAs revealed that there is no intron or reputable open reading frame in either sequence. Despite repeated efforts, we were not able to confirm their expression via ISH or Northern. Over-expression of either cDNA using an expression construct also failed to show any effect on *reaper/hid* induced cell death in S2 cells. Yet, sections of the two non-coding RNAs are strongly conserved in divergent *Drosophil*a genomes. The potential role of these two non-coding RNAs in mediating *reaper/hid* expression and/or blocking of the IRER remains to be studied.

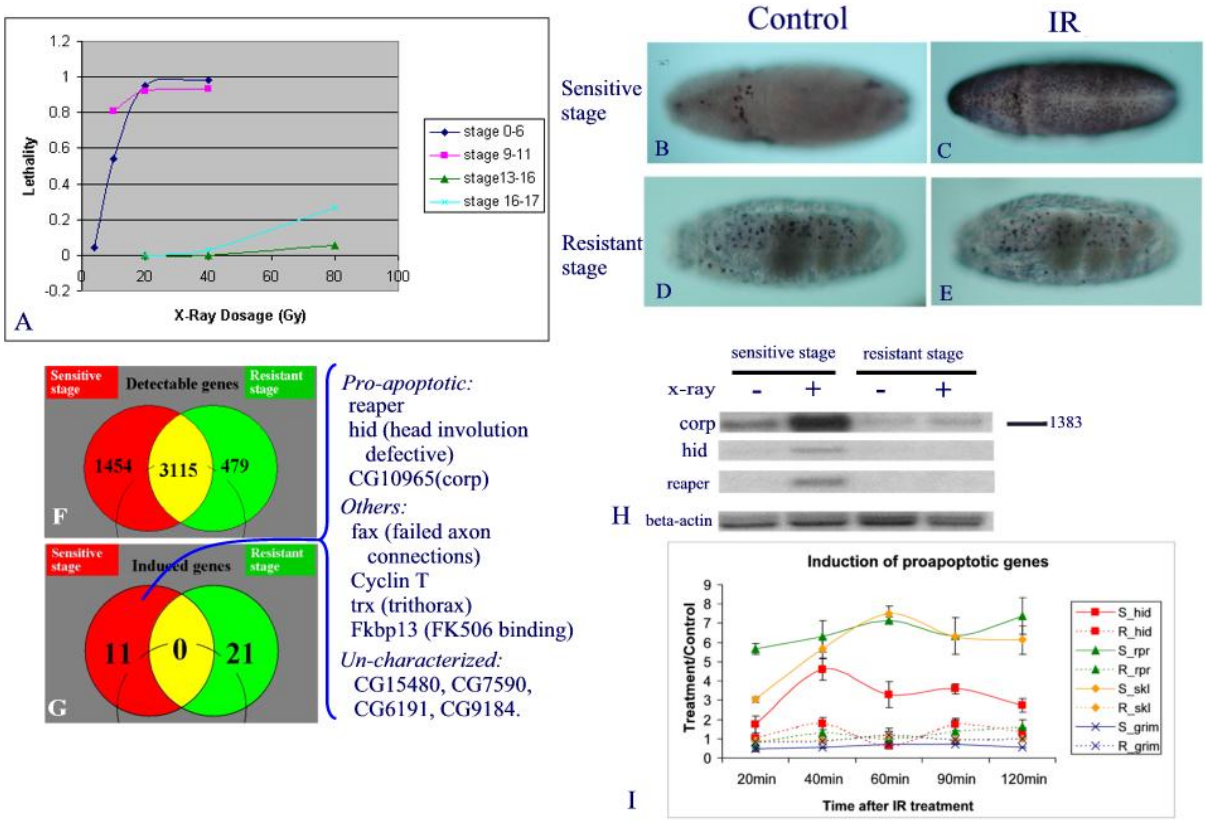

Figure 2-1. Stage–specific sensitivity to γ-ray induced cell death. A) Embryonic lethality induced by γ-ray is dependent on developmental stage. Embryos collected 0-3 hr AEL (developmental stages 0-6), 4-7 hr AEL (stages 9-11), 9-12 hr AEL (stage 13-16), 14-17 hr AEL (stages 16-17) were irradiated with various dosages of γ-irradiation. Each data point represents the average of two to three treatments. Each time an average of 595 eggs were treated. To count for unfertilized eggs, controls were processed in parallel without γ-ray treatment. Embryos that failed to hatch after a 30 hr incubation at 25° C were counted as lethal. B-E) TUNEL labeling of embryos at 75 mins post 40 Gy of γ-irradiation (C, E) or control treatment (B, D). B) and C) are stage 10/11 embryos, D) and E) are stage 16-17 embryos. F) Venn diagram depicting the overlap of detectable genes in sensitive and resistant stage embryos using the pan-genome DNA array. G) Venn diagram indicating no overlap between γ-ray inducible genes detected in sensitive (4-7 hr AEL) and resistant (9-12 hr AEL) embryos. H) Northern hybridization analysis confirms the γ-ray responsiveness of the three cell death genes: *reaper*, *hid,* and *corp (companion of reaper)*, and β-actin was used as a non-responsive control. I) *hid* (red square), *reaper* (green triangle), *sickle* (yellow diamond) and *grim* (blue cross) RNA levels (measured by QPCR) in sensitive (continuous lines) and resistant (dashed line) embryos at 20, 40, 60, 90, and 120 mins following γ-ray treatment. Data were represented as the fold changes comparing γ-ray treated with parallel processed control samples (mean ± Std).

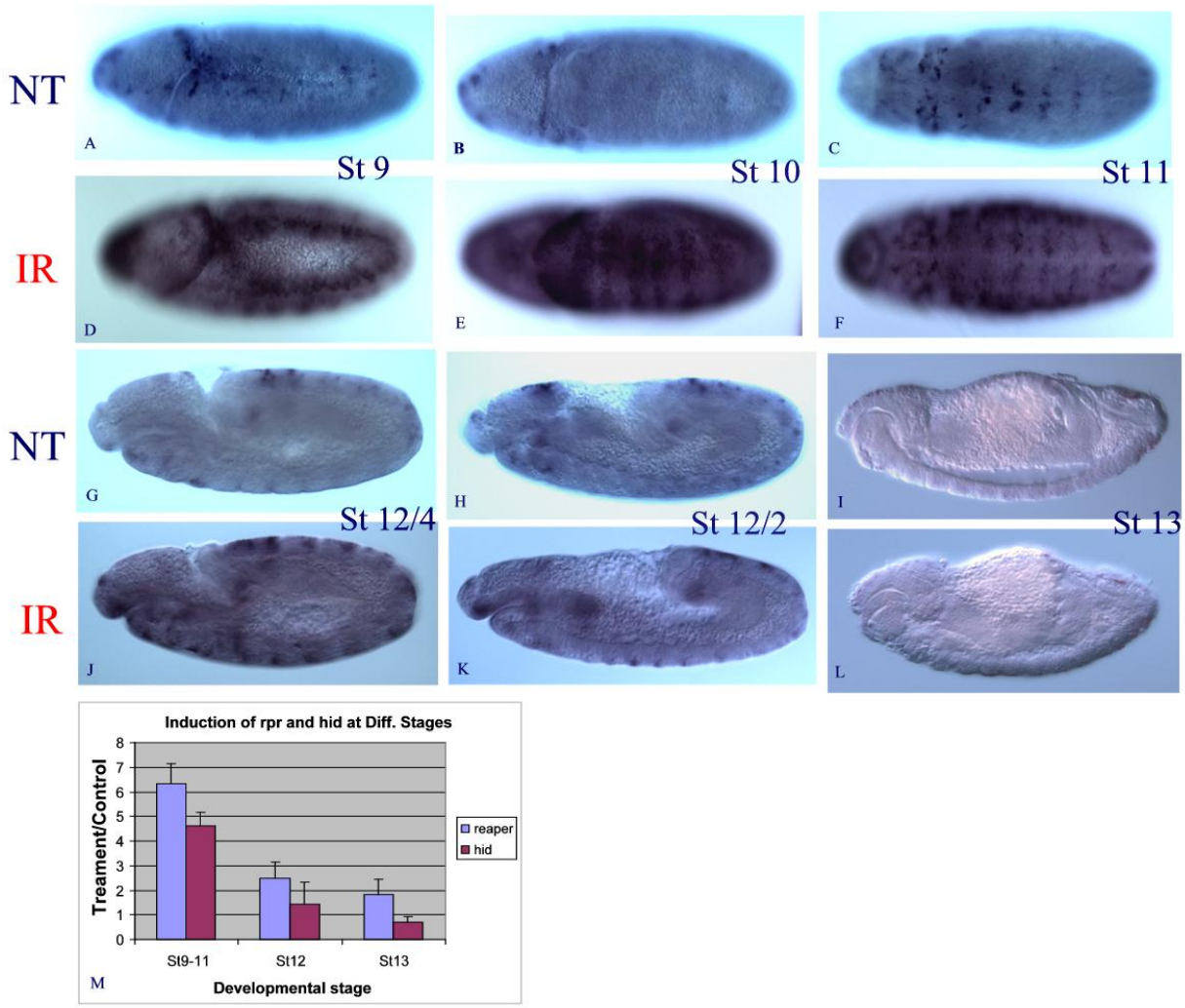

Figure 2-2. Rapid transition of *reaper* sensitivity to irradiation between 8-9 hr AEL. Pooled embryos (0-17 hr AEL) were treated with γ-ray or served as non-treatment control. Significant increase of *reaper* mRNA was observed in stage 7-11 embryos (A-F), with the peak of responsiveness observed in stage 10 embryos (E vs. B). This responsiveness is dramatically decreased once the germ band starts to retract, which happens around 7.5 hr AEL (J vs. G). By the time the germ band is half way retracted on the dorsal side, the responsiveness of *reaper* is almost completely diminished (K vs. H). None of the embryos at the end of stage 12 (8.5-9 hr AEL) or stage 13 has detectable *reaper* responsiveness (L vs. I). A very similar transition is also observed for *hid* responsiveness (Figure 2-3). The sensitive-to-resistant transition was also verified with QPCR (M).

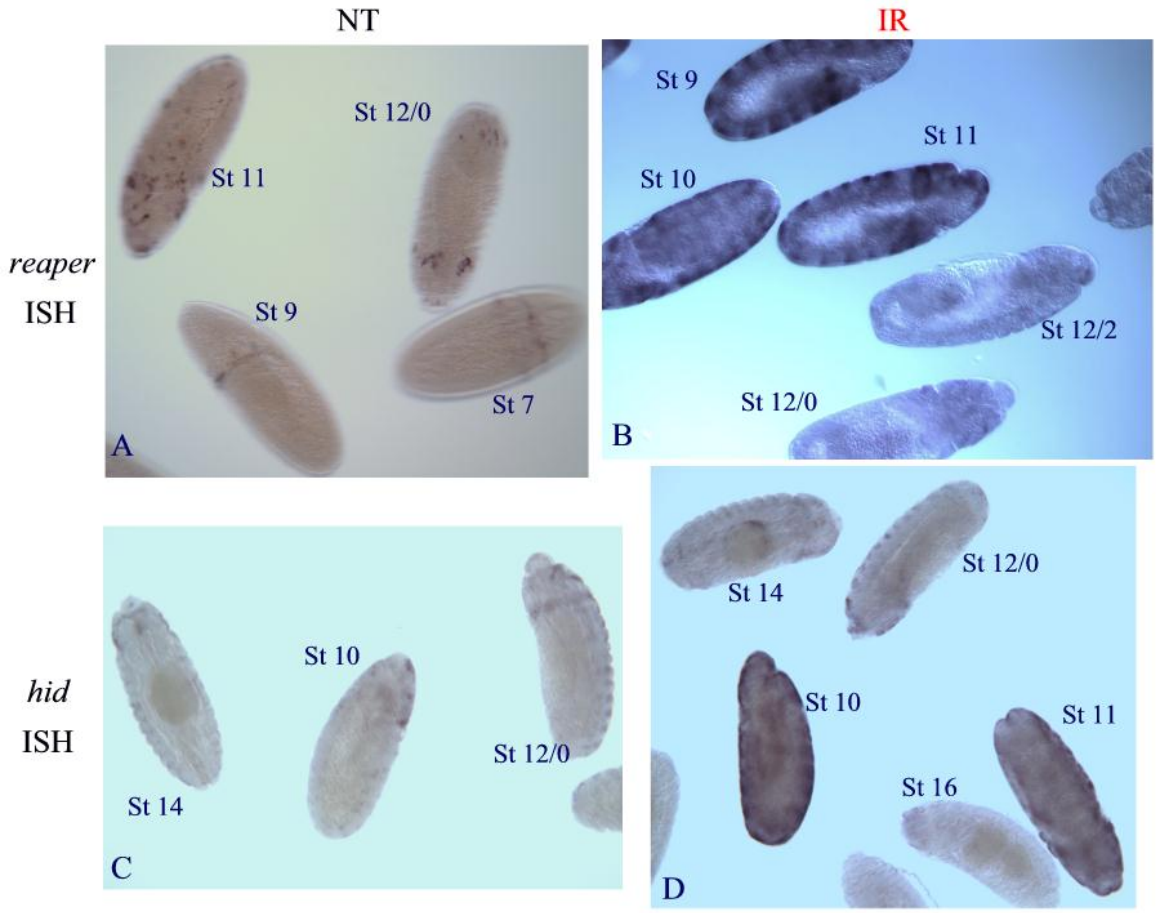

Figure 2-3. Embryos viewed at lower magnifications show the contrast of *reaper* and *hid* responsiveness in embryos at different developmental stages (St). Irradiation induced significant expression of *reaper* and *hid* in germ band extended embryos (St 9-11). In contrast, there is no detectable increase of *reaper* and *hid* expression in dorsal germ band retracting (St 12) or dorsal germ band retracted embryos (St 13-16). Embryos on the same slide were collected and treated together and were processed for ISH in the same tube.

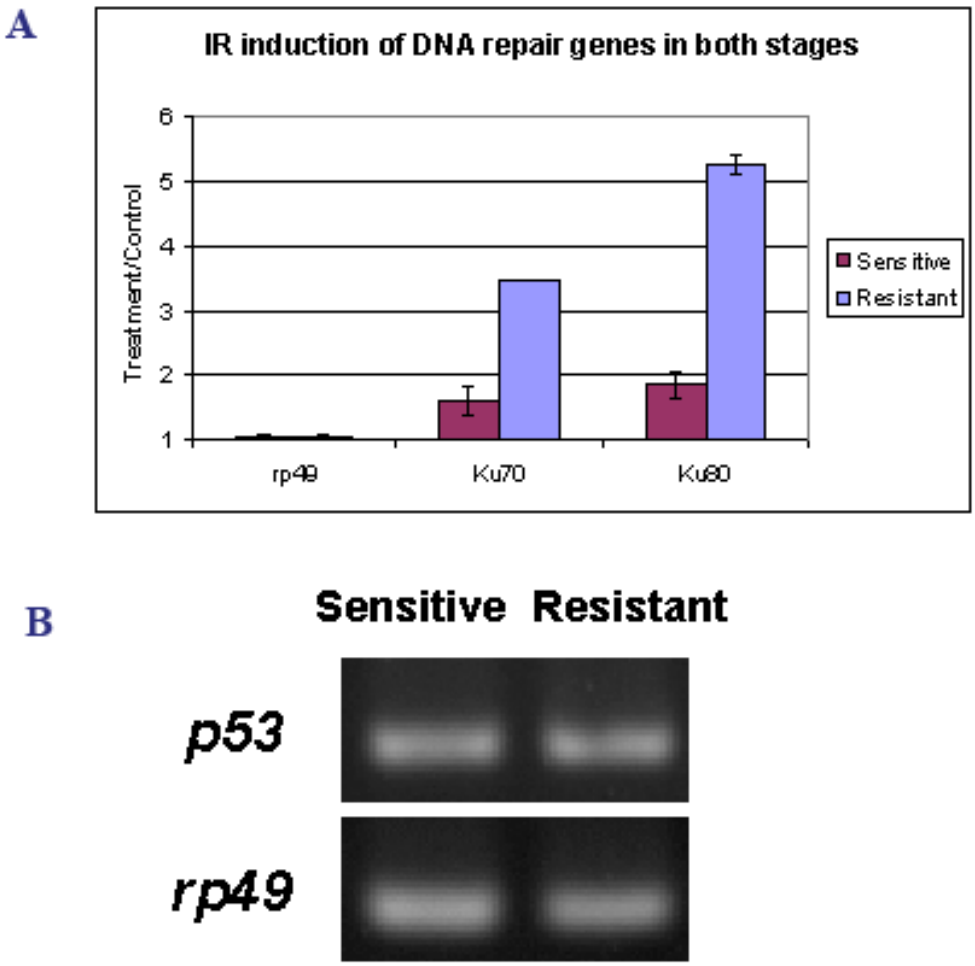

Figure 2-4. Comparable DNA damage induced cellular response and DmP53 expression at both sensitive and resistant stages. A) Two DNA repair genes, *ku70* and *ku80*, are induced upon irradiation at both sensitive and resistant stages. RNA level was measured at 120min after γ-ray treatment by QPCR. The induction fold was indicated by the ratio of IR treated samples and non-treated controls. Housekeeping gene *rp49* was used as the non-responsive control control. Higher induction of DNA repair genes may account for the post irradiation survival at resistant stage. B) Ubiquitous expression of *Drosophila p53* in both sensitive and resistant stages. RNA level was represented by semi-quantitative PCR. *rp49* was used as the endogenous control.

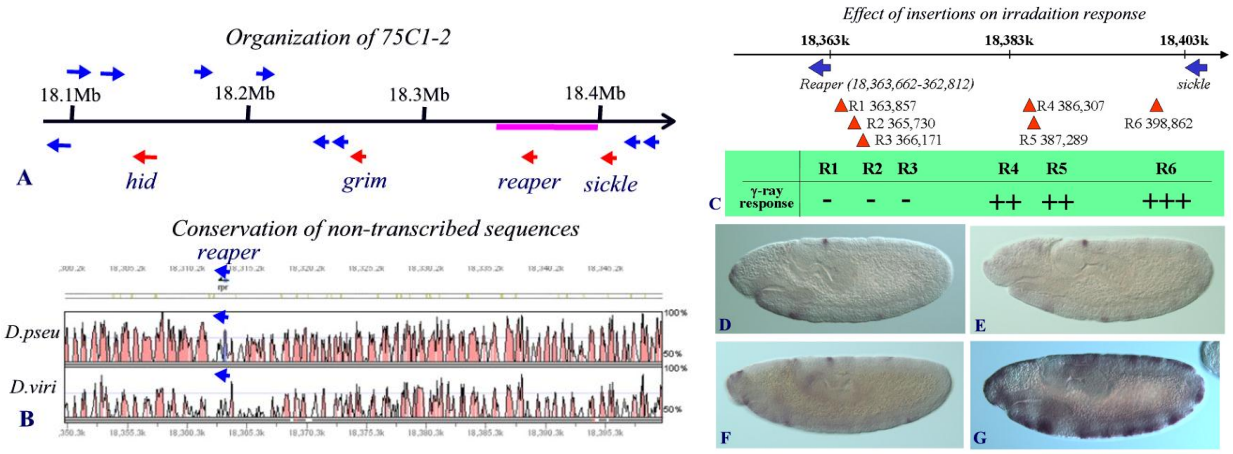

Figure 2-5. Mapping of the irradiation responsive region. A) Organization of the 75C1-2 region that harbors four IAP-antagonist genes (red arrows). Other annotated genes in this region were marked with blue arrows. The region underlined by the red line is represented in B). B) Conservation of the intergenic region around the *reaper* locus. Figure drawn with Vista (Mayor et al. 2000), the curve indicating the percent of identity (window size 100bp). The region is colored if the identity is higher than 75%. Color code: pink - untranscribed or intronic region; light blue – untranslated transcribed region; dark blue – coding region. C) The Exelixis insertions localized between *reaper* and *sickle*, R1(Pd11052), R2 (Pd00909), R3 (PBacf02826), R4(PBacf03056), R5(PBacf07603), and R6(PBacf03389). Induction of *reaper* by γ-ray irradiation was totally blocked by R1, R2, or R3 but is only slightly attenuated by R4 and R5 and is not at all affected by R6. “+++”, wt responsiveness; “-”, no response. For insertion site information, refer to Table 2-2. D) and E) *reaper* ISH of control and irradiated homozygous R3 embryos, respectively. F) and G) *reaper* ISH of control and irradiated homozygous R6 embryos, respectively.

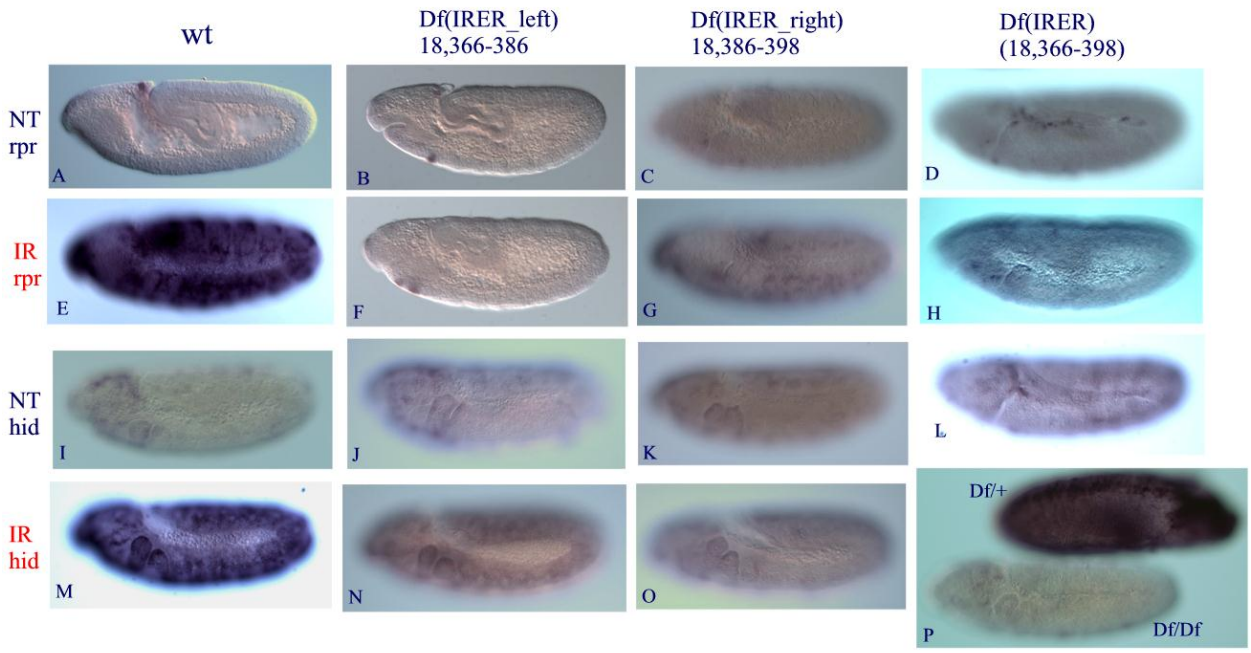

Figure 2-6. IRER is required for the responsiveness of *reaper* and *hid*. Df(IRER_left) abolished the responsiveness of *reaper* to irradiation (B, F). *hid* responsiveness to γ-ray was also significantly reduced (J, N). Df(IRER_right) reduced *reaper* responsiveness (C, G vs. A, E) but blocked *hid* responsiveness (K,O). Df(IRER) blocked the responsiveness of both *reaper* and *hid* (D, H, L, P). In P, the dark embryo is a heterozygous (Df(IRER)/TM3ubi-GFP) embryo that is also stained for GFP.

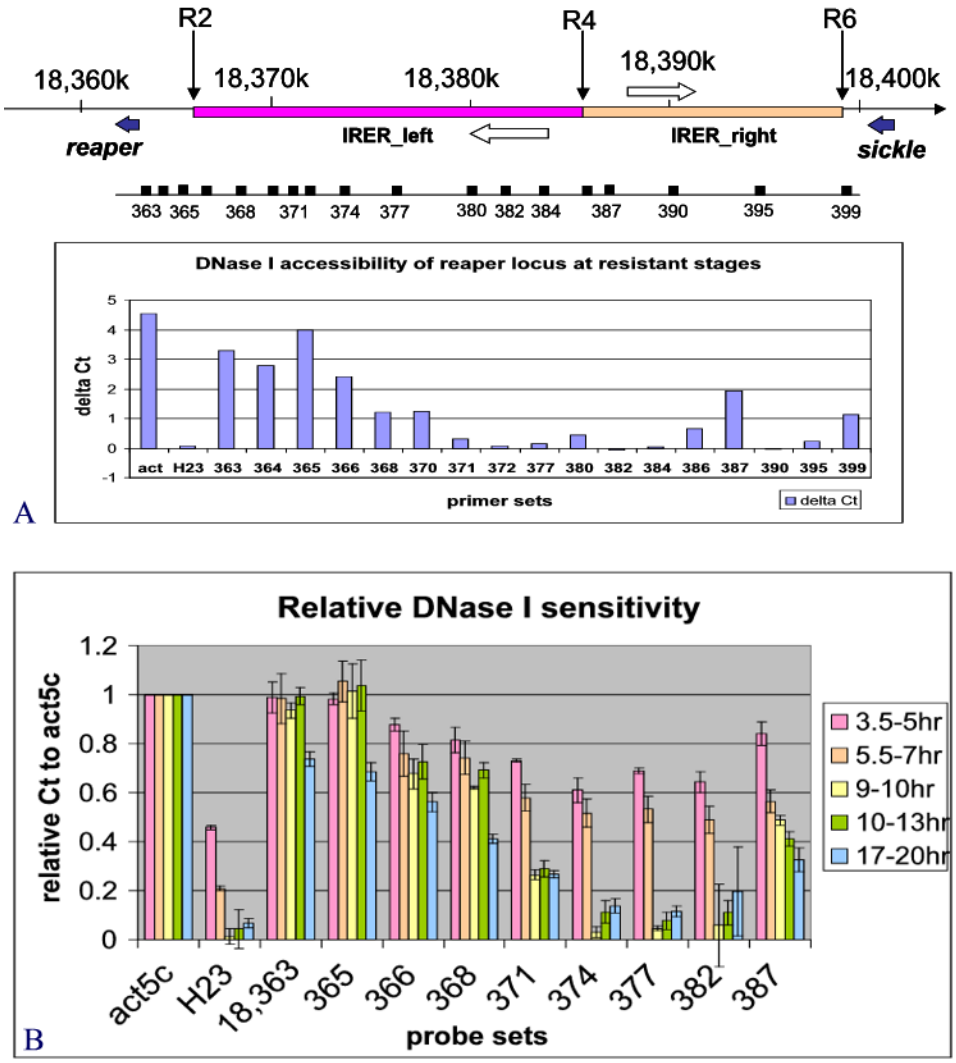

Figure 2-7. Formation of closed heterochromatin structure in the Irradiation Responsive Enhancer Region (IRER). A) DNase I sensitivity assay of the IRER in resistant stage embryos. In resistant embryo, most of the IRER is as resistant to DNase I as the pericentromeric heterochromatin locus H23. The only exception is a relatively open island around 18,387, flanked by two putative non-coding RNAs (open arrows). B) Change of DNase I sensitivity in the IRER in staged embryos. There is a dramatic transition of DNase I sensitivity around 18,368-382 between the 7 hr and the 9 hr AEL. Data were represented as relative ΔCt, which is ΔCt (target region) / ΔCt (act5c). The ΔCt (act5c) values for different stages are: 6.420$\pm$ 0.424 (3.5-5hr), 7.278$\pm$ 0.797 (5.5-7hr), 5.043$\pm$ 0.34 (9-10hr), 4.460$\pm$ 0.339 (10-13hr), 4.988$\pm$ 0.256 (17-20hr). Data represented as mean $\pm$ std; n=3 or 4 for all age groups.

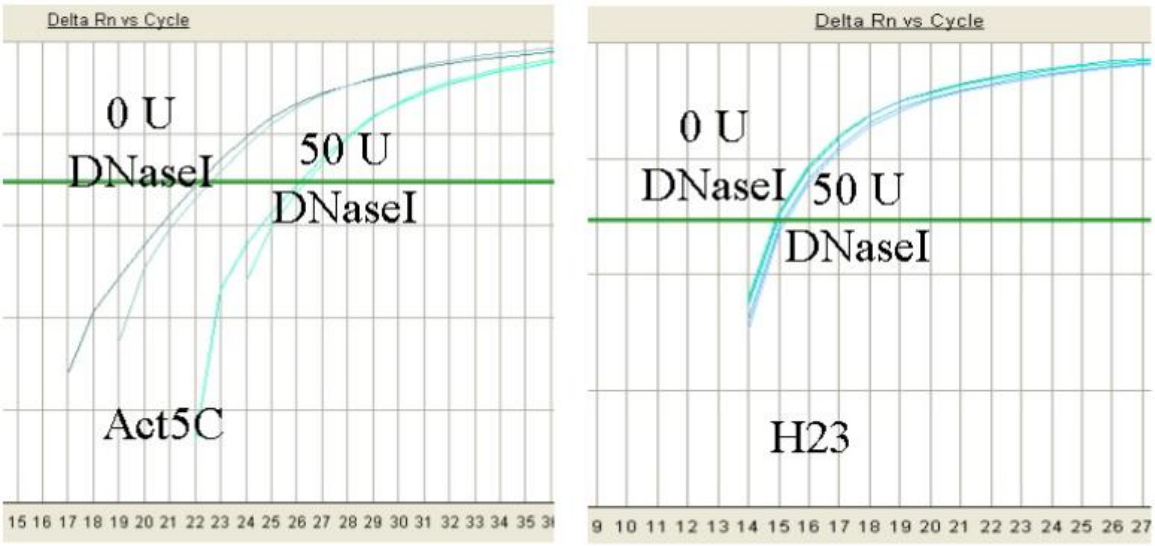

Figure 2-8. Examples of QPCR measurements of DNase I sensitivity. Permeablized nuclei were treated with 0 or 50U of DNase I for 5 min. The Genomic DNA was then extracted. 5ng of genomic DNA were subjected to QPCR analysis for each locus. In open locus (Act5C) there is a significant difference (delta Ct>4) between the treated and untreated samples, indicating over 90% ($1- 2^{-\text{delta Ct}}$) of the DNA in the tested locus has been digested by DNase I. In contrast, in the heterochromatin region (H23), there is little difference between the treated and untreated samples, indicating this locus is un-accessible to DNase I.

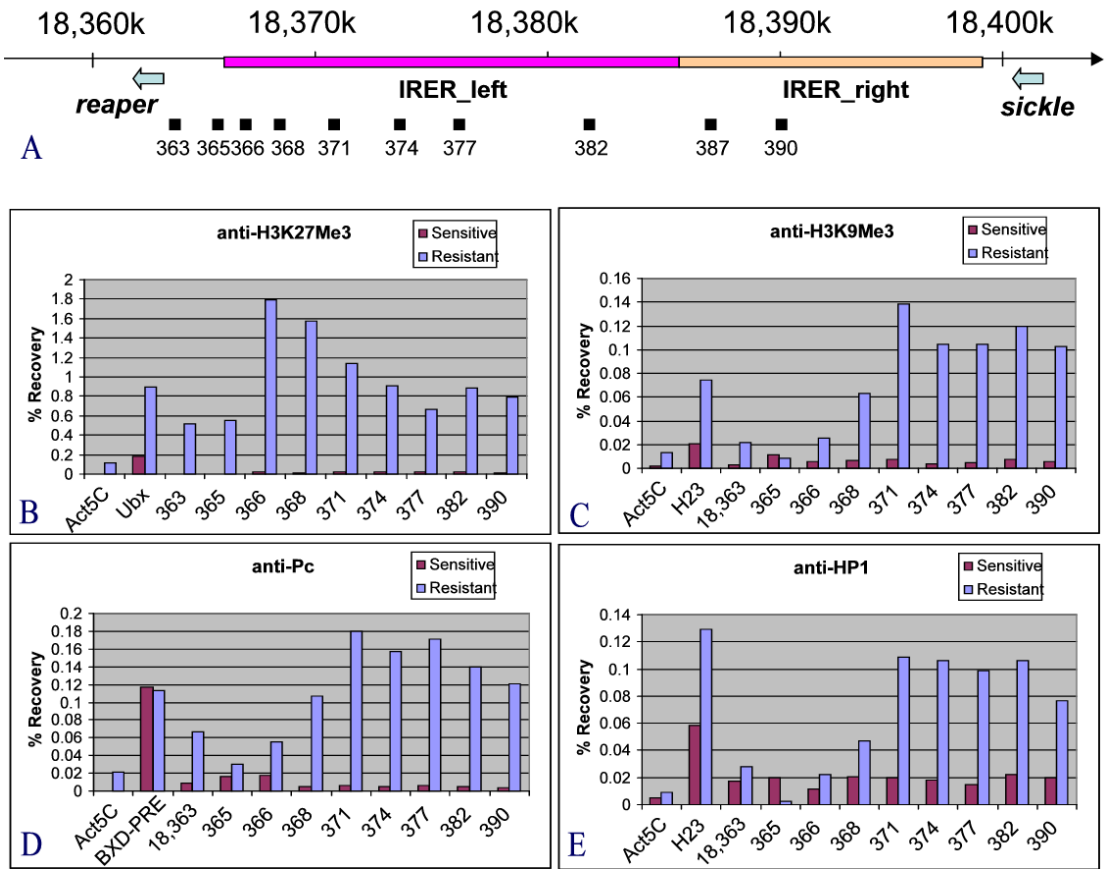

Figure 2-9. Chromatin modification of IRER. A) Schematic representation of the IRER locus, including IRER_left (red bar) and IRER_right (orange). The positions of DNA amplicons for quantification of ChIP results are shown below the IRER map relative to the DNA sequence coordinates of chromosome 3L (Dm genome release 4.3). B-G) ChIP assays performed on embryos at sensitive stage (red) and resistant stage (blue) using anti-H3K27Me3 (B), anti-H3K9Me3 (C), anti-Pc (D), anti-HP1 (E), anti-Psc (F), and anti-Ac-H3 (G). Precipitation of DNA fragments with antibodies was quantified by QPCR and shown in recovery rates. The coding region of *Act5C* was used as background control for all the antibodies. For positive controls, *Ubx* promoter region was chosen for anti-H3K27Me3; H23 for anti-H3K9Me3, anti-HP1 and anti-Ac-H3; and the BXD-PRE for anti-Pc and anti-Psc. Several independent assays were performed for each antibody and a representative figure was shown. H) and I) Timing of H3K27 and H3K9 trimethylation, respectively. ChIP results from embryos at sensitive stage (3-7 hr AEL, red), middle stage (7-9 hr AEL, yellow) and resistant stage (13-16 hr AEL, blue) were normalized to the recovery rate of the positive controls in the resistant stage. Three independent assays were performed for each stage and the values are shown as mean $\pm$ std.

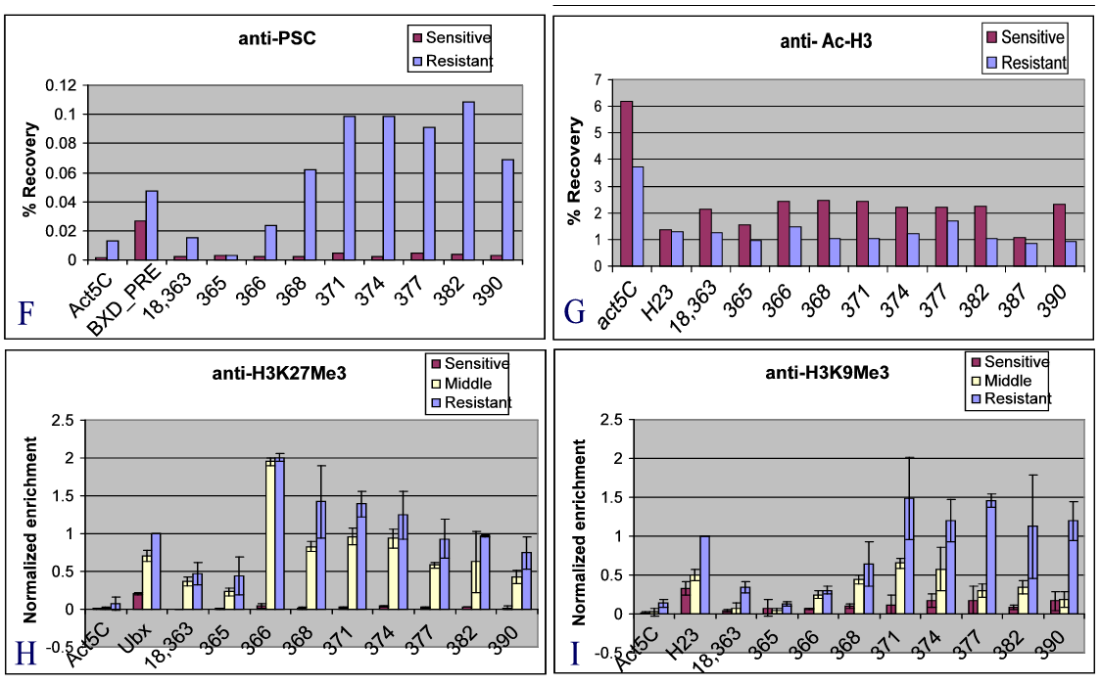

Figure 2-9. Continued.

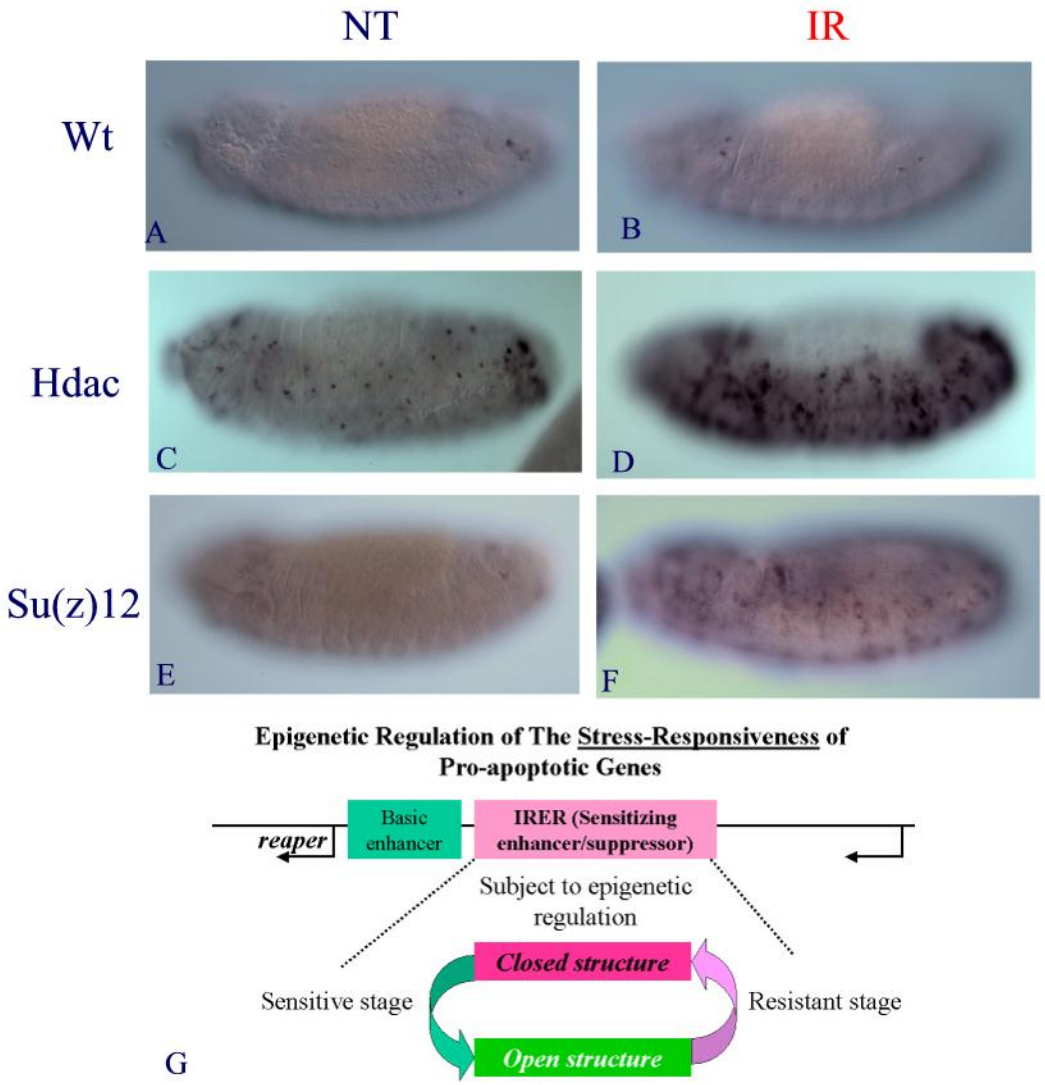

Figure 2-10. Histone deacetylase (Hdac) and Su(z)12 functions are required for the sensitive-to-resistant transition. Responsiveness of *reaper* (and *hid*) following irradiation was measured with ISH in stage 13 embryos. In wild type embryos, there is no response at all (A, B). However, embryos mutated for Hdac (C, D), Su(z)12 (E, F), or Su(v)3-9, Pc, etc. (Table 2-4) remained responsive till stage 13-14. G)Schematic diagram summarize our findings. Epigenetic regulation of the sensitizing enhancer region (IRER) determines whether the pro-apoptotic gene(s) can be induced by cellular stresses such as DNA damage, and thus controls the sensitivity to stress-induced cell death. Such an epigenetic modification may be reversible and regulated by developmental cues.

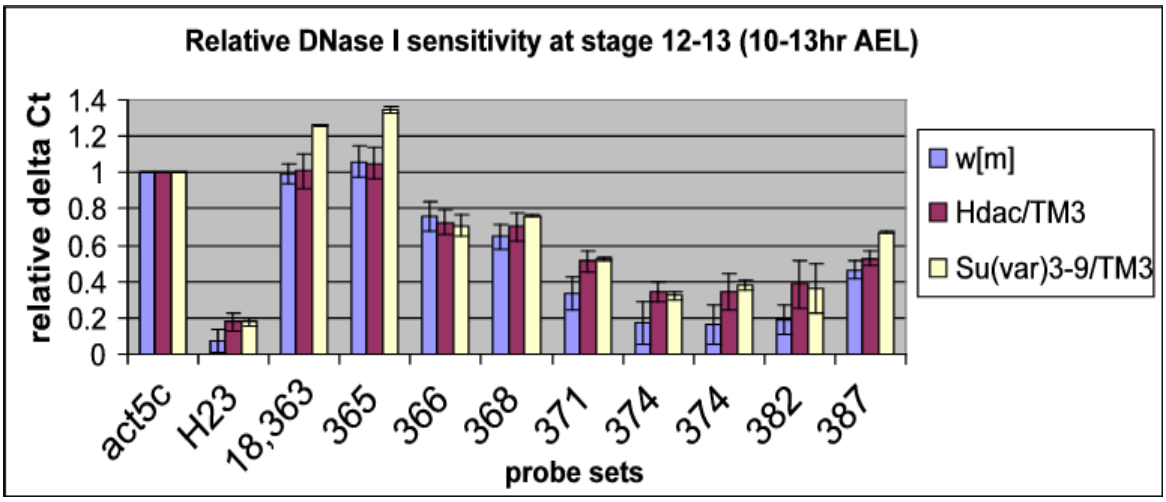

Figure 2-11. Delayed formation of DNase I resistant region in Hdac and Su(var)3-9 mutants. The sensitivity to DNase I digestion was measured for wild type (w[67c23]) embryos and embryos laid by heterozygous parents of Hdac/TM3 and Su(var)3-9/TM3, respectively, at 10-13hr AEL. The measurements were processed as described in the Material and Methods section and normalized against corresponding measurements for the act5c locus. The values represent the average of 3-4 measurements and the error bars represent standard deviation. Since none of the GFP balancers we tested allowed reliable distinction of homozygous mutant embryos at this stage, the assays for mutants were performed using pooled embryos laid by heterozygous parents (1/4 homozygous, ½ heterozygous, and ¼ wt). Because so, the measurements are underestimates of the DNase I sensitivity in homozygous mutants, which should be considerably higher than the values represented here. In wild type embryos, by 10-13 hr AEL the center region of IRER_left (18,371-382) has become inaccessible, however, the DNase I accessibility of the pooled mutant embryos is conceivably higher, indicating a delay in blocking IRER.

Table 2-1. Genes induced in resistant stage (9-12 hr AEL) embryos at 20 minutes following γ-ray irradiation

Probe_set	Name	Function		
142200_at	dib			
148753_at	CG9238	protein phosphatase 1 binding	protein phosphatase type 1\, regulator	
153742_at	polo	protein kinase	protein serine/threonine kinase	mitosis
154516_at	smg	RNA binding	translation repressor	
143339_i_at	Ser99Db	serine-type endopeptidase	digestion	
147469_at	CG15098			
146882_at	CG11804			
143538_at	Top1	larval development (sensu Insecta)	oogenesis	DNA topoisomerase I
143834_at	CycB3	mitotic spindle assembly	cyclin-dependent protein kinase\, regulator	
153799_at	CG1823			
148648_at	CG4300	spermidine synthase		
147364_at	CG14478			
155087_at	CG8390			
154485_at	kel	ring canal formation	oogenesis	actin binding
155049_at	CG7129			
146589_at	CG3305			
152304_at	CG11963	succinate-CoA ligase (ADP-forming)		
154844_at	cdc2	cyclin-dependent protein kinase	G2/M transition of mitotic cell cycle	G1/S transition of mitotic cell cycle
154416_at	BcDNA:LD27979			
154041_at	BcDNA:LD21675			
154399_at	UbcD4	ubiquitin conjugating enzyme	ubiquitin cycle	
154941_at	CG1962			
154506_at	Srp54	mRNA splice site selection	pre-mRNA splicing factor	RNA binding

Table 2-2. Mutant strains used in this study

Name (Flybase ID)	Molecular information	Reference
Point mutations		
Hdac[303]		(Mottus et al. 2000)
Hdac[326]		As above
Hdac[328]		As above
Su(v)3-9[1]		Flybase
Su(v)3-9[2]		Flybase
Su(z)12[3]		(Birve et al. 2001)
Su(z)12[4]		As above
Su(z)12[5]		As above
Deficiencies		
Df(18,366-398)	Deleted region – (3L:18,365,730-18,398,861), replaced by PXP5/PBac5	This study
Df(18,366-386)	Deleted region – (3L:18,365,730-18,386,306), replaced by PXP5/PBac5	This study
Df(18,386-398)	Deleted region – (3L:18,386,306-18,398,861), replaced by PBac5/PBac3	This study
Transposon insertion strains		
P [XPd11052] (referred to as R1)	Inserted after 3L:18,363,856. (Verification by IVPCR indicated that, for the strain we obtained, there were multiple insertions on the 3rd chromosome.)	(Thibault et al. 2004),
P [XPd00909] (R2)	Inserted after 3L:18,365,729	(Thibault et al. 2004), single insertion, position verified by this study.
PBac[WHf02826] (R3)	Inserted after 3L:18,366,170	As above
PBac[WHf03056] (R4)	Inserted after 3L:18,386,307	As above
PBac[WHf07603] (R5)	Inserted after 3L:18,387,288	As above
PBac[WHf03389] (R6)	Inserted after 3L:18,398,861	As above
P(Keyse et al.)rpd3[04556]		Flybase

Table 2-3. Primer pairs used for QPCR measurement of each locus

Symbol	Target region	Forward (f) and backward (b) primers	
Act5c	Act5c	Ac5c_f	CACGGTATCGTGACCAACTG
		Act5c_b	GCCATCTCCTGCTCAAAGTC
H23	Ch 2h (centromeric heterochromatin) 23,000 – 25,000	H23(939)_f	CCAAGTTGGCCAGTTTTGAT
		H24(104)_b	AGTTCAAGCCCGGGTATTCT
363	Ch 3L: 18,363,000-18,363,999 (reaper promoter)	363(689)_f	GCGATGGTTGCTTTTCAACT
		363(972)_b	TGGCAACAACAACACAACCT
364	Ch 3L: 18,364,000-18,364,999	364(552)_f	CAAGGAAGAGTTCCGTTCCA
		364(879)_b	ACTTTAAGCCGCAGGGAAAT
365	Ch 3L: 18,365,000-18,365,999	365(313)_f	GTGCGTCTCAAGTGTTTCCA
		365(741)_b	CGAAAGCAGACCCAAAACAT
366	Ch 3L: 18,366,000-18,366,999	366(325)_f	TGGGAAGTGTGTCAATCGAA
		366(638)_b	CGCAAGTTATCGCATTGTTG
368	Ch 3L: 18,368,000-18,368,999	368(604)_f	TTTTCGGAATGGGTTTTCAG
		368(830)_b	ACACACACGAACCGAATGAA
370	Ch 3L: 18,370,000-18,370,999	370(695)_f	GTCCGATCTCGCAATCAAAT
		370(900)_b	ACATCCGAAAGGCAGAAAGA
371	Ch 3L: 18,371,000-18,371,999	371(263)_f	TTTTGATACCCCGTGATGGT
		371(673)_b	CAACAATTTGAGCAGGAGCA
372	Ch 3L: 18,372,000-18,372,999	372(552)_f	CCCGAGTTGAGCGTAGAGTC
		372(944)_b	ATGAAGTCCCTGGCAAACAC
375	Ch 3L: 18,375,000-18,375,999	375(161)_f	ATGGGATACAGTGCGTGTCA
		375(491)_b	AGGTGAGCAGCTTAGGACCA
377	Ch 3L: 18,377,000-18,377,999	377(539)_f	AGCAGCATCCTGACTGTCCT
		377(683)_b	CGCTTGGTTGAAATTTGGTT
380	Ch 3L: 18,380,000-18,380,999	380(584)_f	AGAAACCACCCACTCACAGG
		380(830)_b	TGACTTTAAGCGGCTTCGAT
382	Ch 3L: 18,382,000-18,382,999	382(413)_f	TTGGGCCCCTTTTAAATACC
		382(610)_b	AAAAACCGGAGCCTAAAGGA
384	Ch 3L: 18,384,000-18,384,999	384(540)_f	ACGAATAAACGTGCCAAAGG
		384(678)_b	CCACACTCCGAATTTCCACT
386	Ch 3L: 18,386,000-18,386,999	386(214)_f	GTTTTGGCATCAGCTTGTGA
		386(354)_b	TGTCGATCCGATTTTCCCTA

Table 2-3. Continued

Symbol	Target region	Forward (f) and backward (b) primers	
387	Ch 3L: 18,387,000-18,387,999	387(463)_f	CGTTTGACCCGTTGAGATTT
		387(862)_b	GATAAGGCCGAAGGAAAAGG
390	Ch 3L: 18,390,000-18,390,999	390(315)_f	TACCAACTCGGTCCTTCCAC
		390(441)_b	TTCTGCACCCATTCTCCTCT
395	Ch 3L: 18,395,000-18,395,999	395(575)_f	TATGCTGGCTGATGGAAGTG
		395(801)_b	GCAGCAGAATGCATAACGAA
399	Ch 3L: 18,399,000-18,399,999	399(296)_f	CAGCATTAGCAAGGCAAACA
		399(716)_b	TATCGGGCGAAAGTCAAAAC
Ubx	Ch 3R, Ubx promoter (Schwartz et al. 2006)	Ubx +54	CCGCTGATAATGTGGATAA
		Ubx -177	CACCCCGATAAACTTAAAC
BXD-PRE	*bxd* PRE region (Wang et al. 2004b)	b4_F	ATGGCCTCATAATCGTTTGC
		b4_B	CTTTTCATAGCCGCTTTTGC

Sequence and coordinates were based on *D. melanogaster* Genome Annotation 4.0.

Table 2-4. Irradiation responsiveness of *reaper* and *hid* in various mutant embryos

Gene	Allele	Responsiveness of *reaper*	Responsiveness of *hid*
w	[67c23]	Stops at stage 12	Stops at stage 12
	[1118]	Stops at stage 12	Stops at stage 12
Su(var)3-9	[1]	Extended+	Extended+
	[2]	Extended+	Extended+
HDAC1 (rpd3)	[04556]	Extended+	Extended+
	[303]	Extended++	Extended++
	[326]	Extended+	Extended+
	[328]	Extended+	Extended+
Su(Z)12	[3]	Extended+	Extended+
	[4]	Extended+	Extended+
	[5]	Extended+	Extended+
trithorax	[1]	No change	No change
	[KG04195]	No change	N/A
	[EY13717]	No change	N/A
brm	[2]	No change	No change
zeste	[a]	No change	N/A
	[ae(bx)]	No change	N/A
	[v77h]	No change	N/A
Polycomb	[1]	Extended++	Extended++
	[3]	Extended+	Extended+
	[7]	Extended+	Extended+
	[1]/[3]	Extended++	Extended++
psc	[e22]	No change	N/A
	[1.d20]	No change	N/A
E(Z)	[S2e]	No change	No change
	[S4e]	No change	N/A
	[S3e]	No change	N/A
	M: [S2e]/ [S2e]	Slightly Extended	N/A
	M: [S2e]/ [S4e]	Slightly Extended	N/A

In wild type embryo, the responsiveness of both genes is turned off at stage 12. “No change” indicates no significant change of the timing of sensitive-to-resistant transition was found in the homozygous mutant embryo. “Extended+” and “Extended++” indicate that in homozygous mutant embryos the gene is still responsive till stage 12/13 or 14/15 (respectively). Mutant strains were balanced with GFP or lacZ balancer and homozygous mutants were identified as lacking anti-GFP or anti-β-Gal staining. M, maternal mutant genotype (parental genotype E(z)[S2e]/TM3 ubi-GFP).

CHAPTER 3
STRESS-RESPONSIVE EPIGENETIC REGULATION OF IRER

Abstract

The irradiation responsive enhancer region (IRER) was originally characterized as a 33 kb intergenic region required for mediating irradiation-induced expression of two pro-apoptotic genes, *reaper* and *hid*. It has been shown that the epigenetic status of the IRER determines the cellular sensitivity to exogenous stimuli such as irradiation. The IRER is better conserved during evolution than the *reaper* coding region, and deletion of this region results in significantly reduced viability, suggesting a vital role of IRER in development. In order to monitor the chromatin accessibility of the IRER region in live animals, we inserted a DsRed reporter gene controlled by an *ubiquitin* promoter into the endogenous IRER locus through homologous recombination. The insertion was verified by Southern blot, and the local chromatin structure was not affected by the insertion. The association of DsRed expression level and the chromatin accessibility of IRER was validated by chromatin immunoprecipitation with sorted DsRed positive and negative cells from IRER{ubi-DsRed} larvae. DsRed positive cells also showed a significant higher level of *reaper* expression than DsRed negative cells, indicating that the cells with open IRER are more sensitive to stress-induced cell death. The DsRed expressing cells were observed at the apex of the testis disc and the tips of the female ovarioles, where the germ line stem cells usually reside. Besides these specific localizations, sporadic DsRed positive cells were also found in various tissues, suggesting that the epigenetic regulation of IRER is not cell lineage-specific. Unexpectedly, rapid induction of DsRed upon irradiation was found in the larval imaginal discs. Also, nutrition-deprivation results in increased DsRed in IRER{ubi-DsRed} larvae. Its dynamic

epigenetic status suggests that IRER is responsive to different environmental stresses and adjust the cellular sensitivity to stress-induced apoptosis by changing its chromatin configuration.

Introduction

Cell death plays an essential role during *Drosophila* embryogenesis. However, it remains an enigma as to what mechanisms determine (or select) the specific cells to be eliminated at a particular developmental stage. Is it mostly dependent on the lineage of the cell and can be viewed as genetically predetermined? Or, is it due to the failure of a cell in the competition for growth factor, which is more or less by chance? Recent developments in studying the molecular mechanism of cell death during *Drosophila* embryogenesis has provided much insight into our understanding of the relative importance of, and the interaction between, these two mechanisms in shaping the embryo.

The fact that almost all developmental cell death is blocked in H99 mutant embryos underscores the importance of the IAP-antagonists in regulating cell death during embryogenesis. In the developing embryo, both Caspases and DIAP1 are ubiquitously expressed. It seems that in all of the analyzed embryonic systems, expression of the IAP-antagonists *reaper*, *hid*, or *grim* is required for inducing cell death.

The expression pattern of *reaper*, *grim*, and *sickle* in post-stage 11 embryos corresponds very well with the cell death pattern, indicating that these genes are specifically expressed in cells destined to die. Hid is the only one of the four IAP-antagonists that are expressed in cells that do not die at the end of embryogenesis, which at least in part is due to the fact that its pro-apoptotic activity can be suppressed by phosphorylation mediated by MAPK. In the case of the MG cells, both *hid* and *reaper*

are expressed in these cells to mediate cell death in a synergistic fashion (Zhou et al. 1997). Removing the function of one of the genes will result in a partial rescue compared to the total blocking of cell death in H99 mutant (Zhou et al. 1997). Coordinated expression of *reaper* and *hid* have also been observed in several other systems, such as ecdysone-induced degeneration of the midgut and salivary gland during metamorphosis (Jiang et al. 1997). In these systems, removing the function of one of the IAP-antagonists often has only mild or minor effect (Peterson et al. 2002; Yin and Thummel 2004). Although all four IAP-antagonists induce cell death mainly through their IAP-binding motif, their functions are not merely redundant (Wing et al. 2001; Zachariou et al. 2003). Reaper, Grim, and Sickle also have a C-terminal motif that could induce cell death at least in over-expression settings (Claveria et al. 2002; Olson et al. 2003; Claveria et al. 2004; Freel et al. 2008).

Interestingly, coordinated expression of *reaper* and *hid* is also observed when embryos at or before stage 11 were irradiated with ionizing irradiation. This coordinated induction is mediated by enhancers within the IRER upstream of *reaper*, as discussed in Chapter 2 (Zhang et al. 2008a). When this enhancer region is deleted, both *reaper* and *hid* lost their responsiveness to irradiation, suggesting that the same set of enhancers can regulate the expression of both genes. The responsiveness of *reaper* and *hid* to irradiation-induced DNA damage is developmental stage specific. Both genes became irresponsive to irradiation in embryos post stage 12. It turned out that this sensitive-to-resistant transition is due to epigenetic regulation of the IRER. Around stage 12, this region forms a heterochromatin-like structure that is inaccessible to DNase I, accompanied with the enrichment of repressive chromatin marks, such as H3K27me3

and H3K9me3, and the binding of HP1 and Polycomb group proteins (Zhang et al. 2008a).

It seems that understanding the transcriptional regulation of the IAP-antagonistss will hold the key to understand how cells are specified to die during embryogenesis. Even for the MG cells, although the EGFR pathway is responsible for determining the number of cells survival during embryogenesis, the specific expression of *hid* (and *reaper*) in these cells appears to be the pre-requisite for cell death in this lineage (Figure 3-1). However, fully characterization of the transcriptional regulation of the IAP-antagonists will unlikely to be a simple task. The four genes are located in a 350kb region that is conserved as synteny in the sequenced *Drosophila* genomes (Figure 3-2). All four genes transcribe toward the same direction (telomere of Chr. 3L). Remarkably long geneless intergenic regions (99kb and 40 kb, respectively) are flanking the *reaper* transcripts. These two long intergenic regions are highly conserved in distantly related *Drosophila* species and are enriched for Highly Conserved Non-coding Elements (HCNE). HCNEs are 50-150bp genomic sequences that are over 90-95% identical in different species. The clustering of HCNE, such as the pattern associated with the IAP-antagonists' region, is often associated with syntenies that form a genomic regulatory block (GRB) in both insects and vertebrates (Engstrom et al. 2007; Kikuta et al. 2007). GRBs often have several genes that are coordinated regulated by the enhancers located in HCNE. It is very likely that the four IAP-antagonists are in a genomic regulatory block. However, identifying all of the enhancers and interactions between/among the enhancers and promoters will be a challenge that demands much dedicated effort.

Materials and Methods

Fly strains

B11 (Df(3L:18,366-398)), L1 (Df(3L:18,366-386)) and JR44-1 (Df(3L: 18,365-367) deletion mutants are partially lethal. The homologous flies were grown for embryo collection. The overnight pool embryo collection was used for *reaper* ISH, and the stage 9-12 embyros (4.5-10.5 hr AEL) were collected for QPCR detection of pro-apoptotic genes. X3 reporter line (IRER{ubi-DsRed}) is viable. Homozygous flies were used in this study.

In Situ Hybridizaition

Embryos were collected and processed for immunocytochemistry and *in situ* hybridization as described previously (Zhou et al. 1995). cDNA clones 13B2 (*rpr*) and 5A1B (*hid*) were used to generate single-stranded digoxigenin-labeled cRNA probes using T3 RNA polymerase (Roche).

Southern Blot

The genomic DNA was extracted by phenol/chloroform from adult files, followed by restriction digestion for 5-6 hr. The digested DNA was loaded on 0.7% agarose gel and run overnight at low votage. The gel was then treated by Denaturization buffer (1.5M NaCl, 0.5M NaOH) for 45 min and washed twice by Neutralization buffer (1.5M NaCl, 0.5M Tris, pH7.5) for 30 min. The DNA was transfered to the membrane (Amersham HybondTM-XL) in the presence of 10x SSC buffer overnight. The membrane was then removed and rinse briefly with 6x SSC, followed by UV cross-linking. The hybridization was performed using Amersham Rapid-Hyb Buffer (GE Healthcare, RPN1635 or RPN1636). The DNA probe was prepared with Amersham Rediprime II Random Prime Labelling System (GE Healthcare, RPN1633 or RPN1634). The membrane was washed

with stringency washing steps. The membrane was dried and visualized by Typhoon Fluorescence Imaging system (Amersham Biosciences, Typhoon 9410).

Fluorescence-Activated Cell Sorting (FACS) with Whole Larvae

Raising animal

The overnight collection of eggs was washed and treated with 50% bleach for 3 minutes, then transfered to a 10cm culture dish containing SY food (100g sucrose, 100g baker's yeast, 1 L of boiled water, 20 ml 15% Nipagin in ethanol, 3ml propionic acid). After growing at 25^{o}C or RT for 3 days, the larvae were rinsed and transfered to a new petri dish with fresh SY food. The live larvae were collected by rinsing on the 350um nylon mesh and transered to clean petri dishes with 7% Sucrose, 2ug/ml Amphotericin B (AmB) (fungizone, Fisher BioSci).

Isolation of cells

The live larvae were homogenized with a mortar in the presence of dissociation buffer (Trypsin/EDTA (Sigma T4049)). Homogernized larvae were incubated at 28^{o}C water bath for 10 minutes, followed by the centrifugation at 200g for 1 minute. The tissue chunks was resuspended in Dissociation Buffer (1:1 mixture of T4049 and T4174 (10x trypsin/EDTA from Sigma)), and further processed by homogenizer at low speed for 2-3 minutes. The homogenized tissues were incubated at 28^{o}C for 60-90 minutes with shaking. The remaining large tissue chunks were removed by centrifugation at 200g for 1 minute at 4^{o}C. The supernatant was tranfered to a new 15ml/50ml tube first, and then passed through a 100 um cell strainer mesh into a new 50ml tube. Cells were collected by centrifugation at 600g for 5 minutes at 4^{o}C, then resuspended with Cell Culture Medium (M3 with 10%FBS, 1xP/S, 1ug/ml AmB), followed by another centrifugation at 500g for 3 minutes to remove small cell debris and further enrich

DsRed+ cells. Cells were then resuspended in ~ 10 ml cell sorting medium (M3, without FBS, 1xP/S, 1ug/ml AmB) per gram of original tissue. At least 20 min prior to FACS analysis, Hoechst 33342 was added to the sample at a final concentration of 1 ng / ml (up to 500 ng / ml), followed by a short vortex. FACS data were collected (DAKO MoFlo High Speed Sorter) and analysed with Summit software.

RNA/DNA Ratio

The 3rd instar lavae of IRER{ubi-DsRed} strain were homogenized, and the DsRed positive and negative cells were sorted by Fluorescence-Activated Cell Sorting (FACS). The simultaneous purification of genomic DNA and total RNA were performed with AllPrep DNA/RNA mini kit (Qiagen Cat#80204). Reverse transcription of RNA samples was done with High-Capacity cDNA Archive Kit (ABI). The DNA fragments containing the target sequences were PCR amplified and purified for the preparation of standards. Measure the DNA concentration by OD and calculate the molecular concentration based on the following formula: nmole DNA = (OD_{260} units x 90) / (length of DNA). The absolute quantification of DNA and RNA was performed by real-time PCR with standards.

Results

IRER Is Invovled in the Regulation of *reaper* During Development

Understanding the transcriptional regulation of the IAP-antagonists is crucial to understand how cells are specified to die during embryogenesis. A reporter construct containing the immediate 11kb sequence upstream of the *reaper* transcribed region gives a much broader expression pattern in transgenic animals than that of the endogenous *reaper* mRNA (Nordstrom et al. 1996), suggesting that there are missing elements that regulate endogenous *reaper* expression in the embryo.

The irradiation responsiveness was greatly decreased or completedly abolished in our IRER deletion mutants, suggesting this region contains *cis*-element(s) responsible for the stress-induced cell death. Also, deletion of IRER results in significantly reduced viability at the organism level; only 10-15% of homozygous animals survive to adulthood. So it is very likely that IRER is not only required for irradiation responsiveness, but also plays an important role in developmental process. Indeed, we found greatly reduced *reaper* expression in stage 10-11 embryos in three homozygous deletion mutants (Figure 3-3 and Figure 3-4A): B11 (Df(3L:18,366-398)), L1 (Df(3L:18,366-386)) and JR44-1 (Df(3L: 18,365-367)), especially in the segmental strips where the cell competition-induced apoptosis (cell death by chance) happens during development. However, the *reaper* expression in CNS was not affected. The stage 9-12 homozygous embryos (4.5-10.5 hr AEL) were collected and the expression of pro-apoptotic genes was measured by QPCR. Only a slightly decreased expression level of *reaper* was observed compared to wild type (Figure 3-4B). The discrepancy between QPCR and ISH may be attributed to the disruption of normal embryonic development in the mutants. The pool of embryos with the same age for QPCR may vary in developmental stage between muant and wild type embryos. Whereas the embryos for ISH were checked under the microscope to make sure they were at the same stage.

The deleted region in B11 and L1 flies contains one at least one putative P53 response element (P53RE, 3L:18,368,516-535) that conforms to the patterns of mammalian P53 binding sites (Brodsky et al. 2000). Correspondingly, genetic analysis indicated that the function of *Drosophila* P53 (DmP53) is required for mediating ionizing irradiation induced *reaper* expression and apoptosis (Lee et al. 2003; Sogame et al.

2003; Brodsky et al. 2004). It is possible that the reduction of *reaper* expression is due to the loss of binding of DmP53 or other transcription factors which is required for developmental cell death in some tissues at stage 10-11.

Monitor the Accessibility of IRER *in vivo*

The IRER is important for regulation of developmental apoptosis through recruiting regulatory transcription factors such as DmP53. It has been shown at least one P53RE reside in the IRER region (Brodsky et al. 2000). However, over-expression of DmP53 failed to induce *reaper* expression or apoptosis in many tissues, indicating that DmP53 alone is not sufficient in inducing *reaper* expression, or (and) the P53RE is not always accessible. As discussed in Chapter 2, IRER is subject to epigenetic regulation during the embryogenesis. Around stage 12, this region forms a heterochromatin-like structure that is inaccessible to DNase I, accompanied with the enrichment of repressive chromatin marks, such as H3K27me3 and H3K9me3, and the binding of Heterochromatin Protein 1 and Polycomb group proteins (Zhang et al. 2008a). This epigenetic modification of IRER may also make it inaccessible to transcription factors, probably including DmP53, that bind to this region otherwise. The developmental consequence of epigenetic regulation of the IRER is tuning down (off) of the responsiveness of the pro-apoptotic genes, and thus decreasing cellular sensitivity to stresses such as DNA damage (Figure 2-10G).

We generated a reporter line X3 (IRER{ubi-DsRed}) to monitor the accessibility of IRER. The ubi-DsRed reporter gene was inserted into the endogenous IRER region (18,375,553) through homologous recombination (Figure 3-5A and Figure 3-6A). The insertion locus is within the region that has the highest enrichment of H3K27me3 and H3K9me3 at resistant stage. The DsRed gene is controlled by *ubiquitin* promoter so that

the expression level will reflect the chromatin accessibility of its surrounding IRER. The insertion was verified by southern blot (Figure 3-5B). And the ChIP assays in homozygous embryos showed that the insertion does not interrupt the chromatin accessibility of the endogenous IRER region (Figure 3-6), consistent with the DNaseI accessibility assay (unpublished data by Can Zhang).

Before we use the X3 line to study the accessibility of IRER during *Drosophila* development, we need to validate the association between DsRed fluorescence signal and the chromatin structure of the insertion site. We used fluorescence-activated cell sorting (FACS) to separate DsRed positive and negative cells, and did ChIP assays around the insertion site. As we expected, DsRed negative cells had much higher H3K27me3 level at inserted reporter gene locus than positive cells (Figure 3-7A), indicating that the DsRed signal is indeed associated with open chromatin. Accordingly, DsRed positive cells showed higher *reaper* expression level than DsRed negative cells, indicates a more permissive chromatin state of IRER in positive cells with which the related *trans*-factors might interact (Figure 3-7B). With these validations, we have confidence to use the reporter line to monitor the openness of IRER *in vivo*, which may help us to understand the transcriptional regulation of pro-apoptotic genes.

Unsurprisingly, all cells before embryonic stage 11/12 have DsRed expression, which start to diminish in most cells after stage 12. Following the status of IRER in post-embryonic development brought several interesting findings. For instances, in male third instar larvae, a group of cells at the apex of the testis disc exhibit a much brighter DsRed signal than any other tissues (Figure 3-8 A and B). The location of these DsRed-expression cells suggests that they are male germ line stem cells (GSCs), which will be

verified by staining for GSC specific markers in the future. In contrast, DsRed signal is turned off in the progenies of GSC, i.e. the spermatocytes that situated just posterior to the GSCs. This suggests that the epigenetic regulation of IRER is not cell lineage-specific; rather, it is development stage/differentiation status-specific. Similarly, the most concentrated DsRed signals were found at the tips of the female ovarioles, where the female GSCs are localized (Figure 3-8C). In the 3rd instar larvae eye discs, most cells have no (or very low level) DsRed signal. However, discrete cells have significant levels of DsRed (Figure 3-8D). We also looked at the DsRed pattern in live pupae a high-resolution photoacoustic tomography (PAT) approach, because there is an abundance of proliferation, differentiation, and apoptosis in pupal development. (Figure 3-8E, preliminary results). Some specific areas lighted up by DsRed suggest that those cells are particularly sensitive to developmental stress-induced apoptosis, although it is difficult to distinguish these cells due to the lack of specific markers.

Discussion and Future Directions

As described in Chapter 2, our initial measurement IRER accessibility was through DNase I sensitivity assay performed on nuclei extracted from staged embryos (Zhang et al. 2008a). This approach succeeded because nearly all cells in early stage embryos respond to irradiation, indicating that IRER is open in these cells. In post-stage 12 embryos, most, if not all, cells lost their responsiveness to irradiation, indicating that IRER is closed. However, it is simply not feasible to use this method to follow the status of IRER in tissues after embryonic development or in individual cells. It is well known that later during development, certain tissues, such as the wing and eye discs in 3rd instar larvae, regain responsiveness to irradiation induced cell death (Ollmann et al. 2000; Wichmann et al. 2006). To test whether IRER becomes open again in these

tissues, we generated the IRER{ubi-DsRed} reporter strain in which the DsRed was used as a cellular reporter for monitoring its surrounding chromatin accessibility. The DsRed reporter gene within IRER should only be expressed in cells that have an open IRER, such as the undifferentiated cells in early stage embryos. In this reporter strain, we observed the ubiquitously expressed DsRed in early stage embryos. After stage 12, DsRed mRNA began to decrease. By the end of embryogenesis, only a few cells and the salivary gland have detectable level of DsRed mRNA by ISH (The DsRed protein has a half-life of over 40hrs). At 3rd instar larvae, most cells have no (or very low level) DsRed signal. However, discrete cells in the gut, eye and wing disc, and the male testis have significant levels of DsRed (Figure 3-8).

Some of our observations indicate that the epigenetic status of the IRER is quite dynamic. Significant increased DsRed signals were found in the larvae imaginal discs upon irradiation or heat-shock treatment (unpublished data by Can Zhang). Also, nutrition deprivation resulted in increased DsRed in IRER{ubi-DsRed} larvae (unpublished data by Michael Novo). Therefore, unlike the traditional view of epigenetic regulation, IRER is responsive to different environmental stresses and controls the cellular sensitivity to stress-induced apoptosis by altering its chromatin configuration.

It is possible that the IRER is also required for cell death resulting from the developmental stresses, such as cell competition for growth factors. One of our focuses of this work will be documenting the expression pattern of the IRER{ubi-DsRed} reporter. In addition to addressing the general questions such as "when and in which cells is IRER open/closed?" We will also address questions such as: "Is IRER specifically open in mitotic cells? ", "Is IRER open in cells that undergo programmed cell

death? ", etc. by monitoring DsRed signal together with other cellular markers. The lacks of specific markers may be a limitation. For instant, we are interested in knowing whether the discrete DsRed-positive cells in the midgut are the pluripotent stem cells described by Ohlstein and Spradling (Ohlstein and Spradling 2006). However, there is no specific marker to distinguish these cells. We could potentially perform mosaic clone assay in the background of IRER{ubi-DsRed}, but that would be rather time consuming. Collaboration with other interested groups is a possibility. There is an abundance of proliferation, differentiation, and apoptosis in pupal development. But the DsRed signal from tissues inside the pupa is hard to monitor due to the deflection and reflection of the cocoon shell. We are collaborating with Dr. Huabei Jiang's group in Dept. of Biomedical Engineering (UF) to develop a high-resolution photoacoustic tomography (PAT) approach to monitor the dynamics of DsRed expression in live pupae (Figure 3-8E, preliminary results). The development and optimization of the technology will not and can not be covered by this project. However, if it is successful, this will allow us to perform real-time monitoring of epigenetic status of IRER in live developing animals.

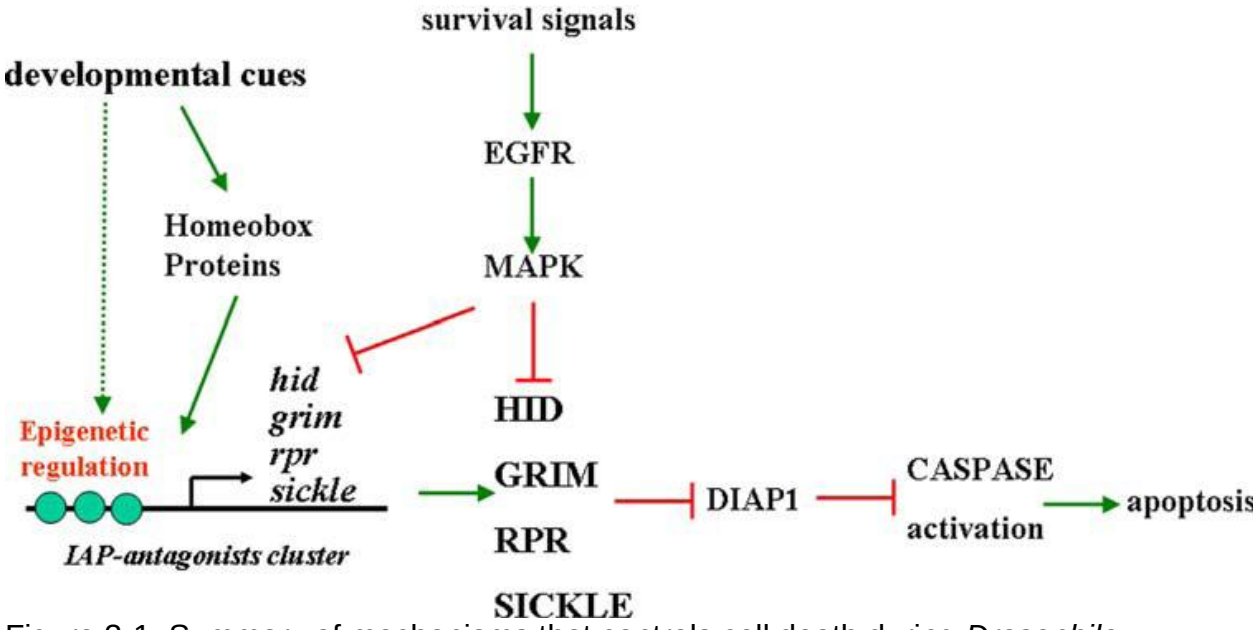

Figure 3-1. Summary of mechanisms that controls cell death during *Drosophila* embryogenesis. Developmental cues control the expression of IAP-antagonists through specific transcription factors and through epigenetic regulation of the enhancer regions. The EGFR pathway suppresses the expression of hid and inhibits the pro-apoptotic activity of HID protein, thus determines the number of cells that can survive.

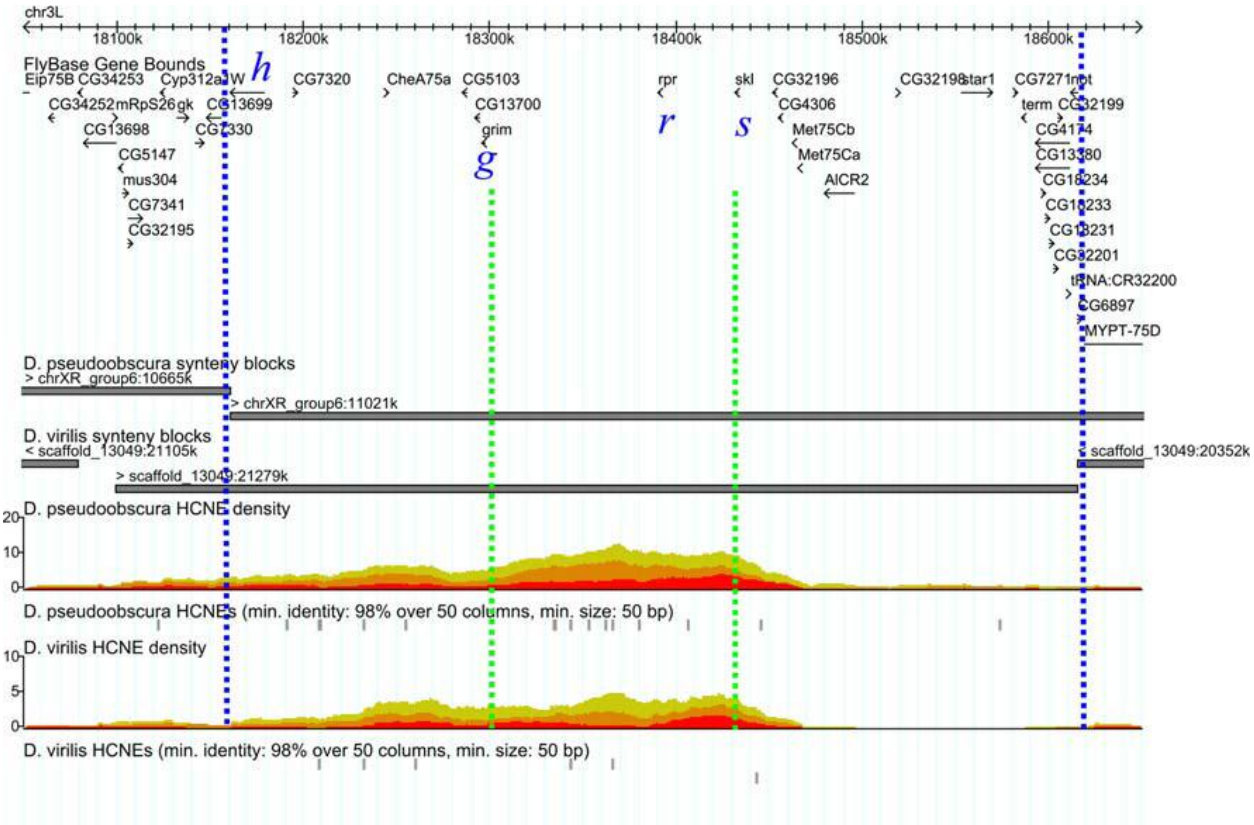

Figure 3-2. Genomic regulatory block of the IAP-antagonists (figure generated in http://ancora.genereg.net/). The four pro-apoptotic genes, *hid* (*h*), *grim* (*g*), *reaper* (*r*), and *sickle* (*s*), are in the same synteny that has high density of HCNE in the middle. The blue dotted lines indicated the minimum syntenic region that is conserved in all sequenced *Drosophila* genomes. The green dotted lines indicate the non-coding genomic regions surrounding *reaper*, which is enriched with HCNE (coordinates based on genome release 5.0).

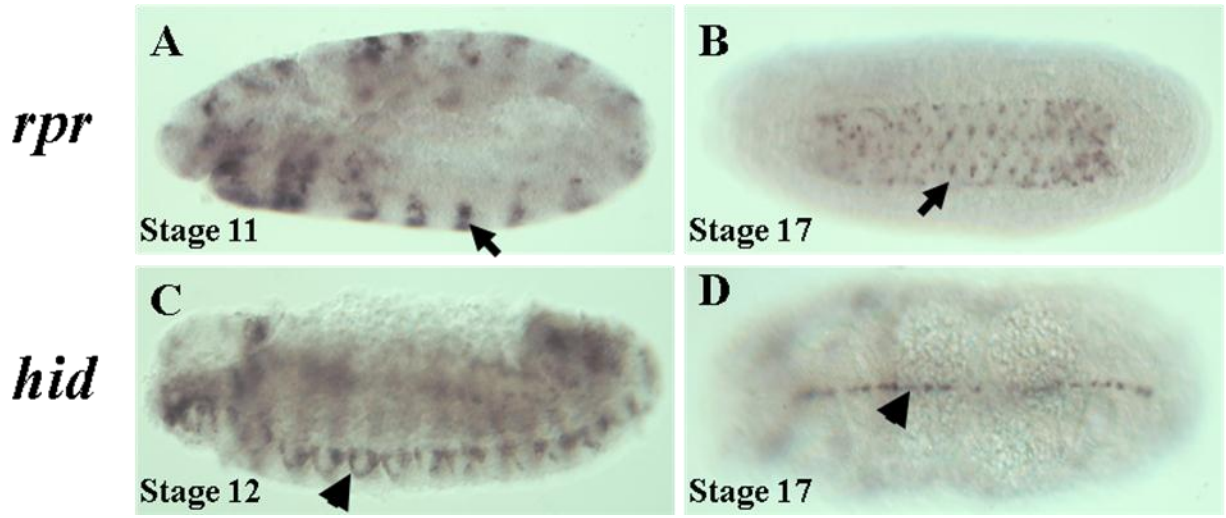

Figure 3-3. Dynamic expression pattern of *reaper* and *hid*. The distribution of *reaper* (A, B) and *hid* (C, D) mRNA in embryos at different stages was revealed via in situ hybridization. (A) Sagittal view of stage 11 embryo, *reaper* is expressed in a segmentally repetitive pattern in the epidermis. However there is significant variation among segments. At later stage (B), *reaper* is only expressed in discrete cells in the ventral nerve cord (arrow). At stage 11–12 (C), *hid* is expressed in the epidermis as well as the CNS midline (arrow head). Some of these *hid*-expressing MG cells remain alive at the end of embryogenesis (D).

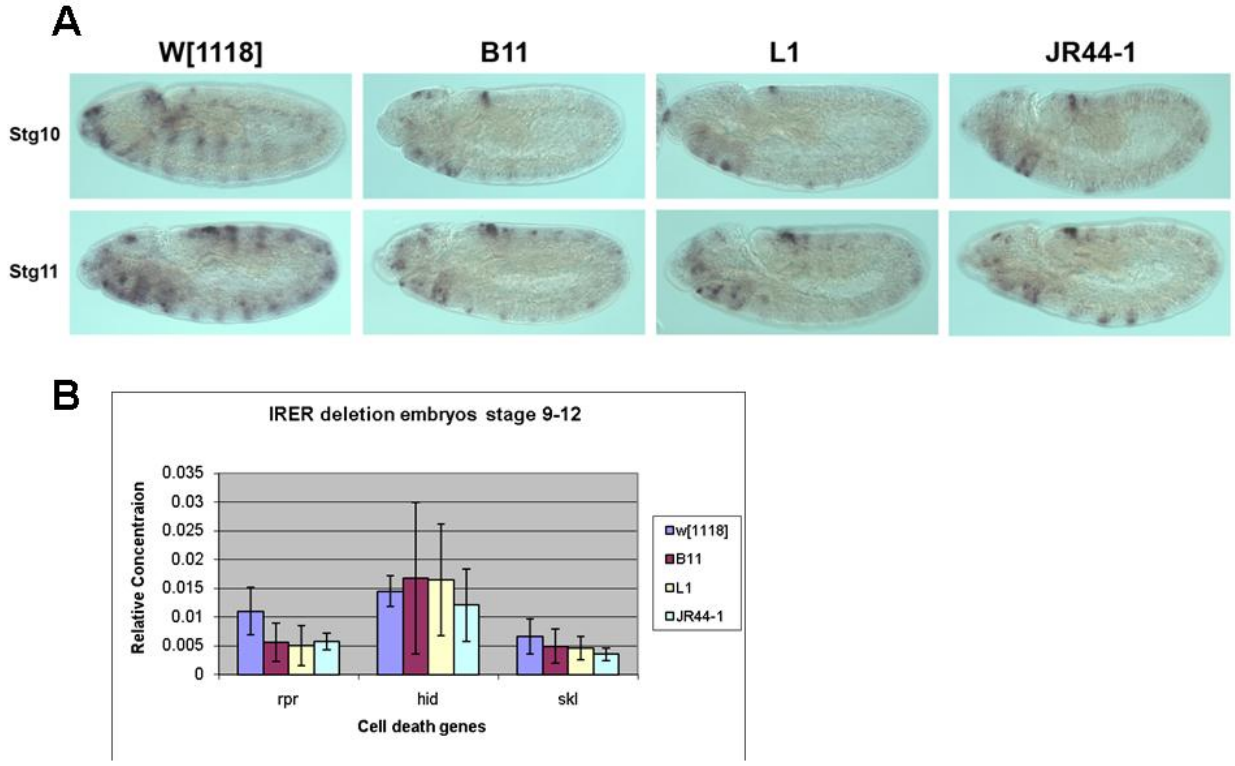

Figure 3-4. Downregulation of *reaper* in IRER deletion mutants. A) ISH signals of *reaper* gene were decreased in IRER deficiency homozygous mutant embryos at stage 10-11, compared to wild-type w^{1118}. B11 (Df(3L:18,366-398)), L1 (Df(3L:18,366-386)) and JR44-1 (Df(3L: 18,365-367)). B) QPCR of three pro-apoptotic genes *reaper*, *hid* and *sickle* in IRER deletion homozygous mutant embryos and wild-type embryos at stage 9-12.

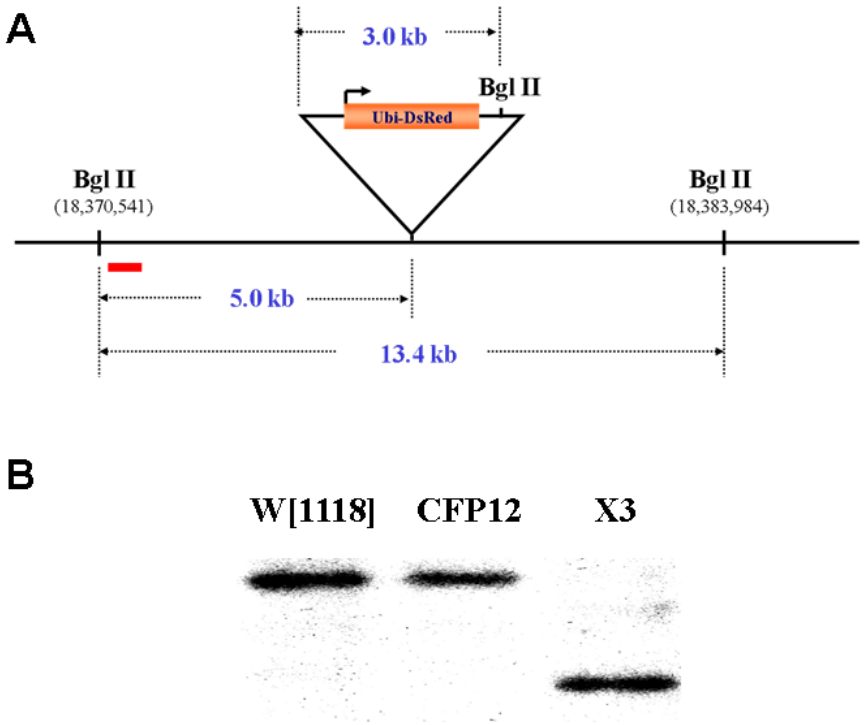

Figure 3-5. Southern blot verification of X3 insertion. A) Schematic map of X3 insertion locus. The ubi-DsRed reporter gene was inserted into the endogenous IRER region (18,375,553) by homologous recombination. Both wild-type and X3 genomic DNAs were digested with BglII and analyzed with the probe near the left BglII site, shown by the red bar. B) Southern blot with genomic DNA from wt, CFP12 donor strain and X3 flies. Both wt and CFP12 had the specific 13.4kb bands, while the band in X3 DNA was about 8kb.

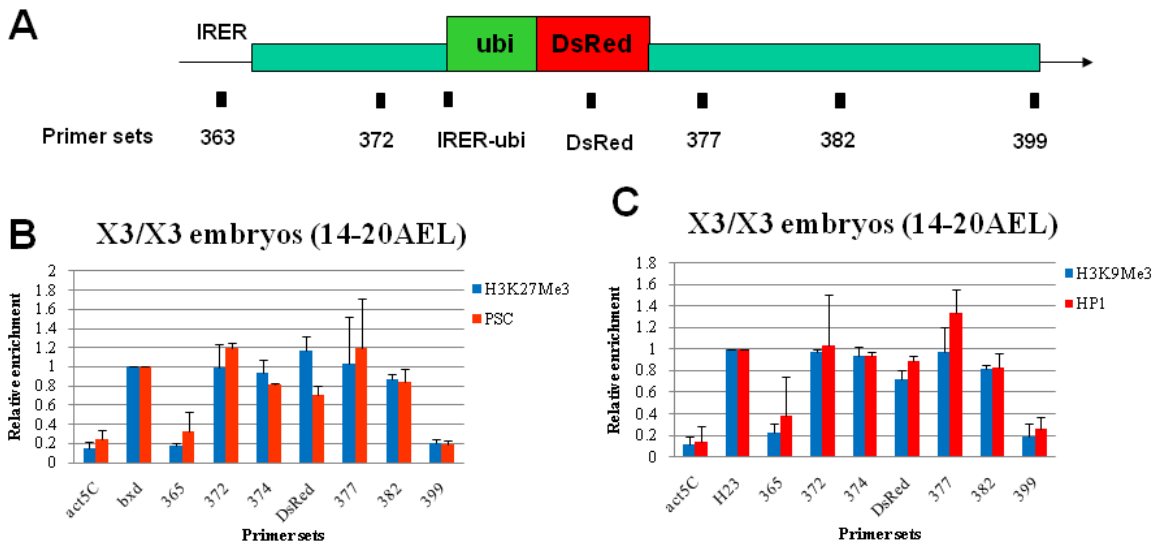

Figure 3-6. Insertion of ubi-DsRed reporter into endogenous IRER region did not alter the chromatin profiles of this region in X3 flies. A) The ubi-DsRed reporter gene was inserted into the endogenous IRER region (18,375,553) by homologous recombination. The black bars below are primer sets for DNaseI sensitivity and ChIP assays. B) and C) ChIP assays with H3K27me3, H3K9me3, PSC and HP1 in X3 homozygous embryos at late stage (14-20 AEL). Act5C was used as negative control. *bxd* PRE region was positive control for H3K27me3 and PSC, while pericentromeric H23 locus was used as positive control for H3K9me3 and HP1.

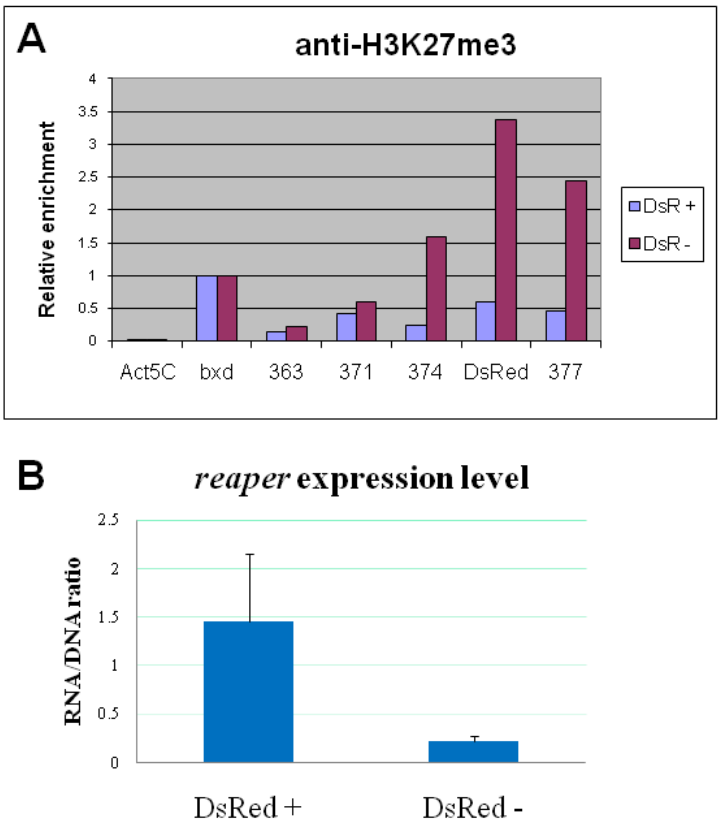

Figure 3-7. Validation of IRER{ubi-DsRed}. A) X3 pupae were collected and homogenized, followed by the Fluorescence-activated cell sorting to separate the DsRed positive and negative cells. The cell sorting and ChIP was done once, QPCR measurement was repeated twice and the results were consistent. Only one set of QPCR data was shown. Both DsRed positive and negative cells are ChIP with H3K27me3 antibody, and the recovery rate was normalized to the positive control bxd PRE locus. B) *reaper* expression levels in DsRed positive cells and DsRed negative cells.

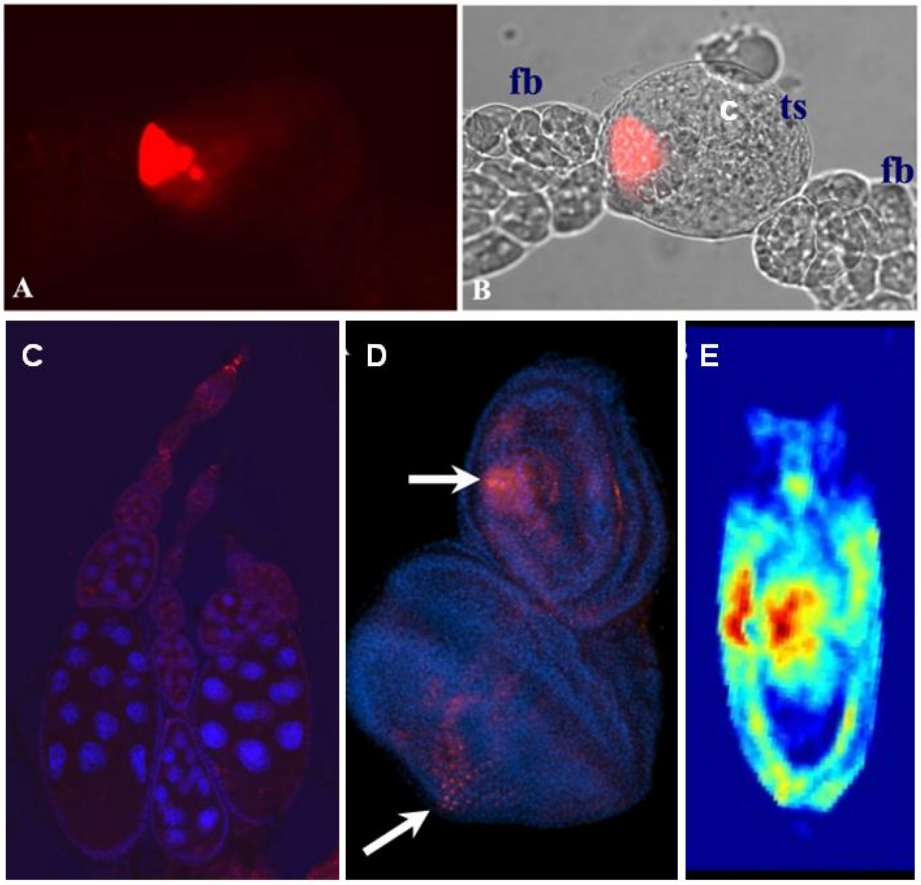

Figure 3-8. The DsRed expression patterns in different tissues of the IRER{ubi-DsRedP reporter flies. A) DsRed signal (red) at the apex of the testis in third-instar larvae. B) Overlay of DsRed and DIC image; “fb”-fat body; “ts”-testis. A) and B) are pictures of the same tissue, however the picture in B is of a slightly different focus plan and was taken with both DIC and fluorescence filters. C) DsRed signal concentrated at the tip of the ovarioles. D) Distribution of DsRed and DAPI signal in the antenna-eye imaginal discs. IRER{ubi-DsRed} is expressed in cells at the posterior tip of the eye disc and at the do (arrow) but not at the morphogenetic furrow. E) Preliminary data of PAT detection of DsRed expression in the pupae.

CHAPTER 4
A NOVEL CHROMATIN BARRIER ELEMENT DELIMITS THE FORMATION OF FACULTATIVE HETEROCHROMATIN WITHOUT BLOCKING ENHANCER FUNCTION

Abstract

Insulators are discrete DNA elements at the boundaries of genes that protect the gene from the positive or negative regulatory influences of its neighboring environment. Insulators have two biological functions: blocking enhancer-promoter interaction and stemming heterochromatin propagation. In this study we identified a chromatin barrier that specifically limits the epigenetic regulation to a distal enhancer region so that repressive histone modification cannot reach the promoter and proximal enhancer regions of *reaper*. Unlike all of the known insulators identified from *Drosophila*, the IRER (irradiation responsive enhancer region) left barrier (ILB) does not contain enhancer-blocking activity. This is in accordance with the fact that epigenetic regulation of IRER is dynamic and reversible following certain stresses, under which circumstances the enhancer function of IRER is required for stress-induced pro-apoptotic gene expression. The barrier activity of ILB requires the binding of *Drosophila* Cut proteins, which might recruit histone modifier enzymes, such as histone acetyltransferase CBP, and change the local chromatin environment into the conformation that favors the euchromatin formation. This study broadens the knowledge about the insulator/boundary elements and their roles in eukaryotic genome organization, and discovers the potential molecular mechanism for the pleiotropic phenotype in Cut mutants.

Introduction

While every cell has a complete genome, only a portion of the genomic information is expressed in accordance with the distinct property of each cell. Histone modifications

play a fundamental role in determining the accessibility and expressivity of the underlying genetic information. We have long known that distinct histone modifications are associated with open (euchromatin) or closed (heterochromatin) conformations (Jenuwein and Allis 2001). Recent high resolution epigenomic analyses further revealed that even within a gene, distinct patterns of histone modifications are associated with different anatomic parts of the gene, such as the promoter, enhancer, or the transcribed region, etc. (Wang et al. 2009). However, the mechanisms that determine the range of a particular histone modification remain enigmatic.

Insulator/boundary elements are regulatory DNA sequences that help to organize the genome into distinct domains and prevent promiscuous gene regulation. Most of the previously characterized insulator/boundary elements in high eukaryotes harbor two activities. One is enhancer-blocking, which prevents the enhancer-promoter interaction when it is positioned in between. The other is chromatin barrier activity, which blocks the spread of heterochromatin formation into euchromatic regions (Gaszner and Felsenfeld 2006).

The molecular mechanisms of insulator/boundary elements are not well understood. Much of our knowledge about the mechanism of the enhancer-blocking activity came from studying insulators in *Drosophila*, where all of the characterized insulators have enhancer-blocking activity (Gurudatta and Corces 2009). Several non-exclusive models have been proposed for the mechanism of enhancer-blocking function, including the promoter decoy model, the physical barrier model, and the loop domain model (Bushey et al. 2008; Raab and Kamakaka 2010).

A few model systems have been exploited to understand the mechanism of chromatin barrier activity. In the yeast mating locus, the binding of specific transcriptional factors creates a gap in the nucleosome array, which prevents the propagation of heterochromatin formation (Bi and Broach 2001). In high eukaryotes, much of what we know about chromatin barrier activity came from studying cHS4, the insulator in the chicken β-globin locus. The complete cHS4 has both enhancer-blocking and barrier activity. However, a series of elaborate dissection indicated that its enhancer-blocking and barrier activities are separable and are carried out by distinct DNA elements (Bell et al. 1999; Recillas-Targa et al. 2002; West et al. 2004; Gaszner and Felsenfeld 2006). Deletion of the CTCF binding site, which is responsible for the enhancer-blocking activity, did not affect the barrier activity of cHS4 (Recillas-Targa et al. 2002). Rather, a binding site for USF1 (upstream stimulatory factor 1) is responsible for the recruitment of chromatin-modifying enzymes, which catalyze euchromatin-specific histone modifications that are incompatible with heterochromatin formation (West et al. 2004; Huang et al. 2007).

Although the enhancer-blocking and barrier activities are clearly separable and are mediated by distinct *cis* elements in the case of cHS4, it is not clear whether this is common for other metazoan insulators. Many insulators have been characterized in *Drosophila*, which could be categorized into at least 5 types based on the responsible binding proteins (Maeda and Karch 2007; Gurudatta and Corces 2009). All of these insulators have enhancer-blocking activity (Maeda and Karch 2007; Gurudatta and Corces 2009). Several of them, such as the Su(Hw)/*gypsy* insulator, also have strong barrier activity (Roseman et al. 1993). However, there is no evidence that the two

functions are mediated by distinct *cis* elements. In the case of Su(Hw)/*gypsy*, it appears that different domains of the binding protein Su(Hw) can interact with distinct proteins for enhancer-blocking and for barrier activity (Kurshakova et al. 2007).

In searching for the mechanism that controls the responsiveness of pro-apoptotic genes following cytotoxic stress, we found that the irradiation responsive enhancer region (IRER) is subject to epigenetic regulation (Zhang et al. 2008b). IRER, located upstream of *reaper,* is actually required for mediating irradiation-induced expression of three pro-apoptotic genes *reaper, hid* and *sickle,* all of which locate in a 200kb region and are transcribed in the same direction. IRER is open in undifferentiated proliferating cells during early embryogenesis, conferring high sensitivity to ionizing irradiation induced apoptosis. However, in most differentiating and differentiated cells in late embryogenesis, IRER forms a heterochromatin-like structure that is inaccessible to DNase I. Consequently, the epigenetic repression of IRER renders the pro-apoptotic genes irresponsive to irradiation in these cells. This epigenetic blocking, signified by enrichment of H3K27me3 and H3K9me3 and binding of Polycomb group (PcG) proteins, is strictly limited to IRER. The promoter and transcribed regions of *reaper* do not have repressive histone marks and remain open in later stage embryos. This restriction of heterochromatin formation is functionally significant. While *reaper* becomes irresponsive to irradiation in later stage embryos, it is expressed under developmental cues in neuroblasts (Maurange et al. 2008) and differentiated motor neurons (Rogulja-Ortmann et al. 2008) and required for programmed cell death at late embryogenesis.

In this study we identified a segment of sequence at the left boundary of IRER that has strong barrier activity in blocking the propagation of repressive histone marks.

However, unlike the Su(Hw)/*gypsy* insulator, the IRER left barrier (ILB) could not block the reporter gene from being activated by the UAS/GAL4 enhancer when placed in between them. Thus it appears that ILB is a barrier-only insulator that lacks enhancer-blocking activity.

Materials and Methods

Constructions of Transgenes

The polylinker sequence was synthesized and cloned into pBluescript KS between EcoR V and BamH I sites. The multiclonal site of the reconstructed vector contains the following restriction sites: Kpn I – Hind III – EcoR V – Nde I – Pst I – Nru I – Nco I – BamH I – Xba I – Not I. The 3'P end and 5'P end sequences were PCR-amplified from pP{EndsOut2} (Jeff Sekelsky) and verified by sequencing, then inserted in the vector restricted with Kpn I/Hind III and BamH I/Xba I respectively. The bacterial attachment (attB) site was amplified from P[acman] vector (Venken et al. 2006) and subcloned at the Nde I site. The 3xP3-DsRed fragment was amplified from M{3xP3-RFPattP} and subcloned at the BamH I site. The 416 bp fragment containing two FRT sequences and a Spe I restriction site in between was inserted at the Nco I site. The experimental ILB fragments were amplified by PCR from w^{1118} flies using primers containing Spe I site and inserted between two FRT sequences in the vectors described below.

- **pBT1:** A 661 bp Nde I - Pst I fragment containing the *Ubx* PRE sequence was kindly provided by V. Pirrotta. This fragment was subcloned between Nde I and Pst I sites in the reconstructed vector mentioned above.
- **pBT3:** The fragment containing a Mlu I restriction site, flanked by two loxP sites, was synthesized and inserted into pBT1 vector at the Pst I site, between the *UBX* PRE and FRT sequences. PCR-amplified Su(Hw) binding region was subcloned into the Mlu I site between the two loxP sequences.
- **pIT1:** The *UBX* PRE sequence in pBT1 was substituted by five tandemly arrayed optimized GAL4 binding sites, amplified from pUAST (Brand and Perrimon 1993).

Fly Strains, Germ Line Transformation and Genetic Crosses

Flies were grown on standard rich media and maintained at 25^{o}C. The transgenic flies were generated by either P-element mediated transformation or ΦC31 integration system (Rainbow Transgenic Flies, Inc., California). The w^{1118} *Drosophila* strain was used for P-element insertion. ΦC31 lines 9752 and 9724 (PBac{y[+]-attP-3B}VK00037 and PBac{y[+]-attP-3B}VK00003a) were used for site-specific integration into the 2nd chromosome (Venken et al. 2006). The transformants were verified by PCR analysis. The transformation efficiency was recorded in Table S1.

Germline excision of the ILB9kb barrier sequence was performed by crossing the BT1-ILB9kb line 47-2 with flies carrying a heat shock-inducible FLP transposase (*y^{1}, w^{1118}, hsFLP*). The progeny were heat shocked for 1.5 hr at 37^{o}C on 3-5 successive days during larval growth. The female progeny were collected and crossed with *TM3/TM6* males. In the following generation, flies were selected for a change in the eye-specific DsRed signals, and PRE excision was confirmed by PCR analysis with the following primers: a1, 5'- CGCCAGCAACAAAGAACTAA-3'; a2, 5'-GGCCGCTCTAGTGGATCTTG-3'; b1, 5'- GATAGGACTACGCGCACCAT-3'; b2, 5'-TGTTCAGCTGCGCTTGTTTA-3'. The BT3 lines with *gypsy* excisions were obtained by crossing the flies with the Cre line (*y^{1}, w^{67c23}; Sco/CyO, Crew1*). The female progeny were crossed with *Sco/Cyo* males, and the desired flies were selected from the next generation based on the eye-specific DsRed signals. The excisions were verified by PCR analysis.

Chromatin Immunoprecipitation (ChIP)

The ChIP method was an adaptation of Cavalli's protocol (Chanas et al. 2004) with some modifications. H3K27me3 and H3K9me3 polyclonal antibodies were kindly

provided by Thomas Jenuwein. 150-200 mg adult flies were collected 5 days post eclosure, and cross-linked in 5 ml of Buffer A1 (60 mM KCl, 15 mM NaCl, 4 mM $MgCl_2$, 15 mM HEPES (pH7.6), 0.5% Triton X-100, 0.5 mM DTT, 10 mM sodium butyrate, and 1% Protease Inhibitors Cocktail (PIC) [Sigma]), in the presence of 1.8% formaldehyde, by homogenization in a Potter and then in a Dounce homogenizer with the “Loose” pestle (three strokes each), followed by incubation for 20 min at room temperature. Cross-linking was stopped by adding glycine to 225mM for 5 min on ice. The homogenate was centrifuged for 5 min, 4000*g* at 4°C, then the supernatant was discarded and the crude nuclei pellet was washed three times in 3 ml Buffer A1and once in 3 ml Buffer A2 (140 mM NaCl, 15 mM HEPES pH 7.6, 1 mM EDTA, 0.5 mM EGTA, 1% Triton X-100, 0.5 mM DTT, 0.1% sodium deoxycholate, 10 mM sodium butyrate, 1% PIC) at 4°C. After the washes, nuclei were resuspended in 3 ml Buffer A2 in the presence of 0.1% SDS and 0.5% N-lauroylsarcosine, and incubated for 10 min in a rotating wheel at 4°C. At the end of the incubation, 0.3g of acid washed glass beads (Sigma, G-1277) were added, and the samples were sonicated on ice using a Branson Sonifer 450 to obtain fragmented DNA with an average size of approximately 500bp. The immunoprecipitation and QPCR quantification were performed as previously described (Zhang et al. 2008b). For primer sequences please refer to APPENDIX A.

Gene Expression Analysis

mRNA was extracted with RNeasy Mini Kits (QIAGEN). cDNA was prepared by reverse transcription of mRNA with a High-Capacity cDNA Archive Kit (Applied Biosystems). Quantitative real-time PCR (QPCR) followed protocols provided by the manufacturer. The real-time PCR step used 10 ng cDNA/PCR well with triplicates per gene per sample. The following primers were used for QPCR: DsRed_f, 5’-

GAAGCTGAAAGACGGTGGTC-3'; DsRed_b, 5'- CGTCCCTCGGTTCTTTCATA-3'; corto_f, 5'- CAACAGCACCAGCAGATGTC-3'; corto_b, 5'- CTCTGGCTCTGGCTCTGACT-3'.

Results

Epigenetic Blocking of IRER Is Restricted to the Upstream Regulatory Region of *reaper*

In our previous work, we showed that in later stage embryos, the Irradiation Responsive Enhancer Region forms a facultative heterochromatin structure that is resistant to DNase I. IRER in later stage embryos is enriched for both H3K27me3 and H3K9me3 and is bound by Polycomb group (PcG) proteins and HP1 (Zhang et al. 2008b). While PcG group genes are required for epigenetic blocking of IRER, the spatial characteristics of epigenetic regulation of IRER is rather different from that of canonical PcG-mediated silencing of homeotic genes. The distribution of repressive histone marks and the binding of the PcG proteins are strictly limited to IRER, which is more than 2 kb away from the basic promoter and coding region of *reaper* (Figure 4-1A).

Chromatin immunoprecipitation (ChIP) analysis with adult flies confirmed that repressive histone modifications remain to be restricted to IRER. The enrichment levels of H3K27me3 and H3K9me3 in the central part of IRER is comparable, or higher than, the respective positive control regions of Ubx promoter and H23 (Figure 4-1B). The homeotic gene *Ubx* is silenced by PRE-mediated suppression in most cells in the adult and H23 is a pericenteremeric heterochromatin locus on the 2nd chromosome. The levels of both repressive marks associated with IRER decrease significantly at the left

boundary of IRER, approximately -2 to -5kb upstream of *reaper* transcription starting site (TSS).

The restriction of the repressive histone marks H3K27me3 to IRER but not the *reaper* transcribed region and the immediate enhancer region was verified by independent ChIP-Seq analysis in cultured *Drosophila* S2 cells. Neither *reaper* nor *hid* is responsive to irradiation in the S2 cells (Lin et al, unpublished data). The distribution of the H3K27me3 upstream of the *reaper* locus resembles what we observed with adult flies (Figure 4-1C). High resolution ChIP-Seq analysis also verified that the *reaper* transcriptional start site is located as previously annotated and is enriched for H3K4me3 and engaged by RNA Polymerase II (Figure 4-1C). Since the level of *reaper* expression is barely detectable in populations of S2 cells, most likely not expressed in most non-dying S2 cells, the significant enrichment of H3K4me3 and Pol II binding indicate that similar to heat shock genes, *reaper* has an engaged but “paused” promoter ready for quick induction (Rougvie and Lis 1988; Zeitlinger et al. 2007).

The restriction of repressive histone marks and heterochromatin formation to IRER but not the *reaper* promoter and coding region is functionally important. Although *reaper* is no longer responsive to irradiation in later stage embryos, it is expressed in late stage embryos and is required for eliminating obsolete neuroblasts (Peterson et al. 2002; Bello et al. 2003). Thus the restricted formation of heterochromatin in IRER but not other enhancer or coding regions of *reaper* is necessary for continued developmental expression of *reaper* while significantly tuning down its responsiveness to environmental stress. Since the transition of repressive histone modifications was about 5kb upstream of *reaper*, it is unlikely that the transition is simply due to the presence of the TSS and

TSS-associated histone modifications. Rather, we hypothesized that a chromatin boundary element is responsible for restricting the repressive histone marks from reaching the *reaper* promoter and the proximal enhancer regions.

Verification and Identification of the IRER Left Barrier (ILB)

Due to the large size of the candidate region that needs to be tested, we developed the construct “p Barrier Tester 1” (pBT1) which allows us to test barrier activity for DNA fragments up to 9 kb via either p insertion or phiC31-mediated docking (Figure 4-2A). In this construct, the compact 3xP3-DsRed reporter/marker gene gives strong DsRed (RFP) expression in the eye (Sheng et al. 1997; Bischof et al. 2007). The Polycomb Response Element (PRE) from the *Ubx* locus was placed upstream of the 3xP3-DsRed. This PRE has been shown to function as a general silencer that can initiate PcG-mediated silencing in different loci (Chan et al. 1994; Sengupta et al. 2004). Restriction sites in between of the PRE and the reporter allow insertion of DNA fragments to be tested for barrier activity. The inserted DNA fragment is flanked by two FRT sites to allow FLP-mediated excision. Similar designs, with different (larger) reporter genes, have been used successfully to demonstrate that the Su(Hw)/*gypsy* and other insulators can block PRE- mediated silencing (Sigrist and Pirrotta 1997; Mallin et al. 1998). We reasoned that if the tested DNA sequence contains a barrier activity that is able to counteract the repressive effect of the PRE, then the DsRed reporter will be expressed and allow the recovering of insertion events.

To test the feasibility of this approach, a 9kb fragment (ILF9kb; Chr3L:18,391,265-18,399,880, *D. melanogaster* genome release 5) that covers from left side of IRER to the *reaper* promoter, was cloned into in pBT1 (Figure 4-2B). P-mediate insertions were recovered by monitoring the 3xP3 DsRed expression in the adult eye (Figure 4-2C, left).

The expression of DsRed suggests that the reporter gene was protected from PRE-mediated silencing by the inserted fragment. To verify that indeed the inserted fragment was responsible for blocking PRE mediated silencing, the transgenic lines were crossed to fly stain carrying *ey*-FLP. This resulted in a great reduction of the DsRed signal in the eye, indicating that the reporter gene is been silenced/suppressed in the absence of ILF9kb (Figure 4-2C, right; Figure 4-3). The successful excision of ILF9kb in flies carrying *ey*-FLP was verified by PCR analysis (Figure 4-4). The level of DsRed expression was fully restored when *ey*-FLP was crossed out (Figure 4-2C, top). Similar findings were confirmed with all of the 7 independent insertion lines, suggesting it is independent of insertion site (Figure 4-3). All the evidence indicate that ILF9kb is capable of blocking PRE-mediated silencing effect of PRE from reaching the reporter gene.

To locate the essential barrier element within the 9kb, and to rule out that the observed suppression of PRE-mediated silencing was simply due to the length of the fragment, we tested a series of DNA fragments within the ILB9kb region to narrow down the region that contains the barrier activity (Figure 4-2B). In order to make the expression level comparable, the testing constructs for the sub-fragments were inserted into the same attP docking site on the 2nd chromosome (line 9752; PBac{y[+]-attP-3B}VK00037). The barrier activities of these fragments were initially screened based on the expression of the marker gene. Positive fragments were then verified by comparing the relative expression levels of the reporter in the absence or presence of *ey*-FLP (Figure 4-2D, Table 4-1 and Table 4-2).

To safeguard against false negatives due to problem associated with generating the transgenic insertion, the F1 progeny of each injection were verified by PCR analysis using a pair of primers flanking the two FRT sequences (Figure 4-5A). This PCR analysis confirmed that the transgenic efficiency of the negative constructs were about the same as the positive ones (Figure 4-6B and Table 4-1). Some of the negative fragments from the original screen were further verified using a modified version of Barrier Tester 1. This construct, pBT3, contains a *gypsy* insulator flanked by two *loxP* sequences in between the PRE and the tested fragment (Figure 4-5C). In the presence of the *gypsy* insulator, both BT3-ILF395bp and BT3-ILF1kb transgenic adults had similar DsRed expression levels in the eye. However, after the removal of *gypsy* insulator with Cre - mediated recombination, BT3-ILF395bp lost the eye expression of DsRed. In contrast, BT3-ILF1kb was not affected by the removal of *gypsy* (Figure 4-5D). This indicates that without the *gypsy* element, only the ILF1kb, but not ILF395bp sequence, could counteract the silencing effect of PRE.

Testing of progressively shorter fragments led to the identification of a 294bp fragment that had full barrier activity as compared to the original longer fragments. The barrier activity associated with this 294bp fragment is orientation independent, as the barrier function was not affected when this sequence was inserted in a reversed orientation between the reporter and PRE (Figure 4-2E).

The expression of the reporter in the presence of ILF294bp and the almost complete diminishing of DsRed signal in the absence of it strongly suggest that ILF294 functions as a chromatin barrier against PRE-mediated silencing. However, one alternative explanation is that the tested ILF fragments contain a strong eye-specific

enhancer, and that the excision of this enhancer resulted in the down-regulation of 3xP3-DsRed expression in the eye. To rule out this possibility, we replaced the PRE with a UAS sequence, and performed the same assay. As shown in Figure 4-7, excision of ILF294bp from UAS>ILF294bp>P3DsRed fly did not cause any reduction of DsRed signal, indicating that ILF294bp fragment does not have enhancer activity. With this validation, we are reasonably confident to conclude that there is a chromatin barrier activity within this 294bp sequence. We will hereby refer to this activity as IRER Left Barrier (ILB). Further verification indicated that most of the barrier activity resides in a smaller 167bp fragment (Figure 4-2B). We will refer to these two fragments as ILB294bp and ILB167bp, respectively.

ILB Prevents PRE-Mediated Transcriptional Silencing of Nearby Genes

QPCR verified that the diminishing of the DsRed signal following removal of the ILB- containing fragments was due to transcriptional silencing of the 3xP3-DsRed reporter gene (Figure 4-8A and B). Crossing the positive Barrier Tester lines with *ey*-FLP reduced the level of DsRed mRNA to less than 10% of that of the original lines which carry one copy of the Barrier Tester. This reduction was largely independent of the insertion site since lines with different original expression level showed similar relative reduction following remove of the ILB-containing sequence. Considering that *ey*-FLP may not led to the excision of the tested ILB-containing fragment in all eye disc cells, the level of mRNA reduction assayed by QPCR suggest that the *Ubx* PRE is very efficient in silencing the transcription of the 3xP3-DsRed reporter gene.

We noticed that for two of the p-mediated insertion lines carrying PRE>ILF9kb>reporter, crossing with *ey*-FLP not only led to suppression of the DsRed signal in the eye, it also led to eye ablation phenotype (Figure 4-8C and Figure 4-3).

Using inverse PCR, we mapped one of the lines, 67-2, to about 400bp upstream of the gene *corto*, with the 3xP3-DsRed at the proximal site and PRE at the distal site (Figure 4-8D). When the ILB-containing sequence was excised by *ey*-FLP, not only was the DsRed mRNA reduced to less than 10 percent of the original line, the level of the *corto* mRNA was also reduced to about 30% of the original level (Figure 4-8E). The eye-ablation phenotype associated with the removal of ILB is reminiscent to what was described for homozygous *corto* mutants (Kodjabachian et al. 1998). The more than 50% reduction of the *corto* mRNA seemed contradictory to the fact that unlike the DsRed reporter, which only had one copy in *cis* with the PRE, there was another copy of *corto* on the homologous chromosome without the PRE. However, it has been shown that PRE mediated silencing can work in *trans* through homologous pairing (Sigrist and Pirrotta 1997), and our observation with *corto* is in accordance with that.

The combination of these evidences indicates that the Ubx PRE could silence multiple genes over a long range. However, the silencing is effectively blocked by the presence of ILB.

ILB Prevents the Propagation of H3K27 Trimethylation

To understand the mechanism of ILB barrier activity, we examined the changes of chromatin structure at the reporter gene before and after the removal of the ILB. The ILB-containing sequence in the transgenic line 47-2 was removed by germline recombination mediated by hs-FLP and verified by PCR analysis (Figure 4-6). The flies without ILB showed complete loss of DsRed signal in the eye (Figure 4-9A). Adult flies of the same age were collected for ChIP analysis. In the absence of ILB, all of the four loci within the tester construct had high levels of H3K27me3 enrichment comparable to that of the *Ubx* PRE locus (Figure 4-9B, -ILB). In contrast, in the presence of the barrier

sequence (+ILB), only the locus before ILB had high level of H3K27me3 while the P3 promoter and DsRed coding regions had significantly lower levels of the suppressive histone mark (Figure 4-9C, +ILB). This indicates that ILB is capable of blocking PRE-initiated propagation of H3K27me3.

It has been shown in cHS4 that the barrier activity is mediated by formation of euchromatic histone marks that are incompatible with repressive histone marks at the barrier site. We first monitored the distribution of euchromatic marks in and around the endogenous ILB locus in later stage embryos in which the IRER is heavily methylated. We found that there are significantly higher levels of H3 acetylation at the ~300bp region encompassing ILB294bp (b1 & b2 loci in Figure 4-9C) than the immediately adjacent regions (-5k and -7k). Specifically, the levels of H3K9 and H3K27 acetylation in ILB is as high, or higher, than the positive control *rp49* locus, respectively. Not surprisingly, the immediate right side of ILB (-7k) has very low levels of histone H3 (K9 and K27) acetylation. However, the levels of H3 acetylations at ILB are also significantly higher than loci left to ILB (such as -5k). This is true not only for late stage embryos, but also for samples prepared from adult fly or the S2 cells. These observations strongly indicate that ILB is subject to specific histone acetylation activity.

ILB Lacks Enhancer-Blocking Activity

As aforementioned, all of the known *Drosophila* boundaries/insulators have enhancer-blocking activity. To test the enhancer-blocking activity of ILB, we modified the Barrier Tester construct by replacing the PRE with the Upstrean Activation Sequence (UAS) (Figure 4-10A). When a *gypsy* insulator was inserted between the UAS and the DsRed reporter, the interaction between UAS/GAL4 and the DsRed promoter was totally blocked as indicated by the absence of epidermal DsRed

expression in the presence of the *en*-Gal4 transgene (Figure 4-10B, panel B and B'). When the *gypsy* insulator was removed in the presence of a copy of UAS-FLP transgene, DsRed became expressed in the *engrailed* pattern (Figure 4-10B, panel C and C'). This validated that this constructs is sensitive and suitable for testing the enhancer-blocking activity of insulators.

However, no enhancer blocking activity was observed for the ILB294bp fragment. The insertion of ILB294 in between of the UAS and the reporter did not affect at all the expression of DsRed in *engrailed* pattern (Figure 4-10B, panel D). To rule out the possibility that enhancer blocking components of ILB was missing or damaged in ILB294bp, we tested a 3.7kb fragment encompassing the ILB294. This much longer fragment failed to block the expression of DsRed in *engrailed* pattern although it was albeit weaker (Figure 4-10B, panel E). Given the length of the fragment, which is much longer than the ~400bp *gypsy* insulator, we consider that this reduction of DsRed expression is likely due to the increased distance between UAS and the DsRed promoter rather than enhancer blocking activity.

Cut Binds to ILB

It has been reported recently that the *Drosophila* ortholog of CREB-binding protein (dCBP or Nej) specifically acetylates H3K27 and antagonizes PcG-mediated silencing (Tie et al. 2009). The analysis of potential binding sites in the 167 bp ILB region identified a site that conforms to the V$CDP_02 matrix (TRANSFAC M00102) (Figure 4-11A). The matrix was generated based on SELEX analysis using the human CCAAT displacement protein (CDP; HGNC: Cutl1(Cut-like 1)) (Andres et al. 1994). CDP is the human orthologs of the *Drosophila* Cut. CDP and Cut demonstrate exceptional conservation at sequence level and display similar DNA binding specificity (Neufeld et

al. 1992). The *Drosophila* gene *cut*, originally named according to the notched wing phenotype associated with hypomorph alleles, was later found to be an essential gene required for the proper development of a variety of distinct tissues and organs such as central and peripheral nervous systems, muscles, and ovarian follicle cells, etc. (reviewed in (Nepveu 2001)). Although it has not been demonstrated for Cut, CDP/Cutl1 interacts with CBP (Li et al. 2000).

In order to verify whether Cut binds to ILB, we performed ChIP with a monoclonal antibody against Cut. In both S2 cells and the Adult fly, Cut specifically binds to ILB (Figure 4-11B). We then carried out experiments to test whether *cut* activity is required for ILB barrier function and whether the Cut-binding site in ILB is essential. Indeed, a reducetion in DsRed singal was found in *cut* mutant ct^{C145} compared to wild type (Figure 4-11C). Therefore, Cut protein is required for ILB barrier activity through the direct interaction.

ILB Is Evolutionarily Conserved

The 167bp ILB sequence is highly conserved even in distantly related *Drosophila* species such as *D. virilis* and *D. mojavensis,* both of which diverged from *D. melanogaster* approximately 60 million years ago (Figure 4-12A). To test whether the function of ILB is conserved, we extracted a 2kb *D. pseudoobscura* genomic sequence harboring the orthologous ILB167bp region and tested its activity in pBT1. We found that this orthologous sequence have complete barrier activity in *D. melanogaster* (Figure 4-12B). This indicates that ILB function existed before the separation of the two species about 40 million years ago and has not changed significantly ever since.

Discussion and Future Directions

Eukaryotic genomes are compartmentalized with euchromatic regions juxtaposed with heterochromatic regions. Heterochromatic regions can be categorized into constitutive heterochromatin and facultative heterochromatin (Trojer and Reinberg 2007). Unlike constitutive heterochromatin, which is consistent and rarely changes, facultative heterochromatic regions are subject to cell-specific regulation and may adopt euchromatic formation in certain cells or under specific conditions. What controls the formation for facultative heterochromatin is not fully understood. However, heterochromatin has an intrinsic property to spread until its propagation is blocked. For instance, PRE could recruit PRC2, which has the enzymatic activity to catalyze the formation of repressive histone mark H3K27me3 in the nearby chromatin. The formed H3K27me3 could in turn recruit PRC1 and PRC2 complex, which leads to the spread of the heterochromatin formation until this cyclic reaction is stopped by a barrier. Several kinds of epigenomic landmarks, such as an active transcribing promoter or a strong enhancer, may serve as a nature barrier to the spread of heterochromatin (Raab and Kamakaka 2010). Yet, under many circumstances specific boundary elements are needed to specifically demarcate the range of heterochromatin formation.

Using a strategy that specifically testing barrier activity against PRE-induced heterochromatin formation, we verified the existence of a chromatin barrier at the left boundary of IRER and narrowed it down to a 167bp DNA region. This boundary element is very efficient at blocking the spread of PRE-initiated heterochromatin formation. Similar to what was described for USF-mediated chromatin barrier activity in the cHS4 insulator, ILB is associated with high acetylation of histone that is incompatible with the H3K27 trimethylation catalyzed by PcG repressive complexes. Unlike any previously

identified boundary elements in *Drosophila*, ILB does not display enhancer-blocking activity.

ILB as A Barrier-Only Boundary Element

Although the barrier activity and enhancer-blocking activity of the cHS4 insulator are mediated by distinct *cis* elements, these elements interpose with each other in close proximity. To our knowledge, ILB is the only boundary element that neither contains nor in close proximity to enhancer-blocking activity. This distinction of ILB, although a little surprising, may suite well with the enhancer-specific epigenetic regulation of IRER.

IRER is an enhancer region that controls the stress-responsiveness of not one, but three pro-apoptotic genes located in the same synteny (Zhang et al. 2008b; Lin et al. 2009). This synteny contains four IAP-antagonist genes, *hid*, *grim*, *reaper*, and *sickle*, which together are required for most development cell death as well as cell death in response to a variety of environmental stimuli (Steller 2008). Coordinate expression of *reaper* and *hid* are observed during development and are required for eliminating obsolete cells (Zhou et al. 1997). These two genes, and *sickle*, are induced within 15 minutes following ionizing irradiation (Brodsky et al. 2004). When IRER is deleted, none of the three genes can be induced by irradiation (Zhang et al. 2008b). While IRER is required for the stress, it is not required for other aspects of transcriptional regulation, such as the expression of *reaper* in differentiated motor neurons or neuroblasts (Bello et al. 2003; Rogulja-Ortmann et al. 2008). Thus the formation of DNase I resistant heterochromatin at IRER serves specifically to block or down-regulate the responsiveness of the three genes to environmental stress. However, at the same time, the basic promoter and other enhancer regions remain open and the genes can still be expressed under other developmental control.

A barrier-only boundary may be necessary for this type of enhancer-specific epigenetic regulation. Using a fluorescent reporter knocked into IRER via homologous recombination, we found that epigenetic blocking of IRER is dynamic and reversible. In specific cells of the developing larval imaginal disc, IRER could change from closed conformation (lack of reporter expression) to open conformation (high level reporter expression) following environmental stress such as heat shock, irradiation, or food deprivation. Consequently, cells with open IRER are sensitive to stress induced *reaper*/*hid* expression. When IRER is open, a boundary with enhancer-blocking activity would have blocked the stress-responsive enhancers in IRER to interact with the *reaper* promoter. Indeed, our earlier work has shown that several *gypsy*-containing p and piggyBac insertions between IRER and the *reaper* promoter totally blocked irradiation induced *reaper* expression (Zhang et al. 2008b).

A Novel Barrier Element?

In searching for the potential trans-factors that is responsible for the barrier activity of ILB, we checked the modENCODE database for the occupancy of all of the known *Drosophila* insulator/boundary-associated proteins, including Su(Hw), CTCF, BEAF32, GAF, CP190 and Mod(mdg4) etc.. Despite the fact that many data sets are available for a variety of tissues and cultured cells, there is no indication that any of these known insulator proteins is enriched in the vicinity of ILB294bp.

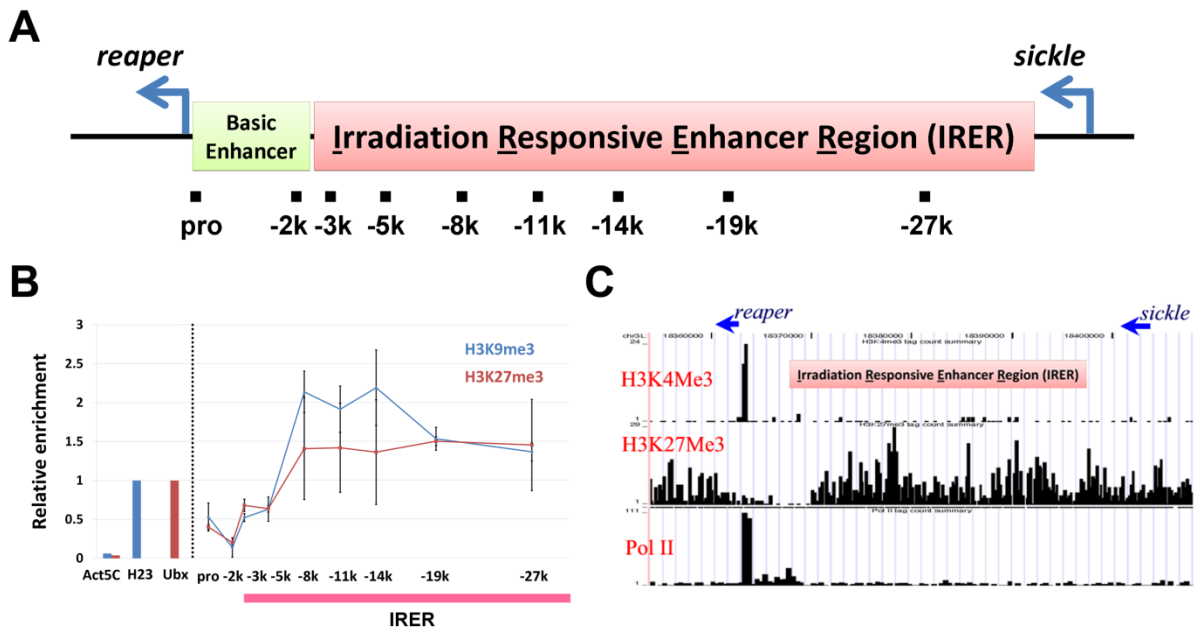

Figure 4-1. Formation of facultative heterochromatin was restricted to IRER and without reaching the *reaper* promoter and proximal enhancer regions. A) Schematic diagram of the intergenic region between *reaper* and *sickle*. IRER (Irradiation responsive enhancer region) is required for mediating irradiation-induced expression of pro-apoptotic genes *reaper*, *hid,* and *sickle* (Zhang et al. 2008b). Accessibility of IRER is controlled by a PcG protein –dependent mechanism, which forms an impermissive structure in irradiation-resistant cells in post-stage 12 embryos. The decrease of DNA accessibility, accompanied by enrichment of repressive histone marks and binding of PcG proteins, was specifically limited to the IRER (red box) without affecting the *reaper* promoter and proximal enhancer region (green box) (Zhang et al. 2008b). B) Chromatin Immunoprecipitation (ChIP) assays performed with wild-type adult fly tissues. Pericentromeric heterochromatin locus H23 (H23) and the *Ubx* promoter region (Ubx) were used as positive controls for repressive histone marks H3K9Me3 (blue) and H3K27Me3 (red), respectively. The coding region of house-keeping gene *Act5C* was used as a background control. Enrichment of the repressive histone marks in IRER was normalized against respective positive controls and presented as Mean ± Std. The high enrichment of both H3K27me3 and H3K9me3 in the central part of IRER drops down significantly at the left boundary of the IRER, about -2kb to -5kb relative to *reaper* TSS. C) Distribution of histone marks H3K4me3, H3K27me3 and binding of Pol II in *Drosophila* S2 cells revealed by ChIP-Seq, which was provided by our collaborator Keji Zhao's laboratory in NIH. The relative locations of *reaper* and *sickle* are indicated by blue arrows. The doted vertical lines denote the region that might possess putative chromatin barrier activity.

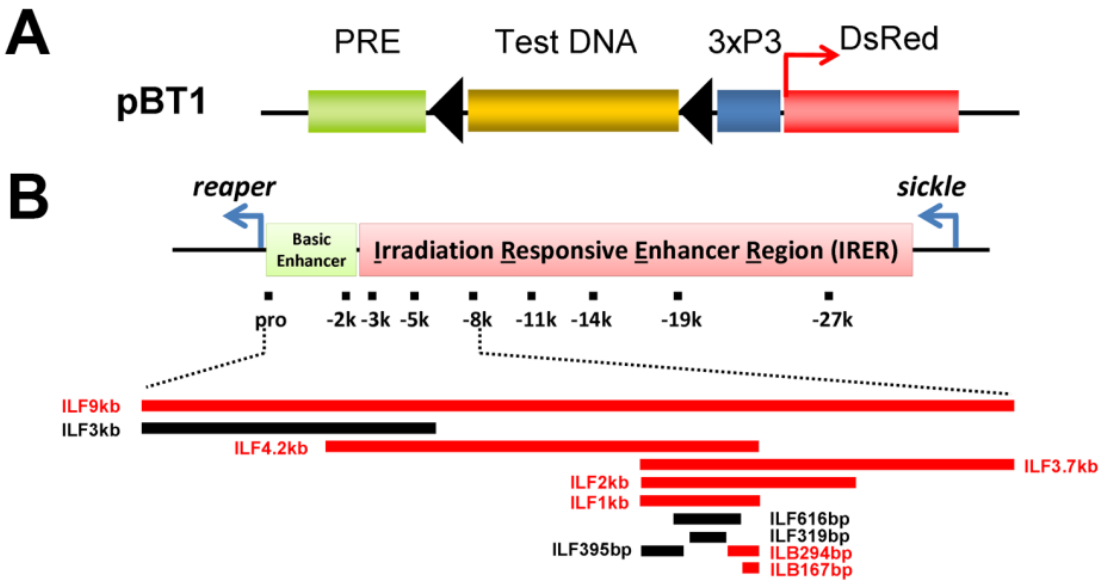

Figure 4-2. Verification of barrier activity and narrowing down the IRER left barrier. A) The Barrier Tester construct pBT1. Eye-specific 3xP3-DsRed served as the reporter/marker. The Polycomb Response Element (PRE) from *Ubx* promoter was placed upstream of the 3xP3-DsRed to initiate the formation facultative heterochromatin. The tested fragments (ILFs) were cloned in between of the reporter gene and PRE, and flanked by two FRT sequences. The transgenic flies were generated by either P- mediated insertion or ΦC31 mediated integration. B) A series of fragments within the IRER left boundary region were tested with the pBT1 vector for barrier activity. The fragments with or without barrier activity are shown as red or black bars, respectively. The essential barrier region was narrowed down to the ILB167bp region. C) An example of verification of barrier activity. The left and right panels show the same group of flies under either the RFP fluorescence channel or bright field, respectively. Transgenic line 47-2 carrying one copy of the pBT1-ILF9kb (>ILF9kb>; the fly head on the left) has strong eye-specific DsRed signal, which was diminished when the ILF9kb fragment was removed by crossing to *ey*-FLP strain (*ey*-FLP; the fly head on the right). The DsRed signal was fully restored when *ey*-FLP was crossed out (top). D) pBT1 constructs carrying sub-fragments of ILF9kb were integrated to the same attP docking site on the 2nd chromosome. Barrier activity was verified as aforementioned. The fly heads of the original transgenic strains are on the left, while the those also have *ey*-FLP are on the right side of each panel. This series of testing indicated that the ILB167 fragment posses full barrier activity as compared to longer fragments. E) The barrier activity was not affected when the ILB294bp fragment was inserted into pBT1 with the reversed direction. Indicating ILB is orientation independent.

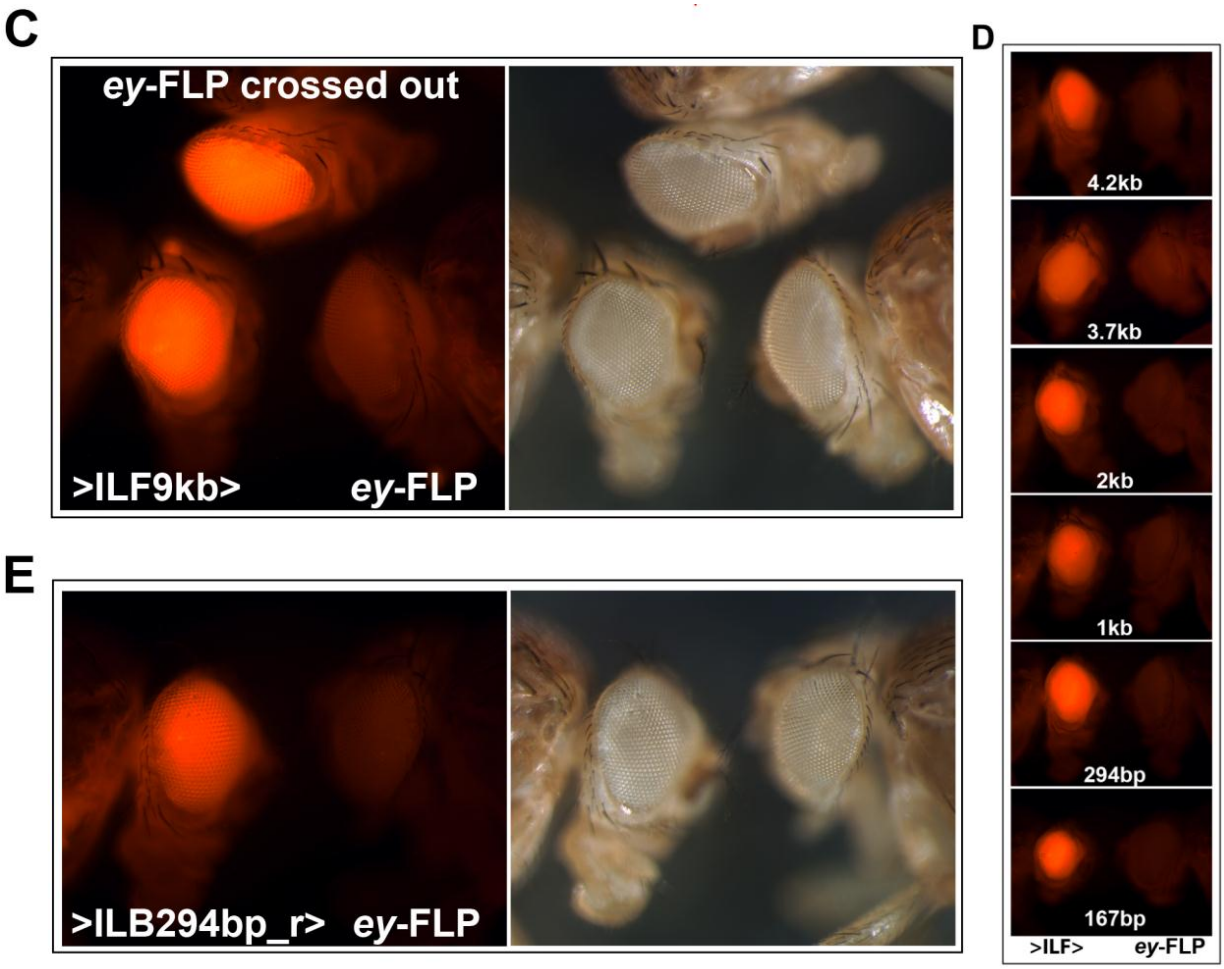

Figure 4-2. Continued.

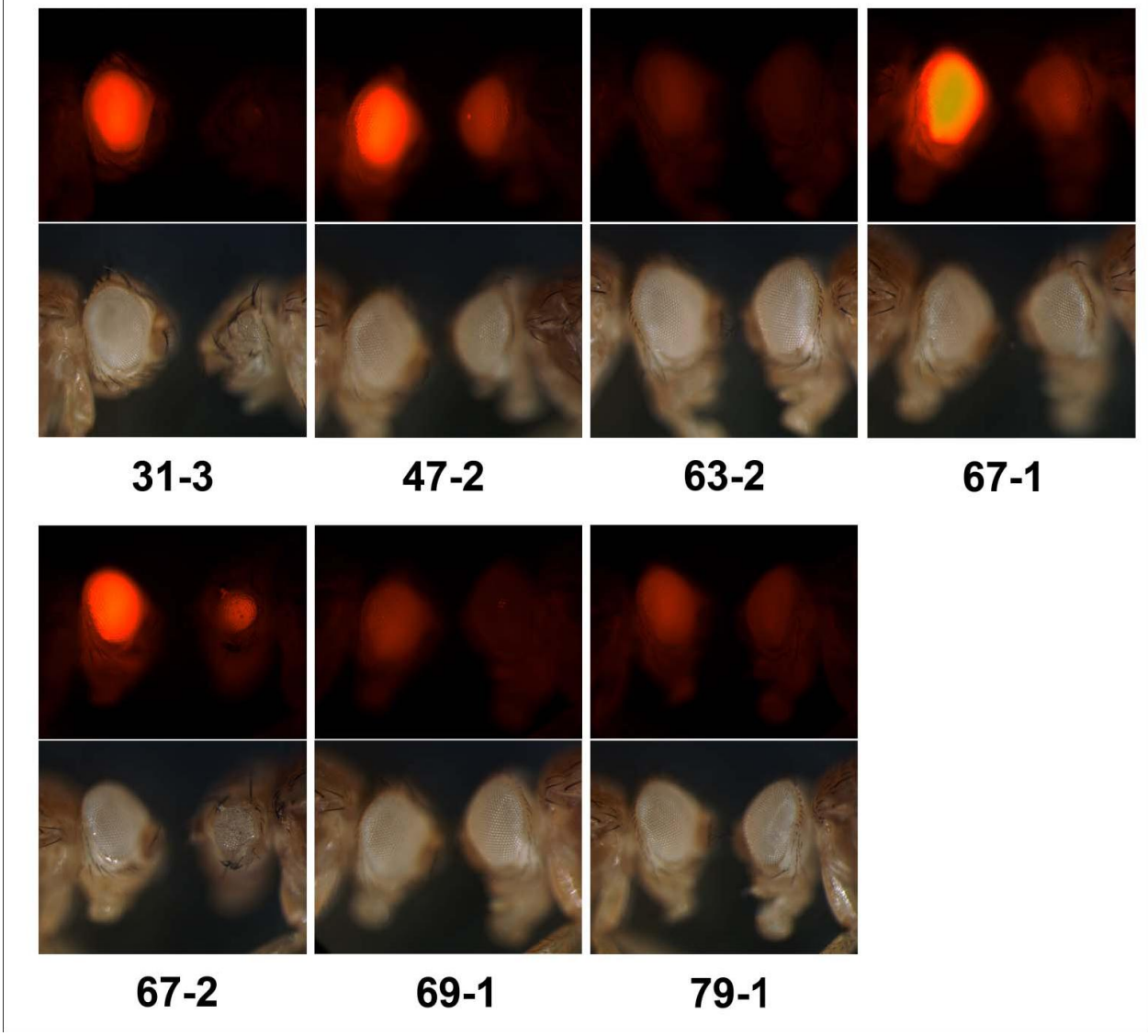

Figure 4-3. The barrier activity in ILF9kb is independent on the insertion sites. Seven independent P insertion lines were recovered for {PRE>ILF9kb>3xP3DsRed}. DsRed channel (bottom panels) and bright light channel (top panels) are shown for the same pair of flies. The one on the left is the original transgenic flies, and the one on the right also contains a copy of *ey*-FLP transgene. All of the seven lines showed decreased DsRed signal after the removal of ILF9kb by *ey*-FLP. Two lines, 31-3 and 67-2, also showed eye-ablation phenotype in the absence of the barrier.

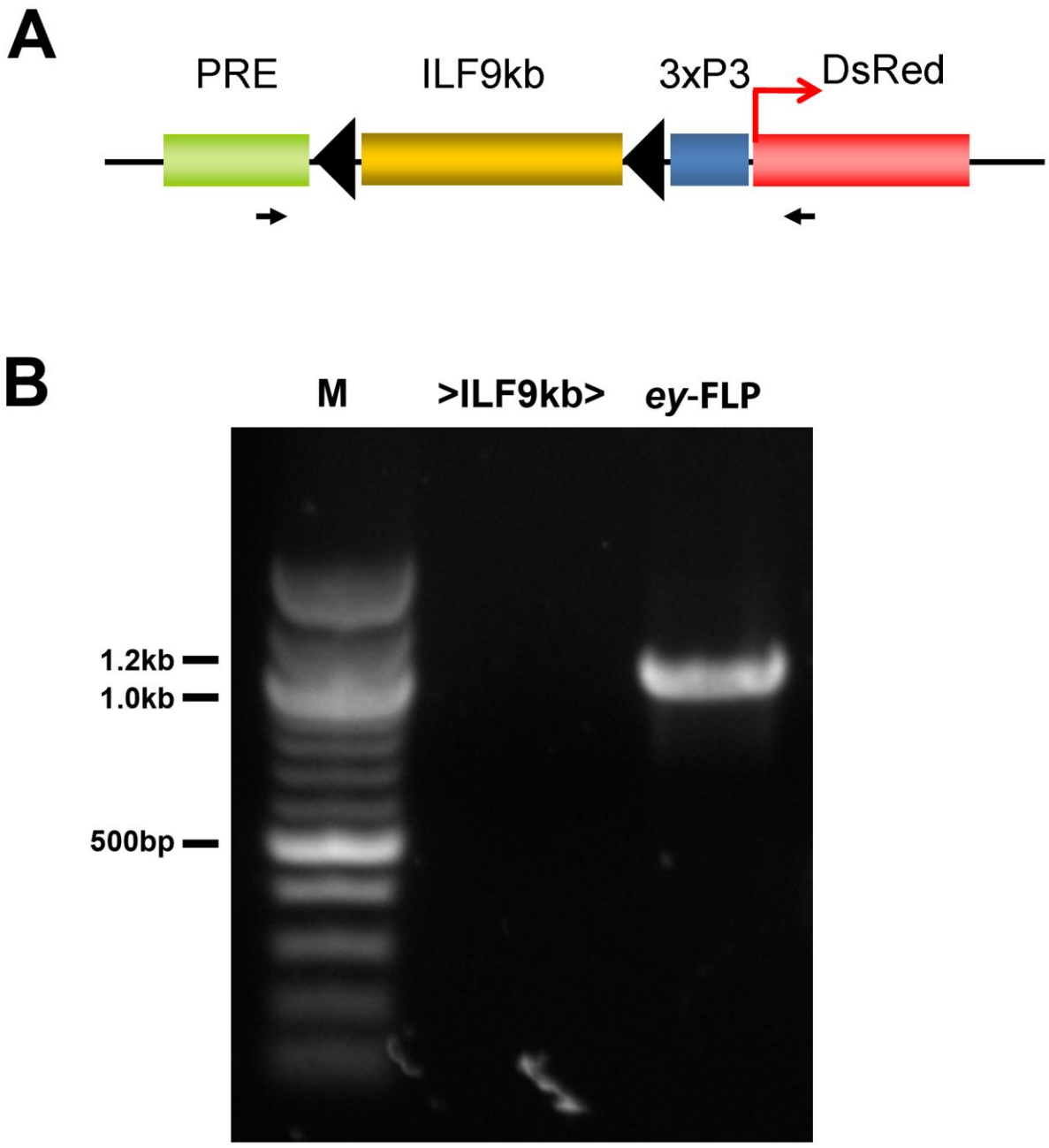

Figure 4-4. Example of PCR verification of somatic excision of ILF fragments. A) The primer set used for the PCR analysis is shown by the black arrows below the schematic structure of the transgene pBT1-ILF9kb. B) In the presence of the 9kb barrier sequence, the PCR reaction failed to amplify the large amplicons. The progeny with *ey*-FLP showed a 1.1kb PCR product, indicating successful somatic excision of the ILF9kb sequence.

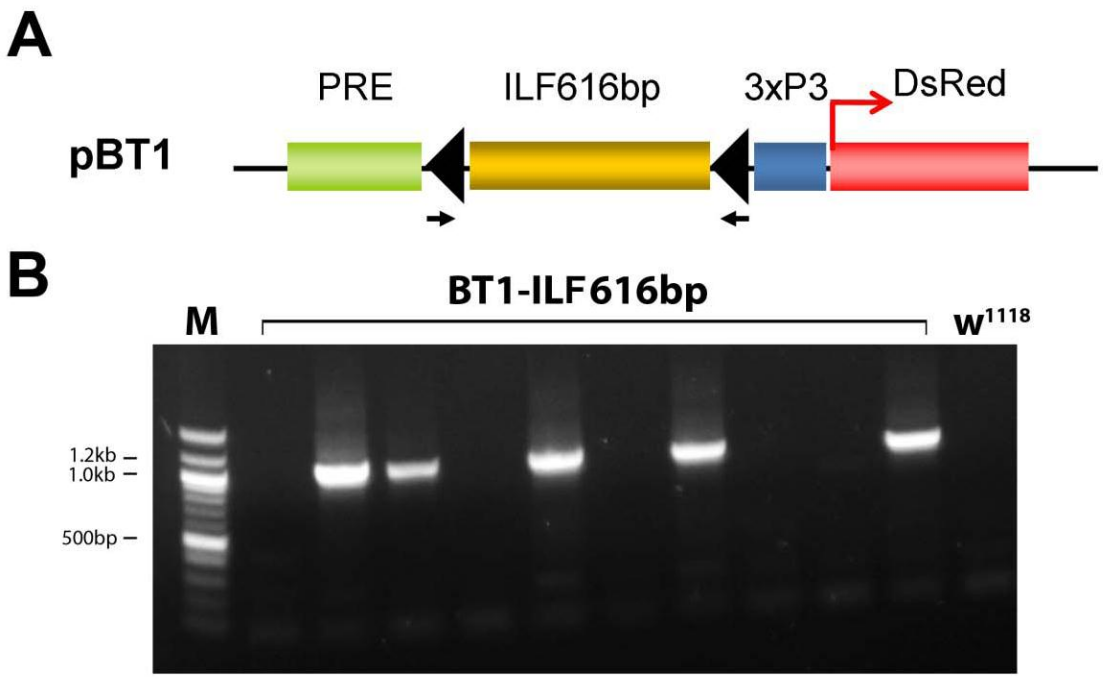

Figure 4-5. Verifying the tested fragments that did not demonstrate barrier activity in the original screen. A) and B) PCR verification of the transformation events with BT1-ILF616bp DNA, from which no DsRed-positive flies was recovered. The progeny from each individual vial were collected for genomic DNA extraction, and PCR analysis was performed with a pair of primers flanking the two FRT sequences (A). The genomic DNA from five out of ten tested vials showed PCR products around 1kb, indicating a ~50% transformation rate (B). These evidence indicate that the failure of recovering BT1-ILF616bp was not due to problem associated with transformation, rather it is due to the silencing of the report gene by PRE, in another word, the lack of barrier activity of the tested fragment. C) Some of the negative fragments were further verified with the reporter construct pBT3, which contains a *gypsy* element flanked by two *loxP* sequences in between of the PRE and the test DNA fragment. Transgenic flies were generated with ΦC31 line 9752. Germline excision of the *gypsy* element was performed by crossing the transgenic flies to a strain providing the source of Cre recombinase (*y w; Sco/CyO,crew1*). ILF395bp was negative while ILF1kb tested positive in the original BT1-mediated assay. Both BT3-ILF395bp and BT3-ILF1kb transgenic files had similar level of DsRed in the presence of the *gypsy* insulator (D, +*gypsy*). However, the level of DsRed in the BT3-ILF395bp line diminished after the excision of *gypsy* (D, left panel, -*gypsy*), indicating that the ILF395bp does not have barrier activity. In contrast, the excision of *gypsy* insulator from BT3-ILF1kb did not lead to any detectable decrease of DsRed signal (D, right panel, -*gypsy*), indicating ILF1kb is sufficient in blocking heterochromatin formation initiated by the PRE.

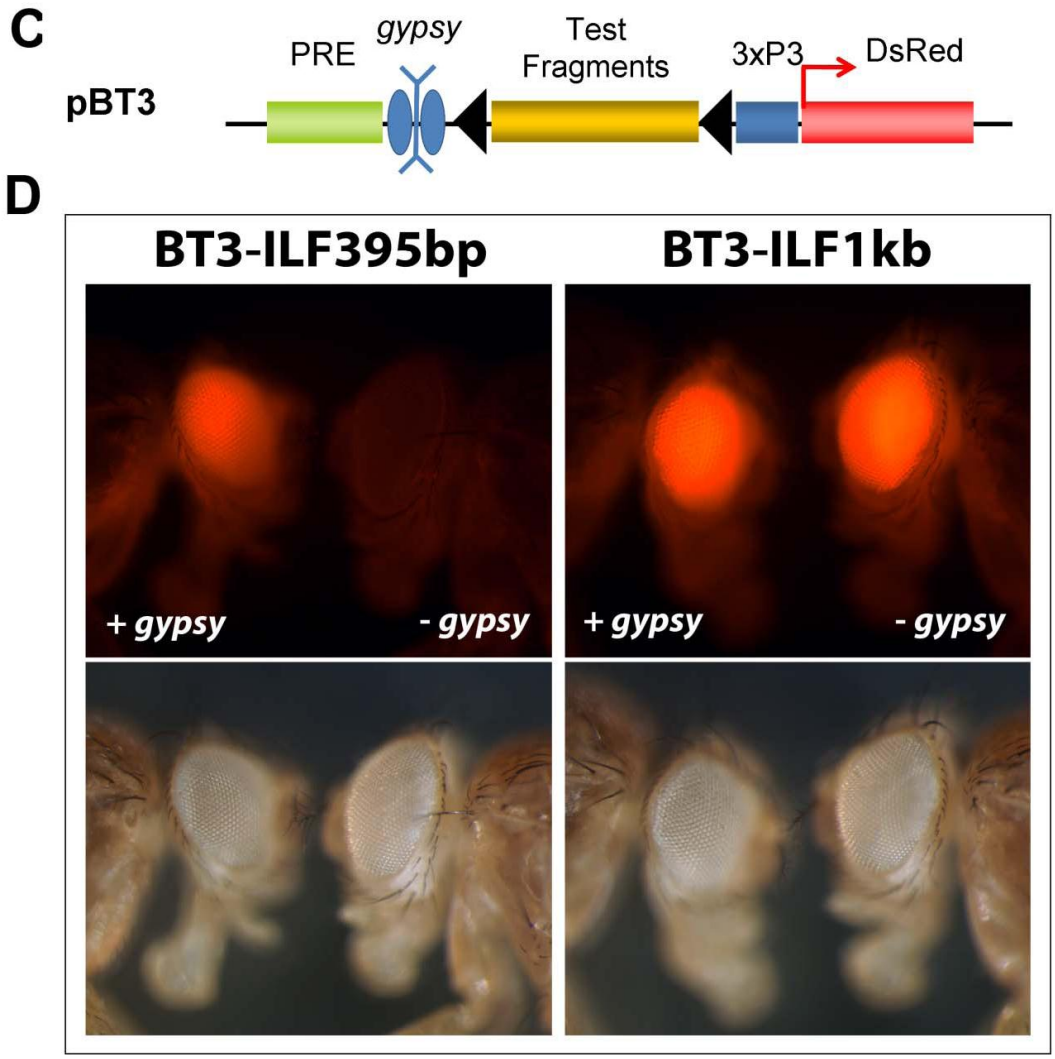

Figure 4-5. Continued.

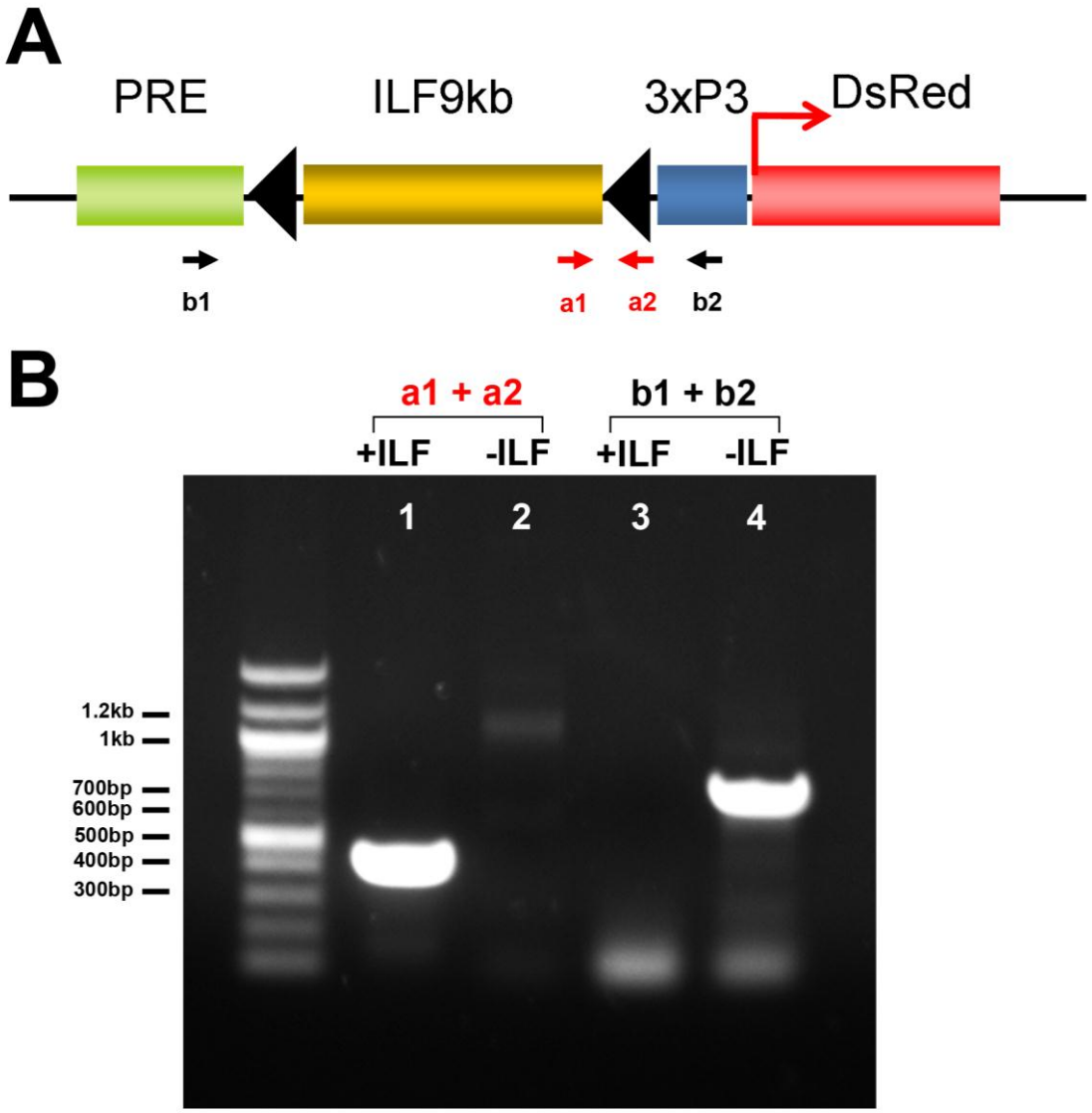

Figure 4-6. PCR verification of the germline excision of ILF9kb from BT1-ILF9kb transgenic line 47-2. A) The two pairs of primers are presented by black and red arrows below the schematic map of the transgene. The ILF9kb sequence was removed by germline excision with hs-FLP. B) The original transgenic flies showed a 400bp PCR band with a1+a2 primers (lane 1), but not with the two primers b1+b2 flanking the 9kb barrier sequence (lane 3). When the ILF9kb barrier was completely removed from the genome, b1+b2 primers produced a 650bp amplicon (lane4), while PCR with a1+a2 primers failed (lane3).

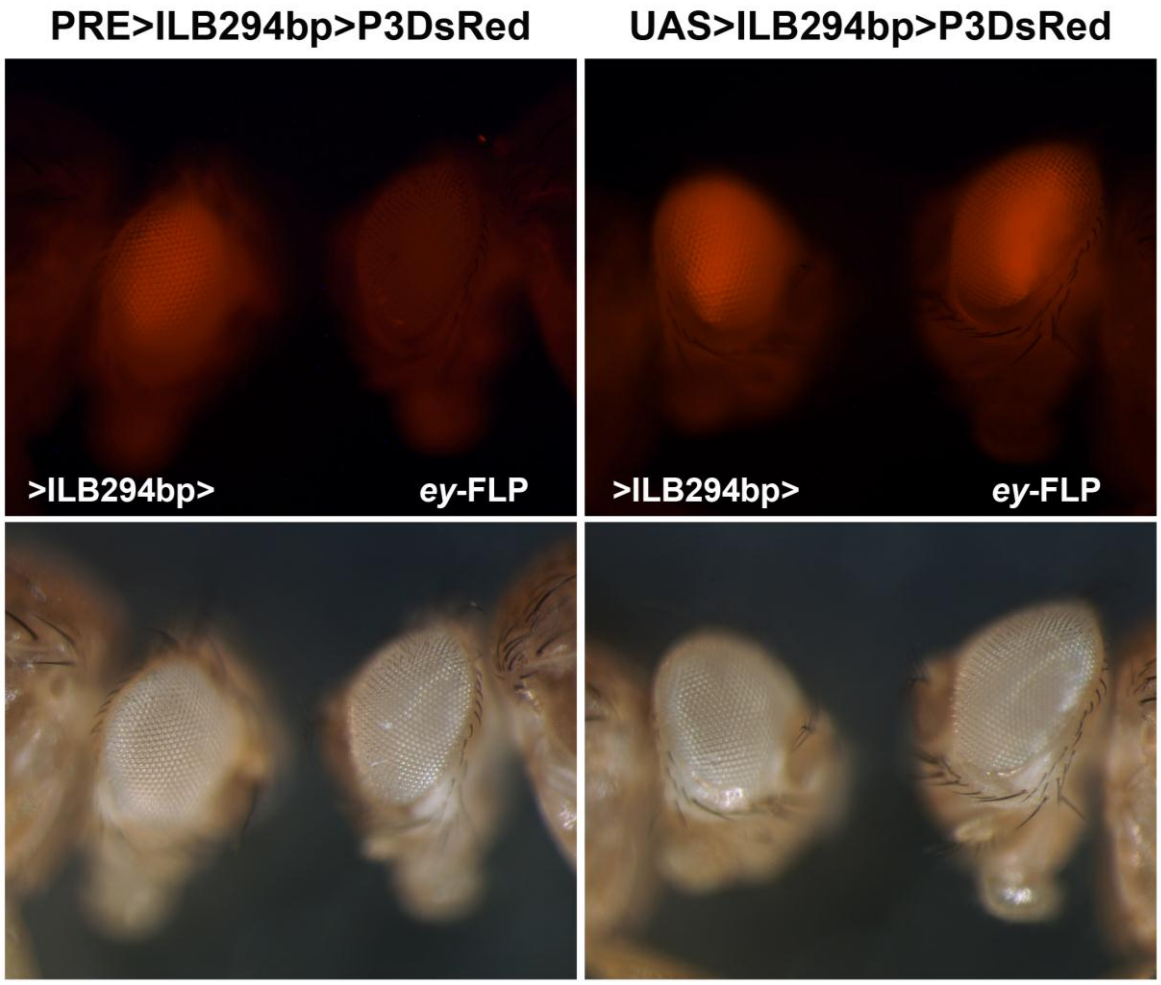

Figure 4-7. ILB294bp does not have eye-specific enhancer activity. Transgenic lines carrying BT1-ILB294bp (PRE>ILB294bp>P3DsRed) or IT1-ILB294bp (UAS>ILB294bp>P3DsRed) were crossed to flies carrying *ey*-FLP. The BT1-ILB294 transformant line showed a significant reduction of DsRed signal after the somatic excision mediated by *ey*-FLP. In contrast, flies carrying IT-ILB294bp had little change after crossing with *ey*-FLP. This indicates that there is no eye-specific enhancer activity associated with the 294bp fragment. The reduction of DsRed expression following removal of ILB is due to PRE mediated silencing of P3DsRed.

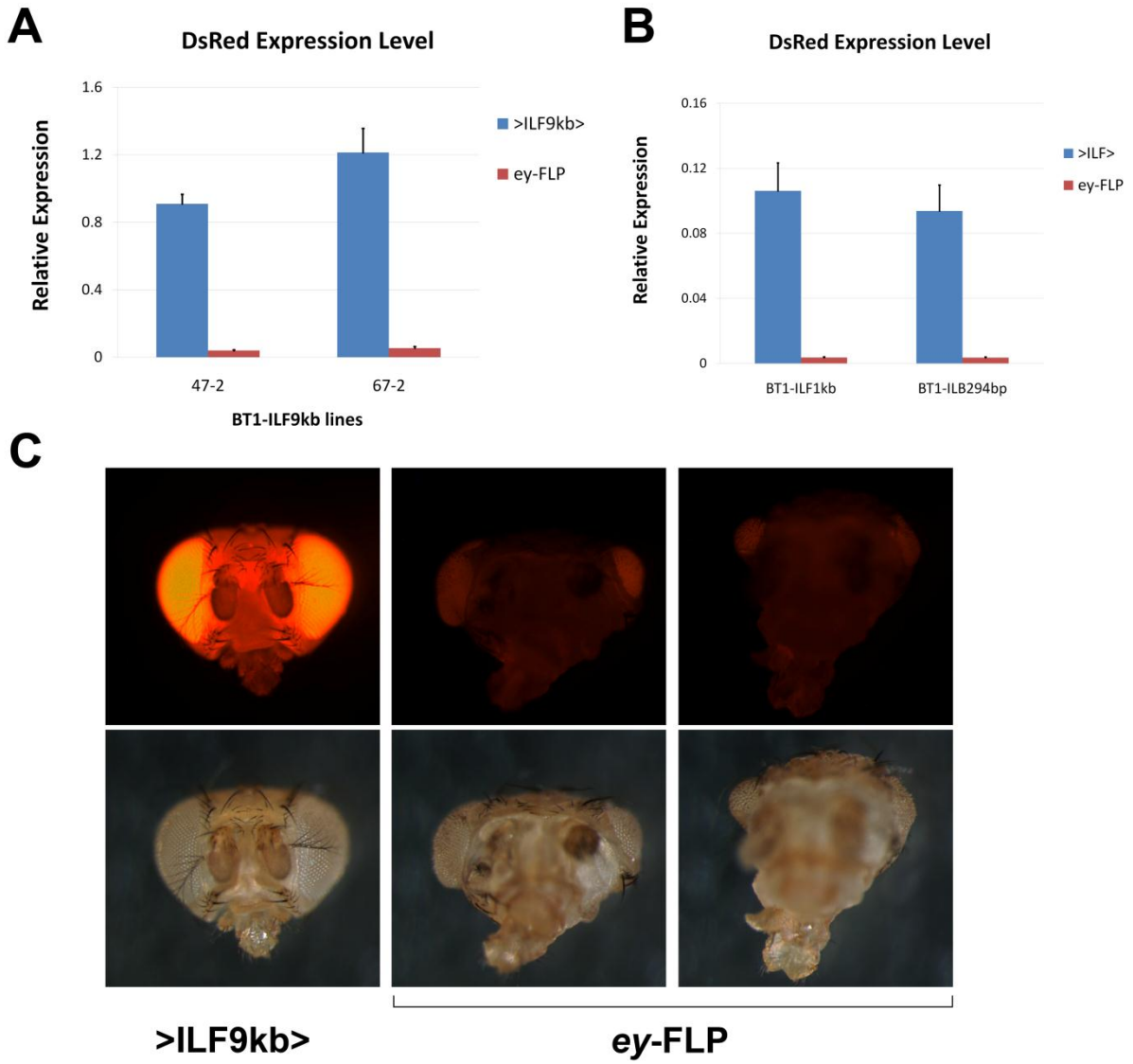

Figure 4-8. ILB prevents transcriptional silencing mediated by PRE. A) and B) The mRNA level of the 3xP3-DsRed reporter gene, detected by QPCR, was significantly reduced after the excision of the ILB-containing fragments by *ey*-FLP. BT1-ILF9kb transgenic lines 47-2 and 67-2 were generated by P insertions (A), while the BT1-ILF1kb and BT1-ILB294bp lines were generated with ΦC31-mediated integration (B). C) When crossed to *ey*-FLP, in addition to decreased DsRed signal, the BT1-ILF9kb transgenic line 67-2 showed eye-ablation phenotype similar to the *corto* mutant. D) inverse-PCR identified that the transgene BT1-ILF9kb in line 67-2 was inserted about 400bp upstream of the gene *corto* by P insertion. E) For Line 67-2, the level of *corto* expression was significantly reduced to less than 50% of the original level after the excision of ILF9kb by *ey*-FLP.

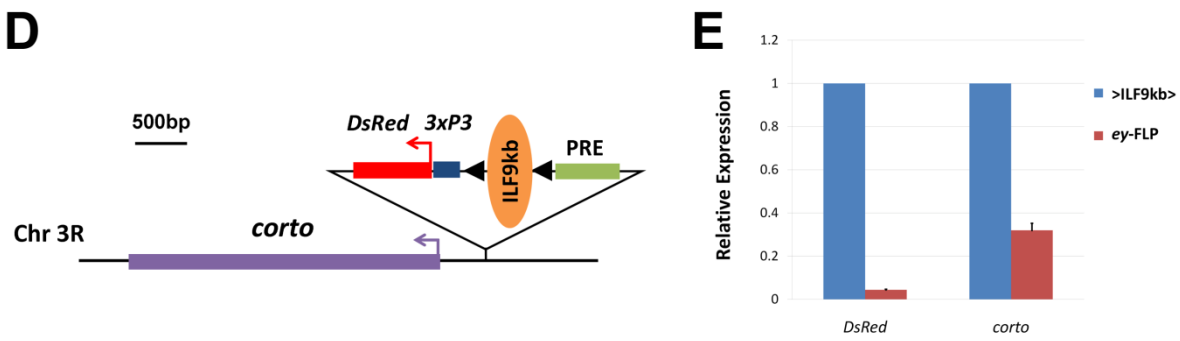

Figure 4-8. Continued.

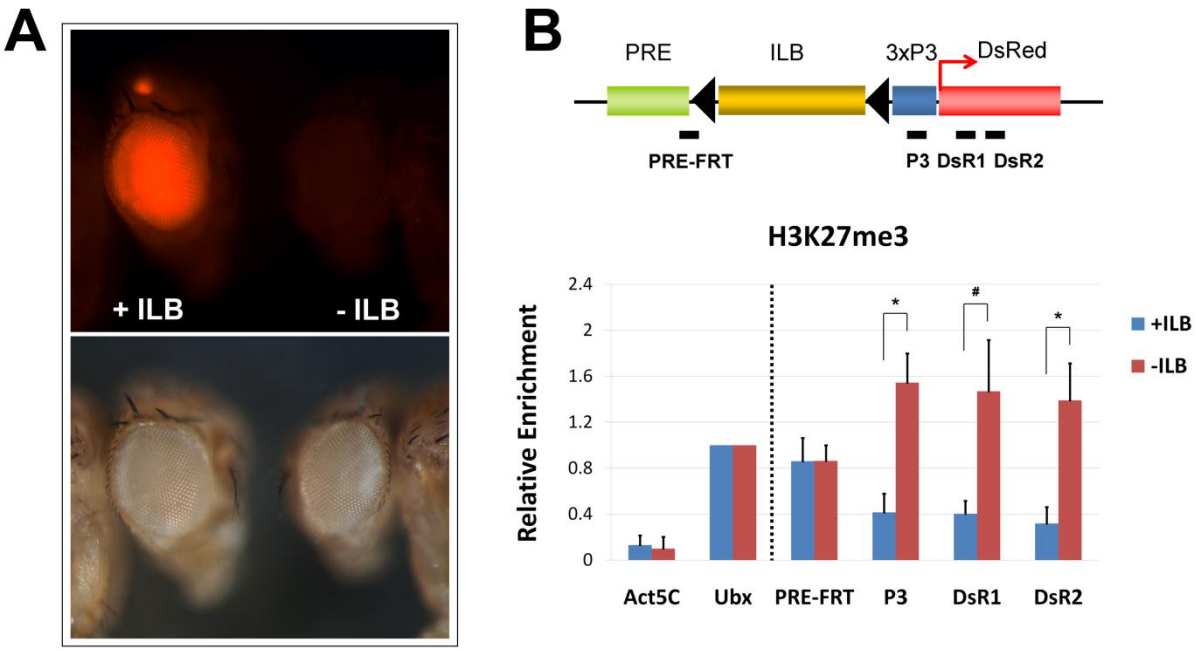

Figure 4-9. ILB blocks the propagation of repressive histone mark initiated by PRE. A) hs-FLP was used to remove the ILB-containing fragment through germline recombination. No DsRed signal was detectable in the resulting PRE>3xP3-DsRed fly (-ILB). B) The enrichment of H3K27me3 in and around the reporter gene before (+ILB) and after (-ILB) the removal of ILB via germline recombination. Targeted loci for primer pairs for the ChIP assays are indicated by black bars below the schematic map of the transgene. Removal of ILB led to significant enrichment of H3K27me3 in the reporter gene loci P3, DsR1, and DsR2 (* $p<0.05$, # $p=0.06847$). Note the level of H3K27me3 remains about the same for the PRE-FRT locus, which is not shielded by ILB. C) Higher levels of histone H3 acetylation at the barrier site. The ILB294bp region (b1 and b2, approximately -6k from the *reaper* TSS) has significantly higher level of H3 acetylation compared to the surrounding region. Specifically, both H3K9 and H3K27 are hyper-acetylated in the ILB294 region. ChIP were performed with late stage embryo (H3Ac & H3K9Ac), S2 cells (H3K27Ac) and adult flies (H3K27Ac). Data were normalized against the recovery rate for the *rp49* locus before statistical analysis.

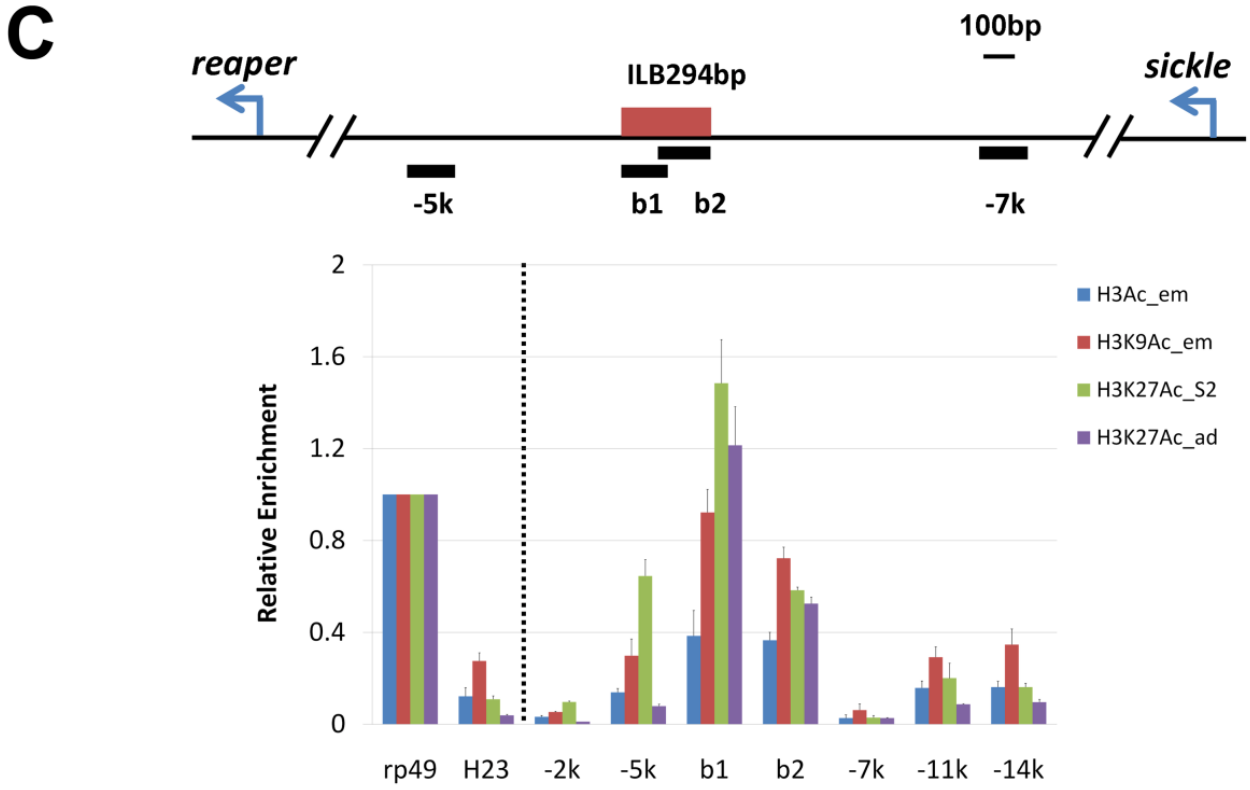

Figure 4-9. Continued.

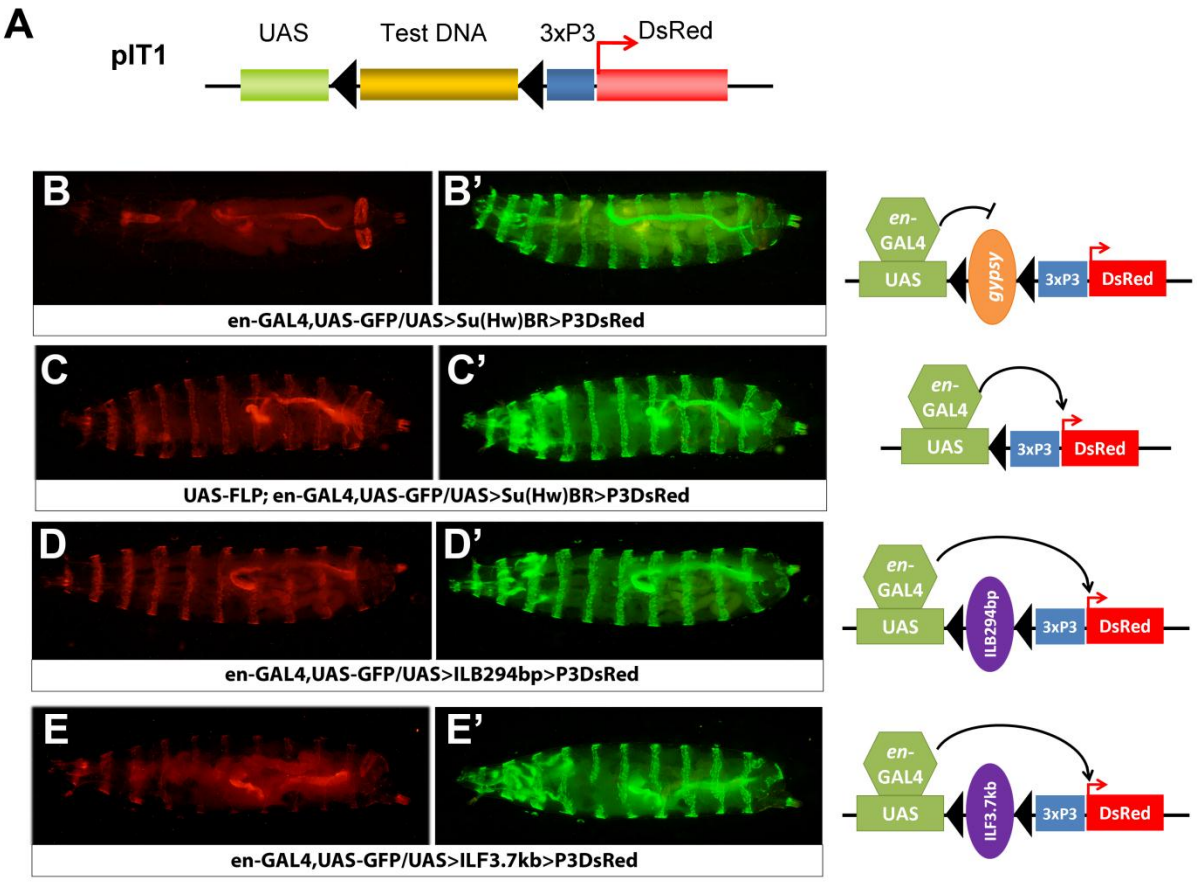

Figure 4-10. The IRER left barrier does not contain enhancer-blocking activity. A) The reporter construct pIT1 was used to test the enhancer-blocking activity. DNA fragments, flanked by FRT, were inserted in between of a UAS sequence and the 3xP3-DsRed reporter. Transgenic fly carrying pIT1 can be crossed to an *engrailed* (*en)*-GAL4, UAS-GFP strain. B) If the DNA fragment has enhancer-blocking activity, such as the *gypsy* insulator, DsRed cannot be expressed in *engrailed* pattern; B') is GFP channel of the same larval representing expression of *en*-Gal4.) C) and C') When the *gypsy* insulator was removed by FLP, DsRed was expressed in the same *engrailed* pattern as the GFP. D) With this testing scheme, the ILB294bp barrier element, which had the complete barrier activity, did not display any detectable enhancer-blocking activity. E) Even a 3.7kb fragment encompassing ILB167 failed to block the expression of DsRed in *engrailed* pattern.

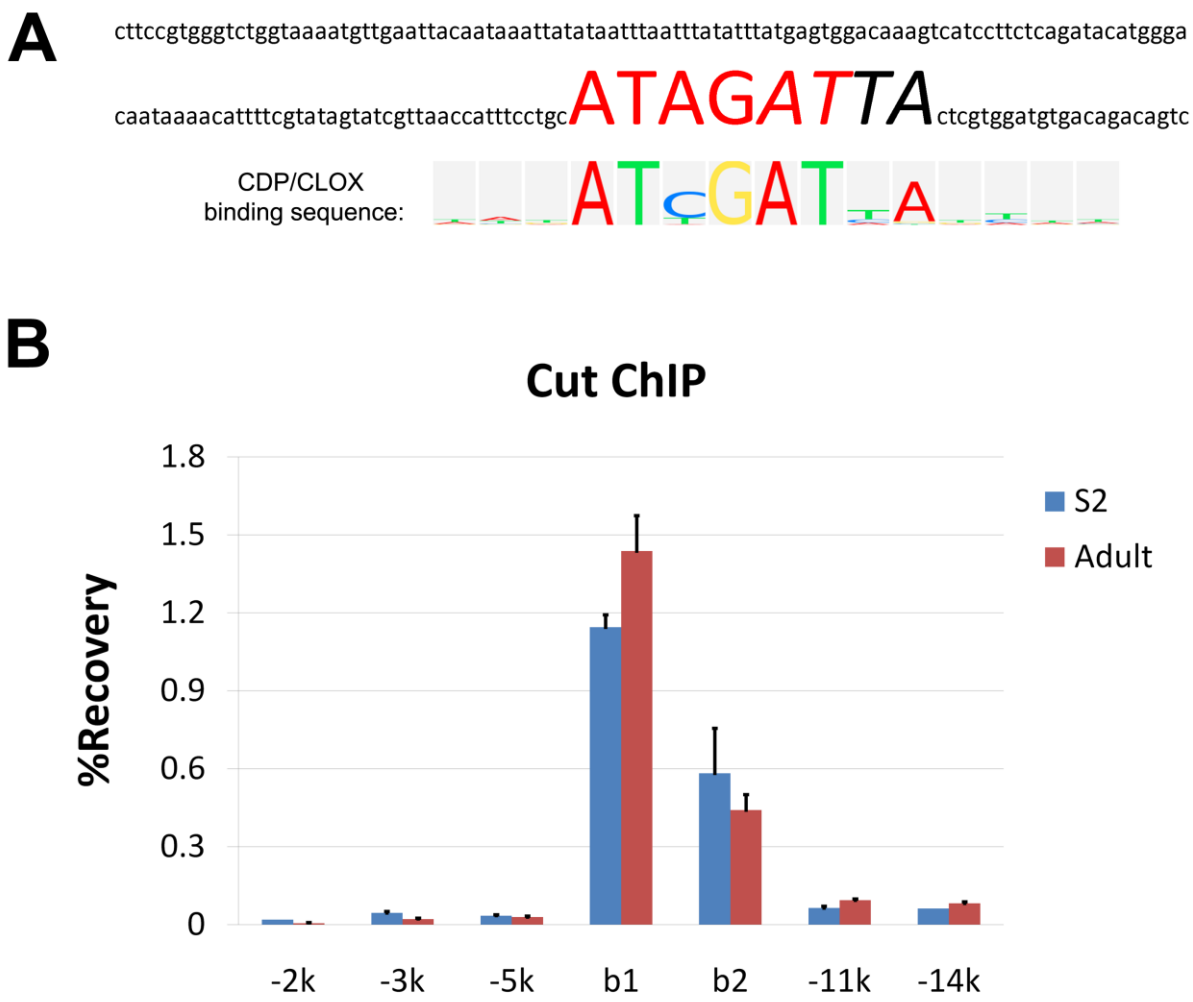

Figure 4-11. Cut is required for the ILB barrier activity. A) Sequence of the ILB167bp fragment that contains a putative CDP/Cut binding site (large font capital letters). The logo representation of the V$CDP_02 matrix was aligned on the bottom, which contains a palindromic ATCGAT motif (highlighted in red in the corresponding putative binding site) overlapping with the homeodomain binding motif ATTA (italic sequence). B) Cut protein was highly enriched in the 300bp region encompassing ILB294bp (b1 and b2) as shown by ChIP analysis in both S2 cells and adult flies. C) BT1-ILB294bp homozygous females were crossed to either w^{1118} males or ct^{C145} males, and the DsRed levels of their female progeny (aged for two days) were shown. A decreased DsRed level was found in ct^{C145} compared to wt.

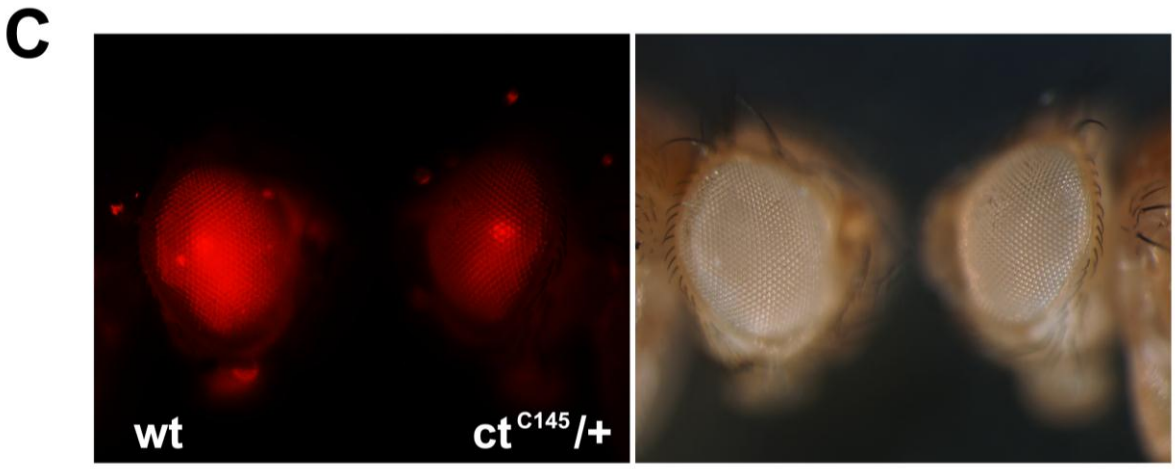

Figure 4-11. Continued.

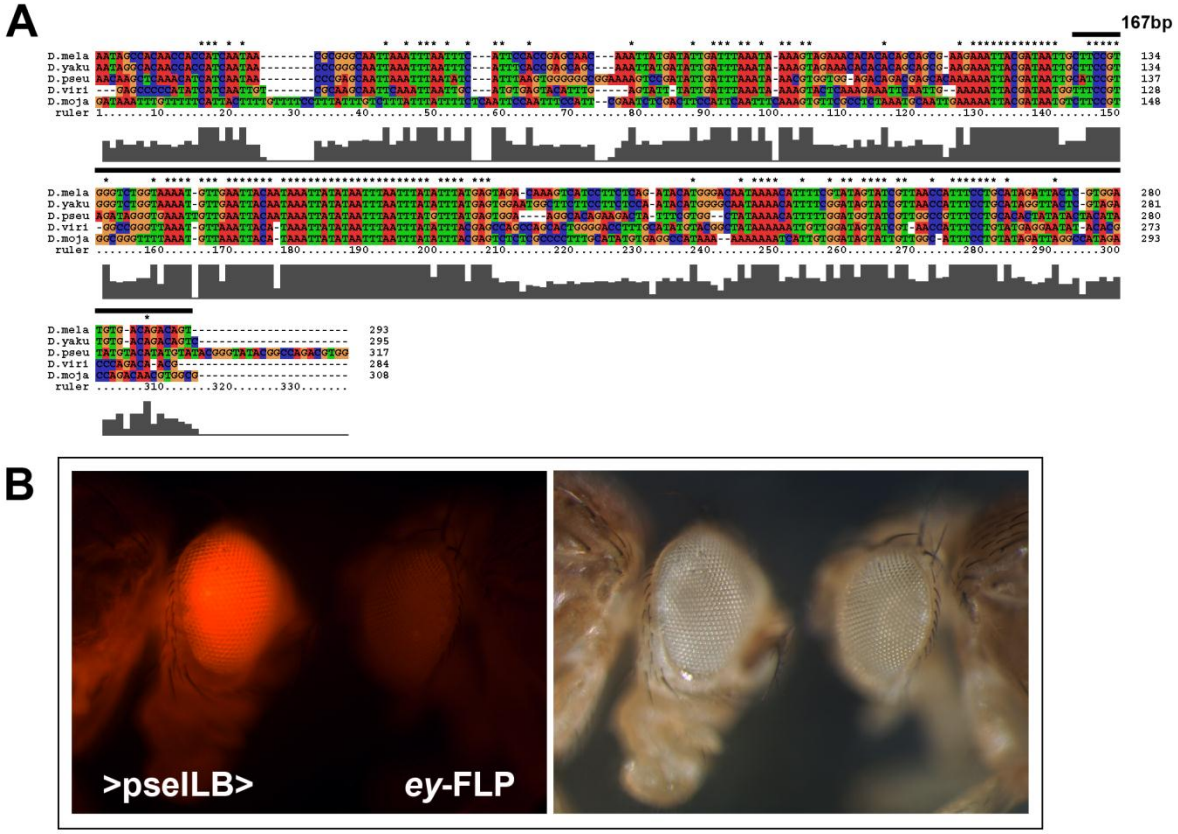

Figure 4-12. ILB is evolutionally conserved. A) The orthologous sequences of the ILB294bp region in 5 *Drosophila* species were aligned using CLUSTAL_X. The 167bp essential barrier sequence (the black line) contains a highly conserved long AT-rich stretch. B) The 2kb *D. pseudoobscura* genomic sequence encompassing the ILB294bp orthologous region (pseILB) displayed similar level of barrier activity in *D. melanogaster* as the native ILB. The transgenic flies were generated by ΦC31-mediated integration.

Table 4-1. Transformant lines

Vectors	Test fragments	attP lines	Cross number (vials)	Recovery number * (vials)	Recovery rate	DsRed intensity **
BT1	ILF3kb	9752	26	0	0%	--
	ILF4.2kb	9752	20	6	30%	++
	ILF3.7kb	9752	22	11	50%	++
	ILF2kb	9752	22	14	63.6%	++
	ILF1kb	9752	26	13	50%	++
	ILF319bp	9752	13	0	0%	--
	ILF616bp	9752	28	0	0%	--
	ILB294bp	9752	17	3	17.6%	++
	ILB167bp	9752	22	7	31.8%	++
	pseILB	9752	24	10	41.7%	++
	ILB294bp_r	9724	18	1	5.6%	++++
BT3	ILF1kb	9752	15	3	20%	++
	ILF395bp	9752	23	10	43.5%	++
IT1	Su(Hw)BR	9752	11	5	45%	++
	ILF3.7kb	9752	22	5	22.7%	++
	ILF3.7kb	9724	13	4	30%	++++
	ILB294bp	9724	12	5	41.7%	++++

* The numbers of vials containing at least one DsRed positive flies were counted.
** In heterozygous flies, two weeks after eclosure.

Table 4-2. BT1-ILB9kb transgenic lines

Individual lines	DsRed intensity *	DsRed intensity after barrier excision *	Homozygous lethality	Chromosome mapping	Insertion sites
31-3	+++	+ **	Lethal	Chromosome 2	N/A
47-2	++++	++	Lethal	Chromosome 3	Chr 3R: 27763042
63-2	+++	+	Viable	Chromosome X	Chr X: 12648036
67-1	+++++	+++	Lethal	Chromosome 3	N/A
67-2	++++	+ **	Lethal	Chromosome 3	Chr 3R:912,861
69-1	++	+	Viable	Chromosome 2	Chr 2R: 16146045
79-1	+++	+	Viable	Chromosome 2	N/A

* In heterozygous flies, 5 days after eclosure.
**Some flies had eye ablation phenotype together with reduced DsRed fluorescence.

CHAPTER 5
PERSPECTIVES

Non-Canonical Epigenetic Regulation of IRER

In this study we showed that the irradiation responsiveness of *reaper* and *hid* is subject to epigenetic regulation during development. To our knowledge, this is the first evidence that epigenetic modification controls the expression of a pro-apoptotic gene. The epigenetic regulation of the Irradiation Responsive Enhancer Region (IRER) is fundamentally different from the silencing of homeotic genes in that the change of DNA accessibility is limited to the enhancer region with the promoter region remaining open. Thus, it seems more appropriate to refer this as “blocking” of enhancer region instead of silencing of the gene.

Much effort has been devoted to understand the transcriptional regulation of *reaper*. Almost all of these studies used transgenic flies carrying reporter constructs inserted into different (mostly unidentified) chromosomal locations (Brodsky et al. 2000; Jiang et al. 2000). The cargo-size limitation of the P-element mediated transgenic technology constrained these analyses to the immediate upstream promoter /enhancer region, with the longest reporter construct containing about 11 kb upstream from the *reaper* 5’ UTR. Dissection of this 11 kb region in the reporter construct led to the identification of an ecdysone-responsive element as well as a P53-responsive element (Brodsky et al. 2000; Jiang et al. 2000). However, there are many discrepancies between the transcriptional regulation of the reporter gene and the endogenous *reaper* gene. While only a few cells in the post-stage 12 embryonic nervous system can be detected as having *reaper* expression by ISH, the reporter constructs gave extensive expression patterns after stage 12 (Nordstrom et al. 1996; Lohmann 2003). There are

also many seemingly conflicting observations in regard to the role of DmP53 in mediating DNA damage (γ-ray) induced *reaper* expression. Like its mammalian orthologs, DmP53 has been implicated in mediating ionizing irradiation-induced cell death (Brodsky et al. 2000; Jin et al. 2000; Ollmann et al. 2000; Sogame et al. 2003). In DmP53 mutant flies, ionizing irradiation induced apoptosis in the wing imaginal discs is greatly reduced, and γ-ray induced expression of *reaper* in the embryo is blocked (Lee et al. 2003; Sogame et al. 2003). However, over-expression of the *DmP53* gene in many tissues failed to induce *reaper* expression or significantly increase the sensitivity to γ-ray induced cell death. A reporter construct containing the putative *reaper* P53RE in front of a hsp70 promoter is responsive to γ-ray, but it remains responsive to irradiation even in stage 16/17 embryos (over 15 hr AEL) long after the endogenous gene lost its responsiveness (Qi et al. 2004). This strongly indicates that the sensitive-to-resistant transition is not due to availability or activation of DmP53.

In light of our data presented here, the discrepancies between the transcriptional regulation of the reporter genes and the endogenous *reaper* are due to the epigenetic silencing of the IRER. This region, containing the putative P53RE and other essential enhancer elements, is required for mediating irradiation responsiveness. Our ChIP analysis indicates that histones in this enhancer region are quickly trimethylated at both H3K9 and H3K27 at the sensitive-to-resistant transition period, accompanied by a significant decrease in DNA accessibility. DNA accessibility in the putative P53RE locus (18,368k), when measured by the DNase I sensitivity assay, did not show significant decrease until sometime after the transition period. It is possible that other enhancer elements, in the core of IRER_left that is quickly transformed into the DNase I resistant

structure, are also required for radiation responsiveness. Alternatively, it could be that the strong and rapid trimethylation of H3K27 and association of PRC1 at 18,366-368 are sufficient to disrupt DmP53 binding and/or interaction with the Pol II complex even though the region remains relatively sensitive to DNase I. Eventually, the whole IRER is closed with the exception of an open island around 18,387.

Coordinated Regulation of *hid* and *reaper*

A surprising outcome of this study is that the IRER upstream of the *reaper* locus is also required for γ-ray responsiveness of *hid* (Figure 2-6). It has been shown that *hid* and *reaper* have different expression patterns during embryogenesis. There is a significant temporal and spatial overlap in the expression of these two genes, especially in cells destined to die during embryogenesis. For example, both genes are expressed in the CNS midline cells before the onset of developmental cell death, and the function of *hid* as well as *reaper* are required for the proper cell death pattern of these cells (Zhou et al. 1997). However, there are also significant differences in the transcriptional regulation of these two genes. In the later stage (stage 12-16) embryos, there is still a significant number of cells expressing *hid*. Many of these *hid*-expressing cells do not seem to be destined for elimination and remain till the end of embryogenesis, presumably because the pro-apoptotic function of the Hid protein is also subject to post-translational modifications (Bergmann et al. 1998a). In contrast, there are only a few scattered cells in the central nervous system expressing *reaper* in post stage 14 embryos.

Despite the apparent difference in expression pattern and the fact that the two genes are more than 200 kb apart, there is a remarkable synchronicity in terms of their

responsiveness to irradiation. Both genes are responsive to γ-ray between stage 6 and stage 11. The responsiveness of both genes is lost in germ band retracting/retracted embryos. In our analysis of the Su(z)12, Hdac, and Su(v)3-9 mutants affecting the epigenetic silencing of the IRER, whenever a mutant allele delayed the sensitive-to-resistant transition of one gene, it affects the sensitivity transition of the other gene to a similar degree. In the Df(IRER) mutant, responsiveness of *hid* to irradiation is lost together with that of *reaper*. This indicates that the IRER is also responsible for mediating γ-ray responsiveness of *hid*. To achieve this, there has to be a formation of higher-order chromosome configuration (looping) to bring the IRER to the proximity of the *hid* promoter region. Such higher-order DNA/chromatin complex has been noticed in mammalian systems as documented by 3C (Chromosome Conformation Capture) assays (Tolhuis et al. 2002) (Dekker et al. 2002). The formation of the higher-order chromatin complex seems to require elements reside between R4 and R6, as the *hid* responsiveness is blocked in Df(IRER_right) even though *reaper* remains responsive. The detailed mechanism of such an arrangement remains to be studied.

Differentiation Stage-Specific Sensitivity to Irradiation-Induced Cell Death

The developmental consequence of epigenetic regulation of the IRER is the tuning down (off) of the responsiveness of the pro-apoptotic genes, and thus decreasing cellular sensitivity to stresses such as DNA damage (Figure 2-10G). Epigenetic silencing of the IRER, and the sensitive-to-resistant transition, happens at a time (7-9 hr AEL) corresponding to the end of major mitotic waves when most cells begin to differentiate (Foe et al. 1993). It is interesting to note that differentiation stage-specific sensitivity to irradiation has long been noticed in mammalian systems. For instance,

proliferating neural precursor cells are extremely sensitive to irradiation-induced cell death while differentiating/differentiated neurons become resistant to γ-ray irradiation (Mizumatsu et al. 2003), even though the same level of DNA damage was inflicted by the irradiation (Nowak et al. 2006). Our findings here suggest that such a dramatic transition of radiation sensitivity accompanying cellular differentiation could be achieved by epigenetic blocking of sensitizing enhancers of pro-apoptotic genes (Figure 2-10G).

The responsiveness of *reaper* to irradiation and its role in mediating irradiation-induced cell death was noticed upon its initial identification (White et al. 1994). Interestingly, the irradiation responsiveness appears to be a highly conserved feature of *reaper*-like IAP-antagonists. A recently identified functional ortholog of *reaper* in mosquito genomes, *michelob_x*(*mx*), was also responsive to irradiation (Zhou et al. 2005). Mosquitoes (*Aedes* and *Anopheles*) were separated from *Drosophila* around 250 million years ago. The resemblance between Mx and Reaper/Hid at the protein sequence level is so low that it could not be identified by a routine sequence similarity search. The conservation of irradiation responsiveness highlighted that stress responsiveness is an essential aspect of functional regulation of upstream pro-apoptotic genes such as *reaper*/*hid*. It is also worth mentioning that several mammalian BH3 domain-only proteins, the upstream pro-apoptotic regulators of the Bcl-2/Ced-9 pathway, are also regulated at the transcriptional level. BH3-only genes such as *puma* are induced upon irradiation and required for mediating irradiation- induced cell death in developing nervous systems as well as hematopoietic cells (Nakano and Vousden 2001; Villunger et al. 2003).

Later in *Drosophila* development, around the time of pupae formation, the organism becomes sensitive to irradiation again, with LD50 values similar to what was observed for the 4-7 hr AEL embryos (Ashburner 1989). Interestingly, it has also been found that during this period, the highly proliferative imaginal discs are sensitive to irradiation-induced apoptosis, which is mediated by the induction of *reaper* and *hid* through P53 and Chk2 (Brodsky et al. 2004). The ability for UV irradiation to induce *hid* in eye imaginal discs appears to be limited to a small time window corresponding to the early highly proliferative period of imaginal disc development and differentiation (Jassim et al. 2003). After this short window, irradiation can no longer induce apoptosis. Our finding here suggests that the sensitive-to-resistant transition could very well be achieved by epigenetic regulation of the IRER. However, it remains to be studied as whether the reemergence of sensitive tissue is due to the reversal of the epigenetic blocking in IRER or the proliferation of undifferentiated stem cells that have an unblocked IRER.

The finding that epigenetic regulation of enhancer region of pro-apoptotic gene controls sensitivity to irradiation induced cell death may have implications in clinical applications involving ionizing irradiation. It suggests that applying drugs that modulate epigenetic silencing may help increase the efficacy of radiation therapy. It also remains to be seen as to whether the hyper-sensitivity of some tumors to irradiation is due to the de-differentiation and reversal of epigenetic blocking in cancer cells. On the other hand, loss of proper stress response to cellular damage is implicated in tumorigenesis (reviewed by (Baylin and Ohm 2006). The fact that the formation of heterochromatin in the sensitizing enhancer region of pro-apoptotic genes is sufficient to convey resistance

to stress-induced cell death suggests it could contribute to tumorigenesis. In addition, it could also be the underlying mechanism of tumor cells evading irradiation-induced cell death. This is a likely scenario given that it has been well documented that oncogenes such as Rb (Narita et al. 2003; Ait-Si-Ali et al. 2004) and PML-RAR fusion protein (Carbone et al. 2006) cause the formation of heterochromatin through recruiting a human ortholog of Su(v)3-9. In this regard, the *reaper* locus, especially the IRER, provides an excellent genetic model system for dissecting the *cis* and *trans* acting mechanisms controlling the formation of heterochromatin associated with cellular differentiation and tumorigenesis.

A Non-Canonical Epigenetic Silencing

The blocking of IRER differs fundamentally with the silencing of homeotic genes in several aspects. First, the change of DNA accessibility and histone modification is largely limited to the enhancer region. The promoter regions of *reaper* (and *hid*) remain open, allowing the gene to be responsive to other stimuli. Indeed, there are a few cells in the central nervous system that could be detected as expressing *reaper* long after the sensitive-to-resistant transition. Even more cells in the late stage embryo can be found having *hid* expression. Yet, the irradiation responsiveness of the two genes is completely suppressed in most if not all cells, transforming the tissues into radiation-resistant state.

Secondly, the histone modification of IRER has a mixture of features associated with pericentromeric heterochromatin formation and the canonic PcG- mediated silencing. Both H3K9 and H3K27 are trimethylated with a large overlapping region. Both HP1, the signature binding protein of the pericentromeric heterochromatin, and the PRC1 are bound to IRER. As demonstrated by genetic analysis, the function of both

Su(var)3-9 and Su(z) 12/Pc are required for the silencing. However, despite the enrichment of trimethylated H3K27 in IRER, we did not observe significant delay of sensitive-to-resistant switch in several E(Z) mutant alleles. When analyzed with the most updated PRE-identification software (Fiedler and Rehmsmeier 2006), only a sub-optimal match was identified around 18,370-371. However, binding of Pc or Psc to this region is about the same as other IRER regions (Data not shown). The fact that none of the mutants tested could completely block the transition seems to suggest that there is a redundancy of the two pathways in modifying/blocking IRER. It is also possible that the genes we tested are not the key regulator of IRER blocking but only have participatory role in the process. Needless to say, the detailed mechanisms await to be explored. The uniqueness of this epigenetic regulation warrants an unbiased screen for key regulators of this process.

In addition, there is no clear Polycomb Response element (PRE) can be predicted in or around IRER using the algorithm developed by Ringrose group based on GAGA factor, PHO and Zeste binding motifs (Fiedler and Rehmsmeier 2006; Ringrose and Paro 2007). However, the ChIP-based genome-wide study of PcG binding sites did not correspond well with the predicted sites (Schwartz et al. 2006), suggesting that additional criteria are necessary to predict most PREs reliably. Moreover, the binding pattern of several PcG proteins to IRER also differs from the pattern observed for homeotic genes such as *Ubx*, where the PcG proteins are tightly associated with their PREs, usually relative small regions of several hundred base pairs (Schwartz et al. 2006). Here in IRER, we found the enrichment of PSC, PC and E(z) across a large chromatin region of more than 30kb (Figure 2-9), similar to the distribution of

H3K27me3. This scenario resembles the distribution patterns of PcG in mammals, in which PRC2 association to chromatin follows the distribution of H3K27me3 on most of target genes (Hansen et al. 2008). This suggests that the mechanisms of the PcG initiation and maintenance between *Drosophila* and mammals might share more features than people have thought.

The observations in IRER{ubi-DsRed} reporter strain indicate that the epigenetic regulation is not cell lineage dependent. For instances, in male third instar larvae, a group of cells at the apex of the testis disc, where the male GSCs usually reside, exhibit a much brighter DsRed signal than any other tissues (Figure 3-8 A and B). Whereas DsRed signal is turned off in the progenies of GSC, such as the spermatocytes that situated just posterior to the GSCs. This is somehow distict from the role of PcG silencing as the epigenetic memory of cell identity (Bantignies and Cavalli 2006; Ringrose and Paro 2007), although dynamic regulation of PcG proteins has previously been reported (Bantignies and Cavalli 2006).

Finally, within the IRER, there is a small region around 18,387 (18,386k-388k) that remains relatively open till the end of embryogenesis (Figure 2-7A). Interestingly, this open region is flanked by two putative non-coding RNA transcripts represented by EST sequences, RE73107 (3L: 18,383-379) and RE07245 (3L: 18,388-392). If they are indeed transcribed in the embryo as suggested by the mRNA source of the cDNA library, then the “open island” within the closed IRER will likely be their shared enhancer region. Sequences of both cDNAs revealed that there is no intron or reputable open reading frame in either sequence. Despite repeated efforts, we were not able to confirm their expression via ISH or Northern. Over-expression of either cDNA using an

expression construct also failed to show any effect on *reaper/hid* induced cell death in S2 cells. Yet, sections of the two non-coding RNAs are strongly conserved in divergent *Drosophil*a genomes. The potential role of these two non-coding RNAs in mediating *reaper/hid* expression and/or blocking of the IRER remains to be studied.

In order to fully understand this kind of non-canonical epigenetic mechanism, we will try to answer the following questions: 1) which *cis* elements are responsible for initiating and setting up the boundary of chromatin modification in IRER? We already knew the answer to the second question, and the results were discussed in detail in Chapter 4; 2) what are the chromatin modulators responsible for histone modification in IRER? 3) What looping structure enables IRER to interact with *hid*? These studies will contribute to our knowledge of sophisticated regulation of apoptosis during normal development and under stress condition.

Functional Significance of the Epigenetic Regulation of IRER

A paramount of evidence suggests that when cell death (apoptosis) occurs in response to cytotoxic stimuli such as ionizing irradiation, it is often mediated through the transcriptional activation of upstream cell death regulators involving transcription factors such as P53 (Zhou et al. 2003). However, this does not explain why there is dramatic difference among tissues and cell types in their sensitivity to irradiation induced cell death. First, the sensitive-to-resistant transition for the induction of pro-apoptotic genes is unlikely due to the unavailability of DmP53, since it is ubiquitously expressed throughout the whole embryogenesis (Jin et al. 2000). In addition, DmP53-mediated DNA repair genes *ku70* and *ku80* remain responsive to irradiation in both sensitive and resistant stage embryos. Furthermore, over-expression of DmP53 failed to induce

reaper expression or apoptosis in resistant stage embryos. All of the evidence suggests that DmP53 alone is not sufficient to determine cellular sensitivity to DNA damage.

Our study in Chapter 2 showed that the epigenetic status of the IRER enhancer region determined the embryonic sensitivity to ionizing radiation induced cell death. Around stage 12, this region forms a heterochromatin-like structure that is inaccessible to DNase I, accompanied with the enrichment of repressive chromatin marks, such as H3K27me3 and H3K9me3, and the binding of HP1 and Polycomb group proteins (Zhang et al. 2008a). The resistence to irradiation at the later stages is likely due to the inaccessibility of the IRER to some upstream transcription factors, such as DmP53, which otherwise binds to the P53RE within the IRER. Indeed, a recent study showed that some p53 target genes could be silenced by E4-ORF3, a small adenovirus protein, through *de novo* H3K9me3 heterochromatin formation upon the virus infection. This epigenetic silencing of p53 target genes prevented p53-DNA binding, and is irrespective of p53 phosphorylation and stabilization (Soria et al. 2010). Therefore, the epigenetic mechanism in transcriptional regulation of stress induced genes might be evolutionally conserved.

Besides its role in regulating the ionizting radiation induced cell death, the IRER might also be required for modulating the cell death resulting from the developmental stresses, such as cell competition for growth factors. Indeed, we found the down-regulation of *reaper* expression in the IRER deletion mutants in the segmental strips where the cell competition induced cell death happens (Figure 3-4). This suggests that IRER is also involved in the apoptosis during the normal development.

By investigating the expression pattern of the IRER{ubi-DsRed} reporter, we will be abel to know when and in which cells is IRER open/closed. And our cell sorting data showed that the accessibility of IRER can reflect the cellular sensitivity to stress induced cell death. It will be intriguing to know whether IRER is specifically open in mitotic cells, such as the cells in the early stage embryos. Our preliminary data suggest that the openness of IRER could be quite dynamic upon various environmental stimuli, such as irradiation, heat shock and starvation. To our knowledge, this is the first established system for *in vivo* mornitoring the chromatin structure of a genomic region in single cell resolution during developmental process or under stress conditions. This will greatly improve people's understanding of this higher level of gene regulation.

A Novel Chromatin Barrier Element ILB Delimits the Ehancer-Specific Epigenetic Regulation without Blockign the Enhancer Function

Eukaryotic genome is composed of two types of functional compartments-euchromatin and heterochromatin, usually juxtaposed to each other. The regions of DNA packed into heterochromatin are found in two varieties: constitutive heterochromatin and facultative heterochromatin, the distinction lies in the inconsistency of the latter form in different cell types within a species. The formation of heterochromatin is launched by the initiating elements bound by repressor proteins which recruit enzymes that modify the chromatin to create binding sites for these repressor proteins, leading to the recruitment of these proteins and the subsequent spread of heterochromatin over several hundreds of kilobase pairs (Raab and Kamakaka 2010). Chromatin barrier is defined as a type of DNA elements that can block the self propagation of heterochromatin into the neighboring regions.

An Efficient Barrier Testing Strategy

The traditional chromatin barrier assay in *Drosophila* is to test the ability of the candidate barrier sequences to protect a reporter gene, usually a mini-white gene flanked by two insulators/barriers, against the position effect when randomly inserted into the genome (Kellum and Schedl 1991). However, there are three problems with this system. First, generating a relatively large amount of transformant lines for each recombinated DNA is necessary for statistic analysis of the eye color variation with or without the flanking insulators/barriers. Secondly, not only the difference of chromatin accessibility at the insertion loci, but also the proximity of an enhancer can result in position effect variation (Weiler and Wakimoto 1995). So both enhancer-blocking and barrier activities of a tested DNA may attribute to the protection against the variation. In addition, insertions of an unprotected reporter gene within a closed genomic region will not be recovered due to the complete heterochromatin silencing, so comparison between the protected and unprotected transgenes based on the variation of eye color could be misleading.

Using a modified version of the previously described reporter construct (Sigrist and Pirrotta 1997) by testing the ability to prevent the heterochromatin spread initiated by a PRE, we identified a chromatin barrier element ILB (chr 3L: 18,397,175-18,397,341) at the transition region between the permissive *reaper* promoter and the highly condensed IRER enhancer region in adult flies. One advantage of this strategy comparing to the traditional assay is that only the barrier activity will be detected, but not the enhancer-blocking activity. Another merit of this barrier testing vector is that it contains two P elements and an attB integration sequence, thus the transgenic flies could be generated by either P-element mediated insertion or ΦC31 system. With ΦC31 integration into a

common genomic locus, the efficiency of different candidate barrier sequences could be compared directly based on the levels of eye-specific expressed DsRed without worrying the position effect, therefore it is not necessary to screen and keep numerous transgenic lines.

A Novel Chromatin Berrier Lacking the Enhancer-Blocking Activity

The ILB barrier does not contain the enhancer-blocking activity because it did not interrupt the interaction between the DsRed promoter and UAS/GAL4 enhancer. This is the first pure chromatin barrier identified in *Drosophila*, as all the currently known *Drosophila* insulator/boundary elements are also enhancer-blockers. In vertebrates, although the barrier and enhancer-blocking activities can be separated as in the case of chicken HS4 insulator, the *cis*-elements responsible for these two activities are intertwined and localized in a relatively small region. However, the situation in ILB region is different from this functional complex. First, ILB barrier resides in between of the *reaper* promoter and IRER enhancer region, any endogenous enhancer-blocking activity in the transition region would prevent the IRER from activating the transcription of *reaper* gene. Indeed, our previous study showed that P or piggyBac transposons containing a *gypsy* insulator inserted between IRER and the *reaper* promoter completely blocked the irradiation responsiveness of *reaper* in early embryos (Zhang et al. 2008b). This ruled out the possibility of the existence of enhancer-blockers within this region. More importantly, here we showed that ILB294bp and the larger 3.7kb fragment did not block the interaction between DsRed promoter and UAS/GAL4 enhancer complex in a reporter assay, while the interaction could be blocked by the *gypsy* insulator. Therefore, the evolutionally conserved ILB barrier probably represents a novel

type of standalone *cis*-elements that maintain the distinct chromatin domain by blocking the spreading of heterochromatin, but do not disrupt the enhancer/promoter interaction.

None of the known *Drosophila* insulator/boundary-associated proteins showing strong enrichment in the essential ILB167bp barrier region confirmed its distinction from these known *cis*-elements. Mutagenesis of the AT-rich region that resembles the mammalian SATB1 binding site did not affect the barrier function, suggesting the barrier may function through a different mechanism from MARs-mediated PEV blocking activity (Girard et al. 1998; Nabirochkin et al. 1998). Isolating and characterizing the ILB-associated *trans*-factor(s) will certainly promote the understanding of its underlying mechanism, and will also facilitate the identification of more of this type of standalone barrier elements.

Our previous work showed that the epigenetic blocking of IRER enhancer region (chr 3L: 18,393,577-18,426,702) controls the sensitivity to the irradiation-induced apoptosis during embryogenesis (Zhang et al. 2008b). Our recent findings suggest that this epigenetic regulation could be quite dynamic upon exogenous or developmental stresses. By inserting a DsRed reporter gene into the middle of IRER region to monitor the real-time chromatin structure of this region, we found an increased DsRed signals in the larvae imaginal discs after irradiation (unpublished data). Also, the IRER region seems to be able to sense the calorie restriction and other stresses by altering the chromatin accessibility (unpublished data). In this study we showed that the ILB barrier at the left boundary of IRER protects the permissive *reaper* promoter from epigenetic silencing by restraining the propagation of the facultative heterochromatin initiated by the unknown initiating element(s) within the IRER. The pure barrier activity may be

critical for the dynamic epigenetic regulation of IRER by delimiting the particular silenced domain in the enhancer region while allowing the enhancer function on the promoter when the silencing is withdrawn upon stress. Considering its unique role, it will be of great interest to see whether similar standalone chromatin barriers exist in other genomic.

APPENDIX

THE PRIMERS USED FOR QPCR IN CHIP EXPERIMENTS

Act5C: CACGGTATCGTGACCAACTG, GCCATCTCCTGCTCAAAGTC

H23: CCAAGTTGGCCAGTTTTGAT, AGTTCAAGCCCGGGTATTCT

Ubx: GCCATAACGGCAGAACCAAAG, ATGAGGCCATCTCAGTCGC

pro: GCGATGGTTGCTTTTCAACT, TGGCAACAACAACACAACCT

-2k: GTGCGTCTCAAGTGTTTCCA, CGAAAGCAGACCCAAAACAT

-3k: TGGGAAGTGTGTCAATCGAA, CGCAAGTTATCGCATTGTTG

-5k: TTTTCGGAATGGGTTTTCAG, ACACACACGAACCGAATGAA

-8k: GAGCTGGGTGATTTGTGGTT, CAACAATTTGAGCAGGAGCA

-11k: CCATCCACAGGAACTGGACT, GGCAAGTCCCCAGACATTTA

-14k: AGCAGCATCCTGACTGTCCT, CGCTTGGTTGAAATTTGGTT

-19k: TTGGGCCCCTTTTAAATACC, AAAAACCGGAGCCTAAAGGA

-27k: TACCAACTCGGTCCTTCCAC, TTCTGCACCCATTCTCCTCT

PRE-FRT: GATAGGACTACGCGCACCAT, CACTGTTCACGTCGCAAGAT

P3: TCAATTAGGATCCAAGCTTATCG, TGTTCAGCTGCGCTTGTTTA

DsR1: GCAGGATGGCTGTTTCATCT, AATGACCACCGTCTTTCAGC

DsR2: GAAGCTGAAAGACGGTGGTC, CGTCCCTCGGTTCTTTCATA

.

LIST OF REFERENCES

Abrams JM, White K, Fessler LI, Steller H. 1993. Programmed cell death during Drosophila embryogenesis. *Development* **117**: 29-43.

Ait-Si-Ali S, Guasconi V, Fritsch L, Yahi H, Sekhri R, Naguibneva I, Robin P, Cabon F, Polesskaya A, Harel-Bellan A. 2004. A Suv39h-dependent mechanism for silencing S-phase genes in differentiating but not in cycling cells. *Embo J* **23**: 605-615.

Andres V, Chiara MD, Mahdavi V. 1994. A new bipartite DNA-binding domain: cooperative interaction between the cut repeat and homeo domain of the cut homeo proteins. *Genes Dev* **8**: 245-257.

Ashburner M. 1989. *Drosophila. A Laboratory Handbook.* Cold Spring Harbor Laboratory, Cold Spring Harbor, New York.

Bantignies F, Cavalli G. 2006. Cellular memory and dynamic regulation of polycomb group proteins. *Curr Opin Cell Biol* **18**: 275-283.

Barges S, Mihaly J, Galloni M, Hagstrom K, Muller M, Shanower G, Schedl P, Gyurkovics H, Karch F. 2000. The Fab-8 boundary defines the distal limit of the bithorax complex iab-7 domain and insulates iab-7 from initiation elements and a PRE in the adjacent iab-8 domain. *Development* **127**: 779-790.

Baylin SB, Ohm JE. 2006. Epigenetic gene silencing in cancer - a mechanism for early oncogenic pathway addiction? *Nat Rev Cancer* **6**: 107-116.

Bell AC, West AG, Felsenfeld G. 1999. The protein CTCF is required for the enhancer blocking activity of vertebrate insulators. *Cell* **98**: 387-396.

Bello BC, Hirth F, Gould AP. 2003. A pulse of the Drosophila Hox protein Abdominal-A schedules the end of neural proliferation via neuroblast apoptosis. *Neuron* **37**: 209-219.

Bender W, Fitzgerald DP. 2002. Transcription activates repressed domains in the Drosophila bithorax complex. *Development* **129**: 4923-4930.

Bergmann A, Agapite J, McCall K, Steller H. 1998a. The *Drosophila* Gene *hid* Is a Direct Molecular Target of Ras-Dependent Survival Signaling. *Cell* **95**: 331-341.

—. 1998b. The Drosophila gene hid is a direct molecular target of Ras-dependent survival signaling. *Cell* **95**: 331-341.

Bergmann A, Agapite J, Steller H. 1998c. Mechanisms and control of programmed cell death in invertebrates. *Oncogene* **17**: 3215-3223.

Bi X, Broach JR. 1999. UASrpg can function as a heterochromatin boundary element in yeast. *Genes Dev* **13**: 1089-1101.

—. 2001. Chromosomal boundaries in S. cerevisiae. *Curr Opin Genet Dev* **11**: 199-204.

Birch-Machin I, Gao S, Huen D, McGirr R, White RA, Russell S. 2005. Genomic analysis of heat-shock factor targets in Drosophila. *Genome Biol* **6**: R63.

Birve A, Sengupta AK, Beuchle D, Larsson J, Kennison JA, Rasmuson-Lestander A, Muller J. 2001. Su(z)12, a novel Drosophila Polycomb group gene that is conserved in vertebrates and plants. *Development* **128**: 3371-3379.

Bischof J, Maeda RK, Hediger M, Karch F, Basler K. 2007. An optimized transgenesis system for Drosophila using germ-line-specific phiC31 integrases. *Proc Natl Acad Sci U S A* **104**: 3312-3317.

Brand AH, Perrimon N. 1993. Targeted gene expression as a means of altering cell fates and generating dominant phenotypes. *Development* **118**: 401-415.

Breiling A, Turner BM, Bianchi ME, Orlando V. 2001. General transcription factors bind promoters repressed by Polycomb group proteins. *Nature* **412**: 651-655.

Brodsky MH, Nordstrom W, Tsang G, Kwan E, Rubin GM, Abrams JM. 2000. Drosophila p53 binds a damage response element at the reaper locus. *Cell* **101**: 103-113.

Brodsky MH, Weinert BT, Tsang G, Rong YS, McGinnis NM, Golic KG, Rio DC, Rubin GM. 2004. Drosophila melanogaster MNK/Chk2 and p53 regulate multiple DNA repair and apoptotic pathways following DNA damage. *Mol Cell Biol* **24**: 1219-1231.

Brown JL, Fritsch C, Mueller J, Kassis JA. 2003. The Drosophila pho-like gene encodes a YY1-related DNA binding protein that is redundant with pleiohomeotic in homeotic gene silencing. *Development* **130**: 285-294.

Brown JL, Mucci D, Whiteley M, Dirksen ML, Kassis JA. 1998. The Drosophila Polycomb group gene pleiohomeotic encodes a DNA binding protein with homology to the transcription factor YY1. *Mol Cell* **1**: 1057-1064.

Bushey AM, Dorman ER, Corces VG. 2008. Chromatin insulators: regulatory mechanisms and epigenetic inheritance. *Mol Cell* **32**: 1-9.

Busturia A, Lloyd A, Bejarano F, Zavortink M, Xin H, Sakonju S. 2001. The MCP silencer of the Drosophila Abd-B gene requires both Pleiohomeotic and GAGA factor for the maintenance of repression. *Development* **128**: 2163-2173.

Campos-Ortega JA, Hartenstein V. 1985. *The Embryonic Development of Drosophila melanogaster*. Springer-Verlag, Berlin.

Cao R, Tsukada Y, Zhang Y. 2005. Role of Bmi-1 and Ring1A in H2A ubiquitylation and Hox gene silencing. *Mol Cell* **20**: 845-854.

Cao R, Wang L, Wang H, Xia L, Erdjument-Bromage H, Tempst P, Jones RS, Zhang Y. 2002. Role of histone H3 lysine 27 methylation in Polycomb-group silencing. *Science* **298**: 1039-1043.

Cao R, Zhang Y. 2004a. The functions of E(Z)/EZH2-mediated methylation of lysine 27 in histone H3. *Curr Opin Genet Dev* **14**: 155-164.

—. 2004b. SUZ12 is required for both the histone methyltransferase activity and the silencing function of the EED-EZH2 complex. *Mol Cell* **15**: 57-67.

Carbone R, Botrugno OA, Ronzoni S, Insinga A, Di Croce L, Pelicci PG, Minucci S. 2006. Recruitment of the histone methyltransferase SUV39H1 and its role in the oncogenic properties of the leukemia-associated PML-retinoic acid receptor fusion protein. *Mol Cell Biol* **26**: 1288-1296.

Carr A, Biggin MD. 2000. Accessibility of transcriptionally inactive genes is specifically reduced at homeoprotein-DNA binding sites in Drosophila. *Nucleic Acids Res* **28**: 2839-2846.

Cashio P, Lee TV, Bergmann A. 2005. Genetic control of programmed cell death in Drosophila melanogaster. *Semin Cell Dev Biol* **16**: 225-235.

Chan CS, Rastelli L, Pirrotta V. 1994. A Polycomb response element in the Ubx gene that determines an epigenetically inherited state of repression. *Embo J* **13**: 2553-2564.

Chanas G, Lavrov S, Iral F, Cavalli G, Maschat F. 2004. Engrailed and polyhomeotic maintain posterior cell identity through cubitus-interruptus regulation. *Dev Biol* **272**: 522-535.

Chao C, Saito S, Kang J, Anderson CW, Appella E, Xu Y. 2000. p53 transcriptional activity is essential for p53-dependent apoptosis following DNA damage. *Embo J* **19**: 4967-4975.

Chen P, Nordstrom W, Gish B, Abrams JM. 1996. *grim*, a novel cell death gene in *Drosophila*. *Genes Dev* **10**: 1773-1782.

Christich A, Kauppila S, Chen P, Sogame N, Ho SI, Abrams JM. 2002. The Damage-Responsive Drosophila Gene sickle Encodes a Novel IAP Binding Protein Similar to but Distinct from reaper, grim, and hid. *Curr Biol* **12**: 137-140.

Claveria C, Caminero E, Martinez AC, Campuzano S, Torres M. 2002. GH3, a novel proapoptotic domain in Drosophila Grim, promotes a mitochondrial death pathway. *Embo J* **21**: 3327-3336.

Claveria C, Martinez AC, Torres M. 2004. A Bax/Bak-independent mitochondrial death pathway triggered by Drosophila Grim GH3 domain in mammalian cells. *J Biol Chem* **279**: 1368-1375.

Conradt B, Horvitz HR. 1999. The TRA-1A sex determination protein of C. elegans regulates sexually dimorphic cell deaths by repressing the egl-1 cell death activator gene. *Cell* **98**: 317-327.

Czermin B, Melfi R, McCabe D, Seitz V, Imhof A, Pirrotta V. 2002. Drosophila enhancer of Zeste/ESC complexes have a histone H3 methyltransferase activity that marks chromosomal Polycomb sites. *Cell* **111**: 185-196.

Dejardin J, Cavalli G. 2004. Chromatin inheritance upon Zeste-mediated Brahma recruitment at a minimal cellular memory module. *Embo J* **23**: 857-868.

Dekker J, Rippe K, Dekker M, Kleckner N. 2002. Capturing chromosome conformation. *Science* **295**: 1306-1311.

Dellino GI, Schwartz YB, Farkas G, McCabe D, Elgin SC, Pirrotta V. 2004. Polycomb silencing blocks transcription initiation. *Mol Cell* **13**: 887-893.

Dickson J, Gowher H, Strogantsev R, Gaszner M, Hair A, Felsenfeld G, West AG. 2010. VEZF1 elements mediate protection from DNA methylation. *PLoS Genet* **6**: e1000804.

Dienemann A, Sprenger F. 2004. Requirements of cyclin a for mitosis are independent of its subcellular localization. *Curr Biol* **14**: 1117-1123.

Ditzel M, Meier P. 2005. Ubiquitylation in apoptosis: DIAP1's (N-)en(d)igma. *Cell Death Differ* **12**: 1208-1212.

Donze D, Adams CR, Rine J, Kamakaka RT. 1999. The boundaries of the silenced HMR domain in Saccharomyces cerevisiae. *Genes Dev* **13**: 698-708.

Engstrom PG, Ho Sui SJ, Drivenes O, Becker TS, Lenhard B. 2007. Genomic regulatory blocks underlie extensive microsynteny conservation in insects. *Genome Res* **17**: 1898-1908.

Erokhin M, Parshikov A, Georgiev P, Chetverina D. 2010. E(y)2/Sus1 is required for blocking PRE silencing by the Wari insulator in Drosophila melanogaster. *Chromosoma* **119**: 243-253.

Fiedler T, Rehmsmeier M. 2006. jPREdictor: a versatile tool for the prediction of cis-regulatory elements. *Nucleic Acids Res* **34**: W546-550.

Fischle W, Wang Y, Jacobs SA, Kim Y, Allis CD, Khorasanizadeh S. 2003. Molecular basis for the discrimination of repressive methyl-lysine marks in histone H3 by Polycomb and HP1 chromodomains. *Genes Dev* **17**: 1870-1881.

Flaus A, Owen-Hughes T. 2004. Mechanisms for ATP-dependent chromatin remodelling: farewell to the tuna-can octamer? *Curr Opin Genet Dev* **14**: 165-173.

Foe V, Odell G, Edgar B. 1993. Mitosis and Morphogenesis in the Drosophila embryo: Point and counter point. in *The Development of Drosphila Melanogaster* (eds. B M, M-A A). Cold Spring Harbor laboratory Press, Cold Spring Harbor.

Fourel G, Revardel E, Koering CE, Gilson E. 1999. Cohabitation of insulators and silencing elements in yeast subtelomeric regions. *Embo J* **18**: 2522-2537.

Franc NC, Dimarcq JL, Lagueux M, Hoffmann J, Ezekowitz RA. 1996. Croquemort, a novel Drosophila hemocyte/macrophage receptor that recognizes apoptotic cells. *Immunity* **4**: 431-443.

Franc NC, Heitzler P, Ezekowitz RAB, White K. 1999. Requirement for Croquemort in Phagocytosis of Apoptotic Cells in *Drosophila*. *Science* **284**: 1991-1994.

Francis NJ, Kingston RE, Woodcock CL. 2004. Chromatin compaction by a polycomb group protein complex. *Science* **306**: 1574-1577.

Francis NJ, Saurin AJ, Shao Z, Kingston RE. 2001. Reconstitution of a functional core polycomb repressive complex. *Mol Cell* **8**: 545-556.

Freel CD, Richardson DA, Thomenius MJ, Gan EC, Horn SR, Olson MR, Kornbluth S. 2008. Mitochondrial localization of Reaper to promote inhibitors of apoptosis protein degradation conferred by GH3 domain-lipid interactions. *J Biol Chem* **283**: 367-379.

Fritsch C, Brown JL, Kassis JA, Muller J. 1999. The DNA-binding polycomb group protein pleiohomeotic mediates silencing of a Drosophila homeotic gene. *Development* **126**: 3905-3913.

Gaszner M, Felsenfeld G. 2006. Insulators: exploiting transcriptional and epigenetic mechanisms. *Nat Rev Genet* **7**: 703-713.

Girard F, Bello B, Laemmli UK, Gehring WJ. 1998. In vivo analysis of scaffold-associated regions in Drosophila: a synthetic high-affinity SAR binding protein suppresses position effect variegation. *Embo J* **17**: 2079-2085.

Goyal L, McCall K, Agapite J, Hartwieg E, Steller H. 2000. Induction of apoptosis by Drosophila reaper, hid and grim through inhibition of IAP function. *Embo J* **19**: 589-597.

Grether ME, Abrams JM, Agapite J, White K, Steller H. 1995. The *head involution defective* gene of *Drosophila melanogaster* functions in programmed cell death. *Genes & Dev* **9**: 1694-1708.

Gurudatta BV, Corces VG. 2009. Chromatin insulators: lessons from the fly. *Brief Funct Genomic Proteomic* **8**: 276-282.

Hansen KH, Bracken AP, Pasini D, Dietrich N, Gehani SS, Monrad A, Rappsilber J, Lerdrup M, Helin K. 2008. A model for transmission of the H3K27me3 epigenetic mark. *Nat Cell Biol* **10**: 1291-1300.

Hogga I, Karch F. 2002. Transcription through the iab-7 cis-regulatory domain of the bithorax complex interferes with maintenance of Polycomb-mediated silencing. *Development* **129**: 4915-4922.

Horvitz HR. 1999. Genetic control of programmed cell death in the nematode Caenorhabditis elegans. *Cancer Res* **59**: 1701s-1706s.

Huang S, Li X, Yusufzai TM, Qiu Y, Felsenfeld G. 2007. USF1 recruits histone modification complexes and is critical for maintenance of a chromatin barrier. *Mol Cell Biol* **27**: 7991-8002.

Jacobs HW, Knoblich JA, Lehner CF. 1998. Drosophila Cyclin B3 is required for female fertility and is dispensable for mitosis like Cyclin B. *Genes Dev* **12**: 3741-3751.

Jassim OW, Fink JL, Cagan RL. 2003. Dmp53 protects the Drosophila retina during a developmentally regulated DNA damage response. *Embo J* **22**: 5622-5632.

Jeffers JR, Parganas E, Lee Y, Yang C, Wang J, Brennan J, MacLean KH, Han J, Chittenden T, Ihle JN et al. 2003. Puma is an essential mediator of p53-dependent and -independent apoptotic pathways. *Cancer Cell* **4**: 321-328.

Jenuwein T, Allis CD. 2001. Translating the histone code. *Science* **293**: 1074-1080.

Jiang C, Baehrecke EH, Thummel CS. 1997. Steroid regulated programmed cell death during Drosophila metamorphosis. *Development* **124**: 4673-4683.

Jiang C, Lamblin AF, Steller H, Thummel CS. 2000. A steroid-triggered transcriptional hierarchy controls salivary gland cell death during Drosophila metamorphosis. *Mol Cell* **5**: 445-455.

Jin S, Martinek S, Joo WS, Wortman JR, Mirkovic N, Sali A, Yandell MD, Pavletich NP, Young MW, Levine AJ. 2000. Identification and characterization of a p53 homologue in Drosophila melanogaster. *Proc Natl Acad Sci U S A* **97**: 7301-7306.

Jones RS, Gelbart WM. 1990. Genetic analysis of the enhancer of zeste locus and its role in gene regulation in Drosophila melanogaster. *Genetics* **126**: 185-199.

Kahn TG, Schwartz YB, Dellino GI, Pirrotta V. 2006. Polycomb complexes and the propagation of the methylation mark at the Drosophila ubx gene. *J Biol Chem* **281**: 29064-29075.

Kalmykova AI, Nurminsky DI, Ryzhov DV, Shevelyov YY. 2005. Regulated chromatin domain comprising cluster of co-expressed genes in Drosophila melanogaster. *Nucleic Acids Res* **33**: 1435-1444.

Kamakaka RT, Kadonaga JT. 1994. The soluble nuclear fraction, a highly efficient transcription extract from Drosophila embryos. *Methods Cell Biol* **44**: 225-235.

Karcavich R, Doe CQ. 2005. Drosophila neuroblast 7-3 cell lineage: a model system for studying programmed cell death, Notch/Numb signaling, and sequential specification of ganglion mother cell identity. *J Comp Neurol* **481**: 240-251.

Kellum R, Schedl P. 1991. A position-effect assay for boundaries of higher order chromosomal domains. *Cell* **64**: 941-950.

—. 1992. A group of scs elements function as domain boundaries in an enhancer-blocking assay. *Mol Cell Biol* **12**: 2424-2431.

Ketel CS, Andersen EF, Vargas ML, Suh J, Strome S, Simon JA. 2005. Subunit contributions to histone methyltransferase activities of fly and worm polycomb group complexes. *Mol Cell Biol* **25**: 6857-6868.

Keyse SM, Amaudruz F, Tyrrell RM. 1988. Determination of the spectrum of mutations induced by defined- wavelength solar UVB (313-nm) radiation in mammalian cells by use of a shuttle vector. *Mol Cell Biol* **8**: 5425-5431.

Kikuta H, Laplante M, Navratilova P, Komisarczuk AZ, Engstrom PG, Fredman D, Akalin A, Caccamo M, Sealy I, Howe K et al. 2007. Genomic regulatory blocks encompass multiple neighboring genes and maintain conserved synteny in vertebrates. *Genome Res* **17**: 545-555.

Kim CA, Gingery M, Pilpa RM, Bowie JU. 2002. The SAM domain of polyhomeotic forms a helical polymer. *Nat Struct Biol* **9**: 453-457.

King IF, Emmons RB, Francis NJ, Wild B, Muller J, Kingston RE, Wu CT. 2005. Analysis of a polycomb group protein defines regions that link repressive activity on nucleosomal templates to in vivo function. *Mol Cell Biol* **25**: 6578-6591.

King IF, Francis NJ, Kingston RE. 2002. Native and recombinant polycomb group complexes establish a selective block to template accessibility to repress transcription in vitro. *Mol Cell Biol* **22**: 7919-7928.

Klymenko T, Papp B, Fischle W, Kocher T, Schelder M, Fritsch C, Wild B, Wilm M, Muller J. 2006. A Polycomb group protein complex with sequence-specific DNA-binding and selective methyl-lysine-binding activities. *Genes Dev* **20**: 1110-1122.

Kodjabachian L, Delaage M, Maurel C, Miassod R, Jacq B, Rosset R. 1998. Mutations in ccf, a novel Drosophila gene encoding a chromosomal factor, affect progression through mitosis and interact with Pc-G mutations. *Embo J* **17**: 1063-1075.

Kurshakova M, Maksimenko O, Golovnin A, Pulina M, Georgieva S, Georgiev P, Krasnov A. 2007. Evolutionarily conserved E(y)2/Sus1 protein is essential for the barrier activity of Su(Hw)-dependent insulators in Drosophila. *Mol Cell* **27**: 332-338.

Kuziora MA, McGinnis W. 1988. Different transcripts of the Drosophila Abd-B gene correlate with distinct genetic sub-functions. *Embo J* **7**: 3233-3244.

Lavigne M, Francis NJ, King IF, Kingston RE. 2004. Propagation of silencing; recruitment and repression of naive chromatin in trans by polycomb repressed chromatin. *Mol Cell* **13**: 415-425.

Lee JH, Lee E, Park J, Kim E, Kim J, Chung J. 2003. In vivo p53 function is indispensable for DNA damage-induced apoptotic signaling in Drosophila. *FEBS Lett* **550**: 5-10.

Levine SS, King IF, Kingston RE. 2004. Division of labor in polycomb group repression. *Trends Biochem Sci* **29**: 478-485.

Lewis EB. 1978. A gene complex controlling segmentation in Drosophila. *Nature* **276**: 565-570.

Lewis SE, Searle SM, Harris N, Gibson M, Lyer V, Richter J, Wiel C, Bayraktaroglir L, Birney E, Crosby MA et al. 2002. Apollo: a sequence annotation editor. *Genome Biol* **3**: RESEARCH0082.

Li S, Aufiero B, Schiltz RL, Walsh MJ. 2000. Regulation of the homeodomain CCAAT displacement/cut protein function by histone acetyltransferases p300/CREB-binding protein (CBP)-associated factor and CBP. *Proc Natl Acad Sci U S A* **97**: 7166-7171.

Lin N, Zhang C, Pang J, Zhou L. 2009. By design or by chance: cell death during Drosophila embryogenesis. *Apoptosis*.

Lohmann I. 2003. Dissecting the regulation of the Drosophila cell death activator reaper. *Gene Expr Patterns* **3**: 159-163.

Lowe SW, Schmitt EM, Smith SW, Osborne BA, Jacks T. 1993. p53 is required for radiation-induced apoptosis in mouse thymocytes. *Nature (London)* **362**: 847-849.

Lu BY, Ma J, Eissenberg JC. 1998. Developmental regulation of heterochromatin-mediated gene silencing in Drosophila. *Development* **125**: 2223-2234.

Lupo R, Breiling A, Bianchi ME, Orlando V. 2001. Drosophila chromosome condensation proteins Topoisomerase II and Barren colocalize with Polycomb and maintain Fab-7 PRE silencing. *Mol Cell* **7**: 127-136.

Maeda RK, Karch F. 2007. Making connections: boundaries and insulators in Drosophila. *Curr Opin Genet Dev* **17**: 394-399.

Magrassi L, Lawrence PA. 1988. The pattern of cell death in fushi tarazu, a segmentation gene of Drosophila. *Development* **104**: 447-451.

Majumder P, Roy S, Belozerov VE, Bosu D, Puppali M, Cai HN. 2009. Diverse transcription influences can be insulated by the Drosophila SF1 chromatin boundary. *Nucleic Acids Res* **37**: 4227-4233.

Mallin DR, Myung JS, Patton JS, Geyer PK. 1998. Polycomb group repression is blocked by the Drosophila suppressor of Hairy-wing [su(Hw)] insulator. *Genetics* **148**: 331-339.

Martinez AM, Colomb S, Dejardin J, Bantignies F, Cavalli G. 2006. Polycomb group-dependent Cyclin A repression in Drosophila. *Genes Dev* **20**: 501-513.

Maurange C, Cheng L, Gould AP. 2008. Temporal transcription factors and their targets schedule the end of neural proliferation in Drosophila. *Cell* **133**: 891-902.

Mayor C, Brudno M, Schwartz JR, Poliakov A, Rubin EM, Frazer KA, Pachter LS, Dubchak I. 2000. VISTA : visualizing global DNA sequence alignments of arbitrary length. *Bioinformatics* **16**: 1046-1047.

McGinnis W, Krumlauf R. 1992. Homeobox genes and axial patterning. *Cell* **68**: 283-302.

Min J, Zhang Y, Xu RM. 2003. Structural basis for specific binding of Polycomb chromodomain to histone H3 methylated at Lys 27. *Genes Dev* **17**: 1823-1828.

Mishra RK, Mihaly J, Barges S, Spierer A, Karch F, Hagstrom K, Schweinsberg SE, Schedl P. 2001. The iab-7 polycomb response element maps to a nucleosome-free region of chromatin and requires both GAGA and pleiohomeotic for silencing activity. *Mol Cell Biol* **21**: 1311-1318.

Mizumatsu S, Monje ML, Morhardt DR, Rola R, Palmer TD, Fike JR. 2003. Extreme sensitivity of adult neurogenesis to low doses of X-irradiation. *Cancer Res* **63**: 4021-4027.

Moazed D, O'Farrell PH. 1992. Maintenance of the engrailed expression pattern by Polycomb group genes in Drosophila. *Development* **116**: 805-810.

Mohd-Sarip A, Cleard F, Mishra RK, Karch F, Verrijzer CP. 2005. Synergistic recognition of an epigenetic DNA element by Pleiohomeotic and a Polycomb core complex. *Genes Dev* **19**: 1755-1760.

Mohd-Sarip A, van der Knaap JA, Wyman C, Kanaar R, Schedl P, Verrijzer CP. 2006. Architecture of a polycomb nucleoprotein complex. *Mol Cell* **24**: 91-100.

Mohd-Sarip A, Venturini F, Chalkley GE, Verrijzer CP. 2002. Pleiohomeotic can link polycomb to DNA and mediate transcriptional repression. *Mol Cell Biol* **22**: 7473-7483.

Mottus R, Sobel RE, Grigliatti TA. 2000. Mutational analysis of a histone deacetylase in Drosophila melanogaster: missense mutations suppress gene silencing associated with position effect variegation. *Genetics* **154**: 657-668.

Muller J, Hart CM, Francis NJ, Vargas ML, Sengupta A, Wild B, Miller EL, O'Connor MB, Kingston RE, Simon JA. 2002. Histone methyltransferase activity of a Drosophila Polycomb group repressor complex. *Cell* **111**: 197-208.

Muller J, Kassis JA. 2006. Polycomb response elements and targeting of Polycomb group proteins in Drosophila. *Curr Opin Genet Dev* **16**: 476-484.

Nabirochkin S, Ossokina M, Heidmann T. 1998. A nuclear matrix/scaffold attachment region co-localizes with the gypsy retrotransposon insulator sequence. *J Biol Chem* **273**: 2473-2479.

Nakano K, Vousden KH. 2001. PUMA, a novel proapoptotic gene, is induced by p53. *Mol Cell* **7**: 683-694.

Narita M, Nunez S, Heard E, Lin AW, Hearn SA, Spector DL, Hannon GJ, Lowe SW. 2003. Rb-mediated heterochromatin formation and silencing of E2F target genes during cellular senescence. *Cell* **113**: 703-716.

Negre N, Hennetin J, Sun LV, Lavrov S, Bellis M, White KP, Cavalli G. 2006. Chromosomal distribution of PcG proteins during Drosophila development. *PLoS Biol* **4**: e170.

Nekrasov M, Klymenko T, Fraterman S, Papp B, Oktaba K, Kocher T, Cohen A, Stunnenberg HG, Wilm M, Muller J. 2007. Pcl-PRC2 is needed to generate high levels of H3-K27 trimethylation at Polycomb target genes. *Embo J* **26**: 4078-4088.

Nekrasov M, Wild B, Muller J. 2005. Nucleosome binding and histone methyltransferase activity of Drosophila PRC2. *EMBO Rep* **6**: 348-353.

Nepveu A. 2001. Role of the multifunctional CDP/Cut/Cux homeodomain transcription factor in regulating differentiation, cell growth and development. *Gene* **270**: 1-15.

Neufeld EJ, Skalnik DG, Lievens PM, Orkin SH. 1992. Human CCAAT displacement protein is homologous to the Drosophila homeoprotein, cut. *Nat Genet* **1**: 50-55.

Nordstrom W, Chen P, Steller H, Abrams JM. 1996. Activation of the reaper gene during ectopic cell killing in Drosophila. *Dev Biol* **180**: 213-226.

Nowak E, Etienne O, Millet P, Lages CS, Mathieu C, Mouthon MA, Boussin FD. 2006. Radiation-induced H2AX phosphorylation and neural precursor apoptosis in the developing brain of mice. *Radiat Res* **165**: 155-164.

O'Dor E, Beck SA, Brock HW. 2006. Polycomb group mutants exhibit mitotic defects in syncytial cell cycles of Drosophila embryos. *Dev Biol* **290**: 312-322.

Ohlstein B, Spradling A. 2006. The adult Drosophila posterior midgut is maintained by pluripotent stem cells. *Nature* **439**: 470-474.

Ollmann M, Young LM, Di Como CJ, Karim F, Belvin M, Robertson S, Whittaker K, Demsky M, Fisher WW, Buchman A et al. 2000. Drosophila p53 is a structural and functional homolog of the tumor suppressor p53. *Cell* **101**: 91-101.

Olson MR, Holley CL, Gan EC, Colon-Ramos DA, Kaplan B, Kornbluth S. 2003. A GH3-like domain in reaper required formitochondrial localization and induction of IAP degradation. *J Biol Chem* **13**: 13.

Orlando V, Jane EP, Chinwalla V, Harte PJ, Paro R. 1998. Binding of trithorax and Polycomb proteins to the bithorax complex: dynamic changes during early Drosophila embryogenesis. *Embo J* **17**: 5141-5150.

Papp B, Muller J. 2006. Histone trimethylation and the maintenance of transcriptional ON and OFF states by trxG and PcG proteins. *Genes Dev* **20**: 2041-2054.

Parks AL, Cook KR, Belvin M, Dompe NA, Fawcett R, Huppert K, Tan LR, Winter CG, Bogart KP, Deal JE et al. 2004. Systematic generation of high-resolution deletion coverage of the Drosophila melanogaster genome. *Nat Genet* **36**: 288-292.

Pasini D, Bracken AP, Jensen MR, Lazzerini Denchi E, Helin K. 2004. Suz12 is essential for mouse development and for EZH2 histone methyltransferase activity. *Embo J* **23**: 4061-4071.

Pazdera TM, Janardhan P, Minden JS. 1998. Patterned epidermal cell death in wild-type and segment polarity mutant Drosophila embryos. *Development* **125**: 3427-3436.

Peissner W, Kocher M, Treuer H, Gillardon F. 1999. Ionizing radiation-induced apoptosis of proliferating stem cells in the dentate gyrus of the adult rat hippocampus. *Brain Res Mol Brain Res* **71**: 61-68.

Peterson C, Carney GE, Taylor BJ, White K. 2002. reaper is required for neuroblast apoptosis during Drosophila development. *Development* **129**: 1467-1476.

Phillips MD, Shearn A. 1990. Mutations in polycombeotic, a Drosophila polycomb-group gene, cause a wide range of maternal and zygotic phenotypes. *Genetics* **125**: 91-101.

Pirrotta V. 1998. Polycombing the genome: PcG, trxG, and chromatin silencing. *Cell* **93**: 333-336.

Qi D, Larsson J, Mannervik M. 2004. Drosophila Ada2b is required for viability and normal histone H3 acetylation. *Mol Cell Biol* **24**: 8080-8089.

Qian S, Capovilla M, Pirrotta V. 1993. Molecular mechanisms of pattern formation by the BRE enhancer of the Ubx gene. *Embo J* **12**: 3865-3877.

Raab JR, Kamakaka RT. 2010. Insulators and promoters: closer than we think. *Nat Rev Genet* **11**: 439-446.

Rank G, Prestel M, Paro R. 2002. Transcription through intergenic chromosomal memory elements of the Drosophila bithorax complex correlates with an epigenetic switch. *Mol Cell Biol* **22**: 8026-8034.

Recillas-Targa F, Pikaart MJ, Burgess-Beusse B, Bell AC, Litt MD, West AG, Gaszner M, Felsenfeld G. 2002. Position-effect protection and enhancer blocking by the chicken beta-globin insulator are separable activities. *Proc Natl Acad Sci U S A* **99**: 6883-6888.

Riley PD, Carroll SB, Scott MP. 1987. The expression and regulation of Sex combs reduced protein in Drosophila embryos. *Genes Dev* **1**: 716-730.

Ringrose L, Paro R. 2007. Polycomb/Trithorax response elements and epigenetic memory of cell identity. *Development* **134**: 223-232.

Ringrose L, Rehmsmeier M, Dura JM, Paro R. 2003. Genome-wide prediction of Polycomb/Trithorax response elements in Drosophila melanogaster. *Dev Cell* **5**: 759-771.

Rogulja-Ortmann A, Luer K, Seibert J, Rickert C, Technau GM. 2007. Programmed cell death in the embryonic central nervous system of Drosophila melanogaster. *Development* **134**: 105-116.

Rogulja-Ortmann A, Renner S, Technau GM. 2008. Antagonistic roles for Ultrabithorax and Antennapedia in regulating segment-specific apoptosis of differentiated motoneurons in the Drosophila embryonic central nervous system. *Development*.

Roseman RR, Pirrotta V, Geyer PK. 1993. The su(Hw) protein insulates expression of the Drosophila melanogaster white gene from chromosomal position-effects. *Embo J* **12**: 435-442.

Rougvie AE, Lis JT. 1988. The RNA polymerase II molecule at the 5' end of the uninduced hsp70 gene of D. melanogaster is transcriptionally engaged. *Cell* **54**: 795-804.

Rozen S, Skaletsky H. 2000. Primer3 on the WWW for general users and for biologist programmers. *Methods Mol Biol* **132**: 365-386.

Sanchez-Elsner T, Gou D, Kremmer E, Sauer F. 2006. Noncoding RNAs of trithorax response elements recruit Drosophila Ash1 to Ultrabithorax. *Science* **311**: 1118-1123.

Saurin AJ, Shao Z, Erdjument-Bromage H, Tempst P, Kingston RE. 2001. A Drosophila Polycomb group complex includes Zeste and dTAFII proteins. *Nature* **412**: 655-660.

Scarano MI, Strazzullo M, Matarazzo MR, D'Esposito M. 2005. DNA methylation 40 years later: Its role in human health and disease. *J Cell Physiol* **204**: 21-35.

Schmitt S, Prestel M, Paro R. 2005. Intergenic transcription through a polycomb group response element counteracts silencing. *Genes Dev* **19**: 697-708.

Schwartz YB, Kahn TG, Nix DA, Li XY, Bourgon R, Biggin M, Pirrotta V. 2006. Genome-wide analysis of Polycomb targets in Drosophila melanogaster. *Nat Genet* **38**: 700-705.

Schwartz YB, Pirrotta V. 2007. Polycomb silencing mechanisms and the management of genomic programmes. *Nat Rev Genet* **8**: 9-22.

—. 2008. Polycomb complexes and epigenetic states. *Curr Opin Cell Biol* **20**: 266-273.

Sengupta AK, Kuhrs A, Muller J. 2004. General transcriptional silencing by a Polycomb response element in Drosophila. *Development* **131**: 1959-1965.

Shao Z, Raible F, Mollaaghababa R, Guyon JR, Wu CT, Bender W, Kingston RE. 1999. Stabilization of chromatin structure by PRC1, a Polycomb complex. *Cell* **98**: 37-46.

Sheng G, Thouvenot E, Schmucker D, Wilson DS, Desplan C. 1997. Direct regulation of rhodopsin 1 by Pax-6/eyeless in Drosophila: evidence for a conserved function in photoreceptors. *Genes Dev* **11**: 1122-1131.

Shibue T, Takeda K, Oda E, Tanaka H, Murasawa H, Takaoka A, Morishita Y, Akira S, Taniguchi T, Tanaka N. 2003. Integral role of Noxa in p53-mediated apoptotic response. *Genes Dev* **17**: 2233-2238.

Sigrist CJ, Pirrotta V. 1997. Chromatin insulator elements block the silencing of a target gene by the Drosophila polycomb response element (PRE) but allow trans interactions between PREs on different chromosomes. *Genetics* **147**: 209-221.

Simon J, Chiang A, Bender W. 1992. Ten different Polycomb group genes are required for spatial control of the abdA and AbdB homeotic products. *Development* **114**: 493-505.

Smouse D, Goodman C, Mahowald A, Perrimon N. 1988. polyhomeotic: a gene required for the embryonic development of axon pathways in the central nervous system of Drosophila. *Genes Dev* **2**: 830-842.

Sogame N, Kim M, Abrams JM. 2003. Drosophila p53 preserves genomic stability by regulating cell death. *Proc Natl Acad Sci U S A* **100**: 4696-4701.

Sonnenfeld MJ, Jacobs JR. 1995a. Apoptosis of the midline glia during Drosophila embryogenesis: a correlation with axon contact. *Development* **121**: 569-578.

—. 1995b. Macrophages and glia participate in the removal of apoptotic neurons from the Drosophila embryonic nervous system. *J Comp Neurol* **359**: 644-652.

Soria C, Estermann FE, Espantman KC, O'Shea CC. 2010. Heterochromatin silencing of p53 target genes by a small viral protein. *Nature* **466**: 1076-1081.

Srinivasula SM, Datta P, Kobayashi M, Wu JW, Fujioka M, Hegde R, Zhang Z, Mukattash R, Fernandes-Alnemri T, Shi Y et al. 2002. sickle, a Novel Drosophila Death Gene in the reaper/hid/grim Region, Encodes an IAP-Inhibitory Protein. *Curr Biol* **12**: 125-130.

Steller H. 1995. Mechanisms and Genes of Cellular Suicide. *Science* **267**: 1445-1449.

—. 2008. Regulation of apoptosis in Drosophila. *Cell Death Differ* **15**: 1132-1138.

Struhl G. 1983. Role of the esc+ gene product in ensuring the selective expression of segment-specific homeotic genes in Drosophila. *J Embryol Exp Morphol* **76**: 297-331.

Su TT, Jaklevic B. 2001. DNA damage leads to a Cyclin A-dependent delay in metaphase-anaphase transition in the Drosophila gastrula. *Curr Biol* **11**: 8-17.

Tepass U, Fessler LI, Aziz A, Hartenstein V. 1994. Embryonic origin of hemocytes and their relationship to cell death in Drosophila. *Development* **120**: 1829-1837.

Thellmann M, Hatzold J, Conradt B. 2003. The Snail-like CES-1 protein of C. elegans can block the expression of the BH3-only cell-death activator gene egl-1 by antagonizing the function of bHLH proteins. *Development* **130**: 4057-4071.

Thibault ST, Singer MA, Miyazaki WY, Milash B, Dompe NA, Singh CM, Buchholz R, Demsky M, Fawcett R, Francis-Lang HL et al. 2004. A complementary transposon tool kit for Drosophila melanogaster using P and piggyBac. *Nat Genet* **36**: 283-287.

Thomas BJ. 2005. Cell-cycle control during development: taking it up a notch. *Dev Cell* **8**: 451-452.

Tie F, Banerjee R, Stratton CA, Prasad-Sinha J, Stepanik V, Zlobin A, Diaz MO, Scacheri PC, Harte PJ. 2009. CBP-mediated acetylation of histone H3 lysine 27 antagonizes Drosophila Polycomb silencing. *Development* **136**: 3131-3141.

Tie F, Prasad-Sinha J, Birve A, Rasmuson-Lestander A, Harte PJ. 2003. A 1-megadalton ESC/E(Z) complex from Drosophila that contains polycomblike and RPD3. *Mol Cell Biol* **23**: 3352-3362.

Tolhuis B, de Wit E, Muijrers I, Teunissen H, Talhout W, van Steensel B, van Lohuizen M. 2006. Genome-wide profiling of PRC1 and PRC2 Polycomb chromatin binding in Drosophila melanogaster. *Nat Genet* **38**: 694-699.

Tolhuis B, Palstra RJ, Splinter E, Grosveld F, de Laat W. 2002. Looping and interaction between hypersensitive sites in the active beta-globin locus. *Mol Cell* **10**: 1453-1465.

Toyama Y, Peralta XG, Wells AR, Kiehart DP, Edwards GS. 2008. Apoptotic force and tissue dynamics during Drosophila embryogenesis. *Science* **321**: 1683-1686.

Trojer P, Reinberg D. 2007. Facultative heterochromatin: is there a distinctive molecular signature? *Mol Cell* **28**: 1-13.

Tseng AS, Hariharan IK. 2002. An overexpression screen in Drosophila for genes that restrict growth or cell-cycle progression in the developing eye. *Genetics* **162**: 229-243.

Tusher VG, Tibshirani R, Chu G. 2001. Significance analysis of microarrays applied to the ionizing radiation response. *Proc Natl Acad Sci U S A* **98**: 5116-5121.

Vaux DL, Korsmeyer SJ. 1999. Cell Death in Development. *Cell* **96**: 245-254.

Vaux DL, Silke J. 2005. IAPs, RINGs and ubiquitylation. *Nat Rev Mol Cell Biol* **6**: 287-297.

Venken KJ, He Y, Hoskins RA, Bellen HJ. 2006. P[acman]: a BAC transgenic platform for targeted insertion of large DNA fragments in D. melanogaster. *Science* **314**: 1747-1751.

Villunger A, Michalak EM, Coultas L, Mullauer F, Bock G, Ausserlechner MJ, Adams JM, Strasser A. 2003. p53- and drug-induced apoptotic responses mediated by BH3-only proteins puma and noxa. *Science* **302**: 1036-1038.

Wang H, Wang L, Erdjument-Bromage H, Vidal M, Tempst P, Jones RS, Zhang Y. 2004a. Role of histone H2A ubiquitination in Polycomb silencing. *Nature* **431**: 873-878.

Wang L, Brown JL, Cao R, Zhang Y, Kassis JA, Jones RS. 2004b. Hierarchical recruitment of polycomb group silencing complexes. *Mol Cell* **14**: 637-646.

Wang L, Tu Z, Sun F. 2009. A network-based integrative approach to prioritize reliable hits from multiple genome-wide RNAi screens in Drosophila. *BMC Genomics* **10**: 220.

Wang SL, Hawkins CJ, Yoo SJ, Muller HA, Hay BA. 1999. The Drosophila caspase inhibitor DIAP1 is essential for cell survival and is negatively regulated by HID. *Cell* **98**: 453-463.

Weiler KS, Wakimoto BT. 1995. Heterochromatin and gene expression in Drosophila. *Annu Rev Genet* **29**: 577-605.

West AG, Huang S, Gaszner M, Litt MD, Felsenfeld G. 2004. Recruitment of histone modifications by USF proteins at a vertebrate barrier element. *Mol Cell* **16**: 453-463.

White K, Grether ME, Abrams JM, Young L, Farrell K, Steller H. 1994. Genetic control of programmed cell death in Drosophila. *Science* **264**: 677-683.

Wichmann A, Jaklevic B, Su TT. 2006. Ionizing radiation induces caspase-dependent but Chk2- and p53-independent cell death in Drosophila melanogaster. *Proc Natl Acad Sci U S A* **103**: 9952-9957.

Wing JP, Karres JS, Ogdahl JL, Zhou L, Schwartz LM, Nambu JR. 2002. Drosophila sickle Is a Novel grim-reaper Cell Death Activator. *Curr Biol* **12**: 131-135.

Wing JP, Schwartz LM, Nambu JR. 2001. The RHG motifs of Drosophila Reaper and Grim are important for their distinct cell death-inducing abilities. *Mech Dev* **102**: 193-203.

Wurgler FE, Ullrich H. 1976. Radiaosensitivity of embryonic stages. in *The Genetics and Biology of Drosophila* (eds. M Ashburner, E Novitski), pp. 1269-1298. Academic press, London and New York.

Yin VP, Thummel CS. 2004. A balance between the diap1 death inhibitor and reaper and hid death inducers controls steroid-triggered cell death in Drosophila. *Proc Natl Acad Sci U S A* **101**: 8022-8027.

Yu J, Zhang L, Hwang PM, Kinzler KW, Vogelstein B. 2001. PUMA induces the rapid apoptosis of colorectal cancer cells. *Mol Cell* **7**: 673-682.

Zachariou A, Tenev T, Goyal L, Agapite J, Steller H, Meier P. 2003. IAP-antagonists exhibit non-redundant modes of action through differential DIAP1 binding. *Embo J* **22**: 6642-6652.

Zeitlinger J, Stark A, Kellis M, Hong JW, Nechaev S, Adelman K, Levine M, Young RA. 2007. RNA polymerase stalling at developmental control genes in the Drosophila melanogaster embryo. *Nat Genet* **39**: 1512-1516.

Zhang CC, Bienz M. 1992. Segmental determination in Drosophila conferred by hunchback (hb), a repressor of the homeotic gene Ultrabithorax (Ubx). *Proc Natl Acad Sci U S A* **89**: 7511-7515.

Zhang Y, Lin N, Carroll P, Chan G, Guan B, Xiao H, Yao B, Wu S, Zhou L. 2008a. Epigenetic Blocking of an Enhancer Region Controls Irradiation-Induced Proapoptotic Gene Expression in Drosophila Embryos. *Developmental Cell* **14**: 481-493.

Zhang Y, Lin N, Carroll PM, Chan G, Guan B, Xiao H, Yao B, Wu SS, Zhou L. 2008b. Epigenetic blocking of an enhancer region controls irradiation-induced proapoptotic gene expression in Drosophila embryos. *Dev Cell* **14**: 481-493.

Zhou L, Hashimi H, Schwartz LM, Nambu JR. 1995. Programmed cell death in the Drosophila central nervous system midline. *Curr Biol* **5**: 784-790.

Zhou L, Jiang G, Chan G, Santos CP, Severson DW, Xiao L. 2005. Michelob_x is the missing inhibitor of apoptosis protein antagonist in mosquito genomes. *EMBO Rep* **6**: 769-774.

Zhou L, Schnitzler A, Agapite J, Schwartz LM, Steller H, Nambu JR. 1997. Cooperative functions of the reaper and head involution defective genes in the programmed cell death of Drosophila central nervous system midline cells. *Proc Natl Acad Sci U S A* **94**: 5131-5136.

Zhou L, Steller H. 2003. Distinct pathways mediate UV-induced apoptosis in Drosophila embryos. *Dev Cell* **4**: 599-605.

Zhou L, Yuan R, Lananta S. 2003. Molecular mechanisms of Irradiation induced cell death. *Frontiers of Bioscience* **8:d9-19**.

BIOGRAPHICAL SKETCH

Nianwei Lin was born in 1979, in Longyan, a small mountainous city in south China. He received his B.S. degree from the Department of Biology at Xiamen University (China) in 2002, and continued his graduate study under the supervision of Dr. Runying Zeng. In 2005, he completed his thesis and graduated with a Master of Science degree. In the same year, he traveled from China to the United States of America, and enrolled as a graduate student in the Interdisciplinary Program in Biomedical Sciences (IDP) at the University of Florida. In 2006, he joined the laboratory of Dr. Lei Zhou in the Department of Molecular Genetics and Microbiology. He passed his qualifying exam and became an official Ph.D. candidate in October 2007. He finished his dissertation in November 2010 and received his Ph.D. degree in December 2010.